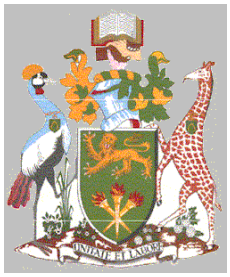

**UNIVERSITY OF NAIROBI**

# MODELING AND SYNTHESIS OF ANTIPLASMODIAL CHROMONES, CHROMANONES AND CHALCONES BASED ON NATURAL PRODUCTS OF KENYA

**BY**

**MANYIM SCOLASTICA**

**I56/79952/2012**

**A Thesis Submitted in Partial Fulfillment of the Requirements for the Award of the Degree of Masters of Science (Chemistry) of University of Nairobi.**

**2016**

## DECLARATION

I declare that this thesis is my original work and has not been submitted elsewhere for examination, award of a degree or publication. Where other people's work or my own work has been used, this has properly been acknowledged and referenced in accordance with the University of Nairobi's requirements.

Signature.....Date....10/5/2016....

**Manyim Scolastica**

**I56/79952/2012**

Department of Chemistry

University of Nairobi

This thesis has been submitted for examination with our approval as research supervisors.

Signature.....Date....11/05/2016....

**Dr. Albert Ndakala**

Department of Chemistry

University of Nairobi

Signature.....Date....11/05/2016....

**Dr. Solomon Derese**

Department of Chemistry

University of Nairobi

**DEDICATION**

*This work is dedicated to my parents, brothers, sisters, Hillary and Harry.*

# ACKNOWLEDGEMENT

First and foremost I wish to acknowledge the almighty God for seeing me through my masters studies.

My deepest gratitude goes to my supervisors Albert Ndakala and Dr. Solomon Derese for their invaluable guidance, support and encouragement throughout the project work. The chairman and staff members of the Department of Chemistry are acknowledged for their support in different ways. My appreciation goes to my colleagues at the Department of Chemistry more so Phylis Ochieng', Caroline Kemboi and my project colleagues Rogo Michael and Oyim James for their collective effort.

Grand challenge Canada is acknowledged for the grant (S4 0260-01) that financially supported the project. Novartis institute of biomedical research for supplying chemicals and computational equipment. OpenEye scientific software company http://www.eyesopen.com for providing the academic license for the computational software used.

I acknowledge Dr. Hoseah M. Akala of United States Army Medical Research unit at Kenya Medical Research institute (KEMRI) for running the antiplasmodial assays and Dr. Matthias Heydenreich of the University of Potsdam, Germany for NMR spectroscopic analysis.

I extend my heartfelt appreciation to my parents Peter Kiptoo Manyim and Regina Kiptoo for their moral and financial support. I acknowledge my brothers and sisters for their support and encouragement throughout my studies.

# ABSTRACT

A significant amount of research has been done on plants of Kenya resulting in the isolation of thousands of natural products, but data on these natural products is not systematically organized in a readily accessible form. This has necessitated the construction of a web-based database of natural products of Kenya. The database is named *mitishamba* and is hosted at http://m*itishamba*.uonbi.ac.ke.

The *mitishamba* database was queried for chromones, chromanones and chalcones that were subjected to structure based drug design using *Fred* (OpenEye) docking utility program with 1TV5 PDB structure of the *Pf*DHODH receptor to identify ligands that bind with the active site. Ligand-based drug design (Shape and electrostatics comparison) was also done on the ligands against query **A77 1726** (**38**) (the ligand that co-crystallized with *Pf*DHODH receptor) using *ROCS* and *EON* programs, respectively, of OpenEye suite. There was an above average similarity among the top performing ligands in the docking studies with shape and electrostatic comparison. This led to the identification of compounds of interest which were targeted for synthesis and antiplasmodial assay.

A chromanone, 7-hydroxy-2-(4-methoxyphenyl) chroman-4-one (**48**) and two intermediate chalcones, 2',4'-dihydroxy-4-methoxychalcone (**45)** and 2',4'-dihydroxy-4-chlorochalcone (**47)**, were synthesized and subjected to antiplasmodial assay. Whereas **45** showed strong activity, **47** and **48** had moderate activity against the chloroquine resistant K1 strain of *P. falciparum* with $IC_{50}$ values of 4.56±1.66, 17.62 ± 5.94 and 18.01 ±1.66 µg/ml, respectively. Since the synthesized compounds showed antiplasmodial potential, there is need for further computational refinement of these compounds to optimize their antiplasmodial activity.

## TABLE OF CONTENTS

# LIST OF TABLES

# LIST OF FIGURES

# LIST OF SCHEMES

# LIST OF APPENDICES

# LIST OF ABBREVIATIONS

ACT: Aspartate carbamoyltransferase

ACTs: Artemisinin-based combination therapies

AUC: Area under the curve

CADD: Computer-aided drug design

CPS: Carbamoylphosphate synthetase

CRS: Chloroquine resistant strain

CSS: Chloroquine sensitive strain

3D7: Chloroquine sensitive strain of *P. falciparum*

D6: Chloroquine sensitive strain of *P. falciparum*

DHODH: Dihydroorotate dehydrogenase

DNA: Deoxyribonucleic acid

FMN: Flavin mononucleotide

HTS: High throughput screening

$IC_{50:}$ Half maximal inhibitory concentration

K1: Chloroquine resistant strain of *P. falciparum*

L-Asp: L-Aspartic acid

LBDD: Ligand based drug design

L-Gln: L-Glutamine

OMPDC: Orotidine 5'-monophosphate decarboxylase

OPRT: Orotate phosphoribosyltransferase

*Pf*DHODH: *Plasmodium falciparum* dihydroorotate dehydrogenase

QSAR: Quantitative structure activity relationship

ROC: Receiver operating characteristic

$R_{F:}$ Retention factor

RNA: Ribonucleic acid

SBDD: Structure based drug design

SD: Standard deviation

SDF: Structure data file

SQL: Structured query language

TS:  Thymidylate synthase

UMP:  Uridine monophosphate nucleotide

VS:  Virtual screening

W2:  Chloroquine resistant strain of *P. falciparum*

# CHAPTER ONE

# INTRODUCTION

## 1.1 Background Information

For many years natural products have been the centre of focus as the main source of new, more effective and safer bioactive metabolites with therapeutic properties against various infectious diseases (Dike *et al*., 2012). Majority of the synthetic drugs used today are either inspired or derived from bioactive compounds in nature (Zhu *et al., 2012)*. Thus, nature continues to be a very important source for new medicines.

The significance of bioactive compounds of natural origin is that they provide novel lead compounds or pharmacological agents for drug discovery. Medicinal plants have played a vital role in the treatment of malaria as well as development of antimalarial drugs. The best known potent antimalarial compound quinine was isolated from the bark of the *Cinchona* tree (Schlitzer, 2007). Over the past decades, the discovery of artemisinin from *Artemisia annua* has boosted research on plants in the search for new antimalarial lead compounds (Biamonte, *et al* 2013). Based on the historically high success rate of natural products, the diversity of chemical compounds found in nature continues to be an important source of molecular templates in search for novel antimalarial drugs (Nogueira and Lopes, 2011).

The African flora comprises of a variety of medicinal plants, which have been extensively utilized by the indigenous people to treat various ailments. For example, in East Africa there are close to 1200 plant species with medicinal value (Kokwaro, 2009). These plant species have been used to treat various diseases and ailments like malaria, typhoid, ulcers, skin diseases, diabetes, reproductive problems, aches and pains. Various studies on medicinal plants of Kenya have led to isolation of a number

of bioactive compounds (Endale *et al*., 2012;Yenesew *et al*., 2003, 2004a, 2005, 2009) with diverse structural scaffolds (Derese *et al.,* 2003; Gumula *et al.,* 2012; Omosa *et al.,* 2010). Despite the enormous body of research existing on natural products of Kenya, this information is not systematically organized in a readily accessible form. This is the reason why a web-based searchable database of natural products of Kenya is developed in this study.

A searchable database of natural products of Kenya would be a source of templates, when combined with modeling, for design and synthesis of drugs for treating various diseases. For example, the chromone (1-benzopyran-4-one), which is a core scaffold in flavonoids has been identified to bind well with diverse receptors (Gaspar *et al*., 2011). This is due to the vast pharmacologically active compounds with this scaffold that have been found to exhibit antimalarial, antibacterial, anticancer, anti-HIV and anti-inflammatory activity (Keri *et al*., 2014). Chromone derivatives have also been found to act as kinase inhibitors, by binding to benzodiazepine receptors (Keri *et al*., 2014). These attractive binding properties as well as biological activities make the chromone scaffold a template of interest for *in silico* design and synthesis of antiplasmodial compounds.

## 1.2 Statement of the Problem

Research on medicinal plants from Kenya has provided a variety of bioactive chemical structures and has become a major source of novel structures that cannot be obtained from sources such as combinatorial synthesis. However lack of collective and comprehensive information of these natural products has restricted further studies.

The diversity (Gumula *et al.,* 2012; Manguro *et al.,* 2006; Yenesew *et al.,* 2000) and outstanding potential (Muiva *et al.,* 2009; Opiyo *et al.,* 2011; Yenesew *et al.,* 2004a, 2009) of these natural products is widely known but the inexistence of a searchable database which properly documents these compounds has limited its application. The establishment of a database of natural products from Kenya will provide systematic information needed by natural products and medicinal chemists hence spur intensive exploration and application in drug discovery.

Considering that majority of antimalarials originated from natural products and that malaria remains a public health challenge due its causative parasites' resistance to the existing drugs, there is need for a continued search for novel antimalarials to stem the looming threat of malaria epidemic. A more efficient strategy for the discovery of antimalarials is through the design using computational methods, synthesis and biological evaluation of lead compounds.

## 1.3 Objectives

### 1.3.1 Main Objective

The main objective of this study was to develop a web-based *in silico* database of natural products of Kenya, for design and synthesis of antiplasmodial lead compounds.

### 1.3.2 Specific Objectives

The specific objectives of this study were to:

1) Develop a web-based *in silico* database of natural products of Kenya.

2) Design antiplasmodial compounds based on chromone, chromanone and chalcone scaffolds through virtual screening of the database against *Plasmodium falciparum* dihydroorotate dehydrogenase enzyme.

3) Synthesize and evaluate the antiplasmodial activity of the promising chromones, chromanones and chalcones from the virtual screening.

### 1.4 Justification and Significance

The establishment of a web-based database of natural products of Kenya will ease the accessibility to information that would facilitate further studies on these natural products. This would lead to discovery and synthesis of important lead compounds against various problematic diseases such as malaria. The new web-based database of natural products of Kenya (*mitishamba* database) will not only be a significant tool for virtual screening but also provide promising scaffolds that can be utilized in the design of novel drugs.

# CHAPTER TWO

# LITERATURE REVIEW

## 2.1 Malaria

According to WHO (2014), there were approximately 198 million malaria cases globally with an estimated 584,000 deaths. Ninety eight percent of the deaths occurred in Africa with children under the age of five accounting for 78 percent deaths (WHO, 2014). Pregnant women and children less than five years of age are mostly affected (WHO, 2014). Malaria therefore, rates as one of the major health, socioeconomic and developmental challenges affecting mainly the world's poorest countries (Biamonte *et al*., 2013).

Malaria is caused by *Plasmodium* parasite, transmitted by the *Anopheles* mosquito. In humans, malaria is caused by five *Plasmodium* species (*P. falciparum, P. vivax, P. ovale, P. malariae and P. knowlesi*) (Birkholtz *et al*., 2012). *Plasmodium falciparum* is by far the deadliest of the five human malarial species (Krungkrai and Krungkrai, 2011). *Plasmodium vivax* is responsible for approximately 25 to 45 percent malaria cases worldwide which are rarely fatal and relapses after the primary infection (Krungkrai and Krungkrai, 2011). *Plasmodium malariae* and *Plasmodium ovale*, although also significant, cause fewer cases and less severe forms of the disease. *Plasmodium knowlesi* has been known to infect nonhuman primates but recent studies have shown that it can also infect human beings (Thera and Plowe, 2012).

Clinical manifestations of the malaria disease occur at the erythrocytic stage (Rudrapal, 2011). Malaria typically produces a string of recurrent attacks, each of which has three stages- chills, followed by fever, and then sweating (Rudrapal, 2011).

Along with chills, an infected person is likely to have headache, fatigue, and muscular pains and occasionally nausea (Rudrapal, 2011). The early symptoms make malaria particularly hard to distinguish from other typical diseases and hampers early diagnosis. As the disease progresses, metabolic acidosis, severe anemia, and cerebral malaria may occur and ultimately prove fatal (Rudrapal, 2011).

Malaria control strategies have been facing a number of challenges. These include, lack of effective vector control, lack of vaccine and the spread of drug resistant malaria parasite to the current antimalarial drugs (Krungkrai and Krungkrai, 2011; Gamo, 2014). The development of new drugs for the treatment and prevention of malaria is therefore essential.

## 2.2 Treatment of Malaria

Malaria treatment strategies employ chemotherapy and vaccine.

### 2.2.1 Malaria Chemotherapy

Since the recognition of malaria as a major health challenge, a great number of plant species have been identified by various communities as having antimalarial properties. As a result, most of the current antimalarial chemotherapies consist substantially of natural products e.g. quinine (**1**) and artemisinin (**4**) and their derivatives. Synthetic antimalarials such as antifolates also play an important role in malaria chemotherapy.

#### 2.2.1.1 Quinine and its Derivatives

Quinine (**1**) an antimalarial drug was the first chemical compound used to treat an infectious disease (Schlitzer, 2007). Quinine is an aminoquinoline alkaloid isolated from the bark of *Cinchona* tree (Nair and Vellalath, 2008) . This alkaloid is one of the oldest and most significant antimalarial drugs still in use that is effective against *Plasmodium falciparum* (Achan *et al*., 2011). The drawbacks in the use of quinine (**1**)

is due to its side effects such as nausea, headache, slight impairment of hearing, vomiting, blurred vision and abdominal pain (Jaeger, 2012). In order to overcome these side effects, the synthetic derivatives such as chloroquine **(2)** and primaquine **(3**) were developed (Kumar *et al*., 2014). The parasite has since developed resistance against chloroquine and primaquine rendering it ineffective for treatment of malaria.

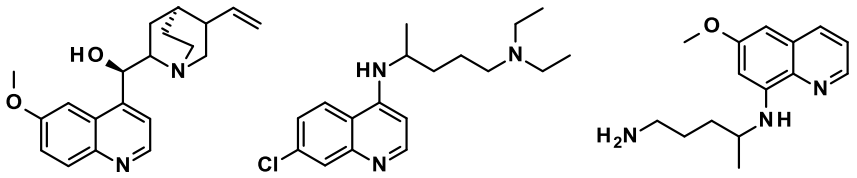


**1** **2** **3**

### 2.2.1.2 Artemisinin and its Derivatives

Artemisinin (**4**) is a component of an ancient Chinese medicine, derived from *Artemisia annua* (Fidock *et al.,* 2004). The discovery of artemisinin (**4**) led to development of many synthetic derivatives such as artesunate (**5**), artemether (**6**) and dihydroartemisinin (**7**). A study investigating the mode of action of artemisinin (**4**) demonstrated that it acts on the electron transport chain where it causes the depolarization of the mitochondrial membrane (Phillips and Rathod, 2010). Since artemisinin and its derivatives have been found to have short half-life, they are recommended for use when combined with drugs that have longer half-life. As a result, the current drugs in use against malaria are artemisinin-based combination therapies (ACTs). Drugs that are commonly combined with artemisinin derivatives include lumefantrine (**8**) and piperaquine **(9**) (Biamonte *et al*., 2013). ACTs have been confirmed to be the first line antimalarial drugs in majority of malaria-endemic countries (WHO *et al*., 2013).

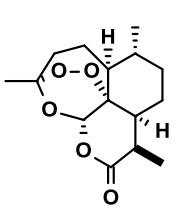

4

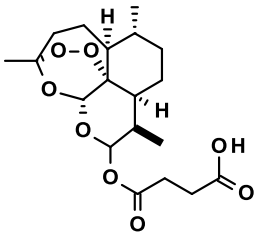

5

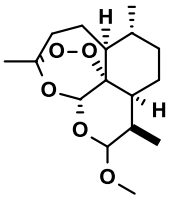

6

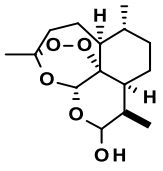

7

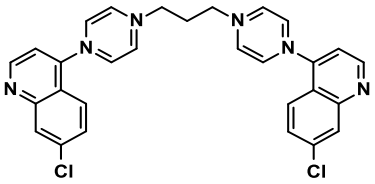

8

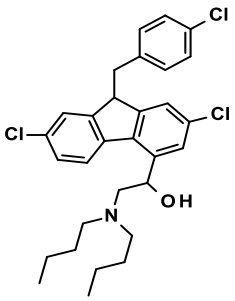

9

### 2.2.1.3 Antifolates

Antifolates are antimalarial drugs that target the dihydrofolate reductase (DHFR) and dihydropteroate synthase (DHPS) enzymes. They include sulfadoxine, dapsone, pyrimethamine, proguanil and cycloguanil (Jana and Paliwal, 2007). Due to their low activity they are combined to increase their effectiveness. For instance, the popularly known fansidar is a combination of sulfadoxine and pyrimethamine (S/P) (Schlitzer, 2008).

### 2.2.1.4 Antimalarial Drug Resistance

Drug resistant malaria is an issue that is of major concern globally. Malaria drug resistance is of particular concern in sub-Saharan Africa, where the burden of malaria is manifested in higher morbidity and mortality (Lee *et al.*, 2013). Antimalarial drug resistance has been associated with the genetic plasticity of the malaria parasite (Castellini *et al.*, 2011). The resistance involves spontaneous mutations that lead to reduced sensitivity to specific drugs or classes of drugs (Castellini *et al.*, 2011). There

are several malaria drugs in use but the increase in resistance of malaria parasite to these drugs poses a challenge to malaria control strategies.

Malaria drug resistance began with the spread of chloroquine resistance across the African continent and resulted in increased disease burden (Klein, 2013). There has been continuous evolution of malaria resistance as new malaria drugs are discovered. The current emergence of *Plasmodium falciparum* resistance to the front-line ACTs calls for the discovery of new antimalarial therapies (Lukens *et al*., 2014). In addition to using combination therapy, there is also need to develop other ways of protecting the existing malarial therapies against resistance.

### 2.2.2 Malaria Vaccines

The traditional approach to malaria vaccine development involves the subunit vaccine strategies whereby the different stages of the *Plasmodium* parasite lifecycle are targeted (WHO 2010). There are several overlapping categories of malaria vaccines (Thera and Plowe, 2012); these include:

- Pre-erythrocytic vaccine targets the liver-stages and the sporozoites.
- Blood stage/asexual vaccines target infected red blood cells specifically antigens expressed on the surface of cells by eliciting an antibody response against attenuated merozoites.
- Transmission blocking vaccines target the sexual stages of malaria parasite and aim to reduce parasite transmission to other hosts.
- Multi-stage vaccines are those vaccines that target a number of antigens that belong to different stages. This is based on the fact that a number of vaccines that target a single antigen have been found to be ineffective.

There are a number of malaria vaccine candidates that are progressing through preclinical and clinical development. Despite the several progresses in search for malaria vaccines, RTS,S (Mosquirix$^{TM}$) remains the most clinically advanced malaria vaccine candidate in development, although it only provides partial immunity (WHO 2012). RTS,S (Mosquirix$^{TM}$) is an example of a pre-erythrocytic vaccine.

Although the use of malaria vaccines would be the best option in the control of malaria, its development has been faced with a number of challenges. The whole process of developing a malaria vaccine is not only very expensive, but also the large size of *P. falciparum* genome which is expressed in the various stages of the mosquito's life-cycle is another significant challenge. Mutation in the liver and blood stages also contributes to the genetic diversity (Thera and Plowe, 2012). Thus anti-malarial control programs still heavily focus on chemotherapy for the treatment and prevention of malaria.

### 2.3 Molecular Modelling in Drug Discovery

Molecular modelling involves the use of computational techniques to predict the behaviour of molecules. It has diverse applications including drug design. Computer aided drug design (CADD) (the use of software and hardware in drug discovery) is a significant tool in the drug discovery process in determination of protein structure and pharmacophore determination as well as docking studies (Ooms, 2000).

The traditional process of drug discovery that involves high-throughput screening (HTS) techniques is cumbersome, time consuming and resource intensive due to the elaborate experimental procedures associated with the process (Tsunoyama *et al*., 2008). The use of virtual screening (VS) in CADD as an alternative for HTS has helped overcome these limitations. VS employs *in silico* techniques to filter vast

chemical space databases in order to obtain promising candidates for lead discovery and optimization (Bielska *et al*., 2011, Hubbard, 2011). The two approaches in CADD are structure based and ligand based drug design.

### 2.3.1 Structure-Based Drug Design

In structure-based drug design (SBDD), the 3D structure of the molecular target must be available. Molecular modeling programs are used to predict the best pose of ligands or small molecules placed in the binding pocket of a receptor (enzyme or protein) through a process known as docking, Figure 2.1 (Nagamani *et al*., 2012). The docking process also predicts the interactions between the ligands and the receptor and the biological implication of the interactions (Udatha *et al*., 2012).

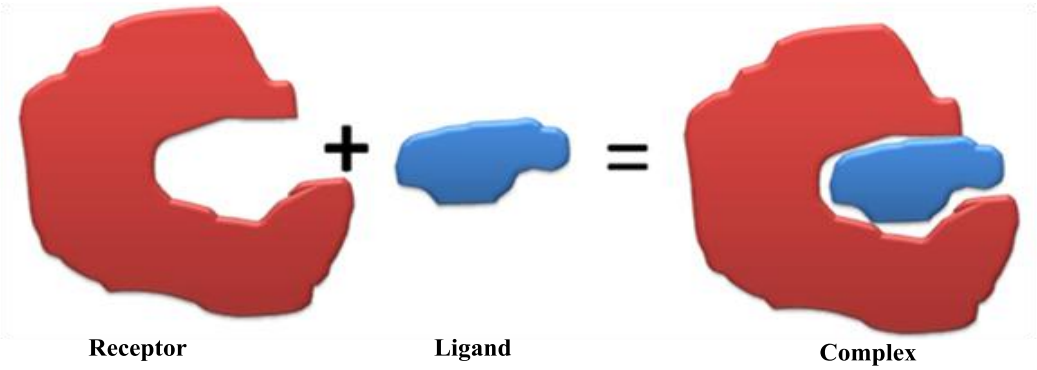


Figure 2.1: Illustration of the docking process

SBDD focuses on finding small molecules that can bring an impact on the functioning of a molecular target (Kuntz, 1992). The success of structure-based drug design is assessed based on the scoring function (Jain and Jayaram, 2005). Depending on the computational program used, docking experiments rank ligands basing on either of the following approaches: force field, knowledge or empirical based approach (Kitchen *et al.*, 2004). Force field-based scoring functions score docking complex basing on atom interactions such as van der waals forces, while knowledge-based scoring function utilize the experimentally determined energy potentials of the ligand

and enzyme to score the docked ligand. On the other hand, empirical-based scoring functions score the docked ligand basing on summation of energies (e.g. hydrogen bonding and desolvation energy) of the complex (Huang *et al*., 2010). The binding program used in this study use an empirical-based scoring function (Chemgauss4) to score the ligands.

### 2.3.2 Ligand-Based Drug Design

Ligand-based drug design (LBDD) is used if the 3D structure of a biological target is not available. It depends on already known active compounds which are used to generate pharmacophores (*Sharma et al*., 2012). The frequently used methods in LBDD are shape and electrostatic similarity searching, quantitative structure-activity relationships (QSAR) and pharmacophore searching (Lee *et al*., 2011).

#### 2.3.2.1 Shape and Electrostatic Similarity Searching

Shape and electrostatic similarity matching involves the use of computer software to superimpose a large set of small molecules on a query molecule (an active compound against the disease of interest) to determine their shape and electrostatic similarity. The small molecules are then scored according to their similarity to the query (Schneider *et al.*, 2006; Wale *et al.*, 2007).

#### 2.3.2.2 Quantitative Structure-Activity Relationships (QSAR)

3D-QSAR models based on molecular descriptors are generated to allow correlation of pharmacological activity and physicochemical properties of compounds for prediction of activity of novel compounds (Shanthi *et al*., 2013). The 3D structures of known active compounds are used to generate QSAR model. Based on the QSAR models various statistical techniques are applied in the formulation of QSAR equations that are used to predict the biological activities of the new compounds.

Molecular descriptors considered in the development of 3D-QSAR models include chiral centres, hydrogen bond acceptors and donors, rotatable bonds, AlogP, among other (Roy and Roy, 2010)

#### 2.3.2.3 Pharmacophore Searching

It involves the construction of a 3D pharmacophore which represents the minimal set of spatially oriented features a compound must possess to be active (Balaramnavar *et al.*, 2014). These features are determined by studying a series of structurally diverse ligands that possess similar features and are active (Van Drie, 2010). The pharmacophore generated is used to screen a database of molecules which are then subjected to assays to determine their activity (Lee *et al*., 2011).

### 2.3.3 Computational Drug Discovery Process

Drug discovery based on computational techniques involves target Identification and Validation, hit Identification, hit to lead and lead optimization.

#### 2.3.3.1 Target Identification and Validation

Target identification is achieved through an understanding of molecular biology of a disease. Bioinformatics has led to the development of computational techniques that can analyze protein structures, interactions, gene sequences and metabolic pathways hence providing novel drug targets (Jiang and Zhou, 2005). Target validation is based on the specific biological function of that target and its relevance to the disease of interest.

#### 2.3.3.2 Hit Identification

Hits are molecules obtained through either traditional library screening or virtual screening. Hit identification involves screening a library of available compounds in order to find small molecules that bind to the active site of the target and modulate its

activity (Wunberg *et al.*, 2006). Hit compounds can be obtained from combinatorial and natural products libraries as well as from ligand design and random screening (Figure 2.2). The libraries of compounds are virtually screened to reduce the size of chemical space hence focus on more promising candidates (Keserű and Makara, 2006). The outcome of this step is a set of hit compounds that bind to the target.

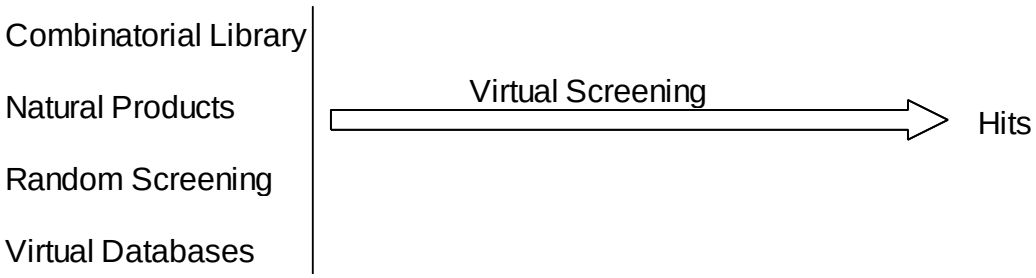


Figure 2.2: Hit identification

#### 2.3.3.3 Hits to Lead Discovery

Leads refer to those molecules obtained when the library of hits is filtered based on pharmacodynamics, Lipinski's rule, pharmacokinetics and bioassays. Hit compounds identified in step one are further explored for their potential to make a lead series. This is achieved through hit evolution, bioisosteric replacements and hit fragmentation (Keserű and Makara, 2006). Hit evolution is whereby hit analogs (generated basing on structure activity relationship) are synthesised and tested while bioisosteric replacement involves substitution of bioisosteres to generate hit analogs with improved physicochemical properties (Meanwell, 2011). On the other hand, hit fragmentation technique is used when the hits are complex molecules in order to generate simpler hit analogs (Keserű and Makara, 2006). The objective of this step is to identify a small number of chemical series with higher activity, more selective, highly stable, less toxic and simplified synthesis (Langdon *et al.*, 2010). The output here is a lead series of compounds that can be optimised (Cheeseright, 2009).

#### 2.3.3.4 Lead Optimization

Modification of the chemical structure of the lead compounds is done to improve their pharmacological and pharmaceutical properties (Nicholls *et al.*, 2010). It involves optimization of compounds' potency, selectivity, affinity and pharmacokinetic properties such as ADMET (Absorption, Distribution, Metabolism, Excretion and Toxicology) (Theil *et al.*, 2003). This stage leads to development of chemical entities that can be considered for clinical trials.

## 2.4 Pyrimidine Biosynthetic Pathway

Pyrimidines are essential metabolites that are precursors for DNA and RNA biosynthesis (Hurt *et al.*, 2006). Pyrimidines are obtained by cells either through *de novo* synthesis or by salvaging the already synthesized pyrimidine bases which include thymine, uracil and cytosine or nucleosides which include thymidine, uridine and cytidine (Biamonte *et al.*, 2013). Whereas human cells can utilize both pathways, *Plasmodium* parasites lack the two necessary pyrimidine salvage enzymes (uridine and thymidine kinase) and therefore relies solely on the *de novo* pathway for DNA and RNA synthesis (Jana and Paliwal, 2007; Ramazani and Borna, 2011).

The pyrimidine *de novo* synthetic pathway (Figure 2.3) begins with ammonia, bicarbonate, and L-Gln. Six enzymes (bifunctional glutamine amidotransferase/ carbamoylphosphate synthetase (GAT/CPS), aspartate carbamoyltransferase (ACT), *Plasmodium falciparum* dihydroorotase (*Pf*DHOtase), *Plasmodium falciparum* (*Pf*DHODH), orotate phosphoribosyltransferase (OPRT) and orotidine 5'-monophosphate decarboxylase (OMPDC) are required by *Plasmodium* parasite to synthesize pyrimidines (Phillips and Rathod, 2010).

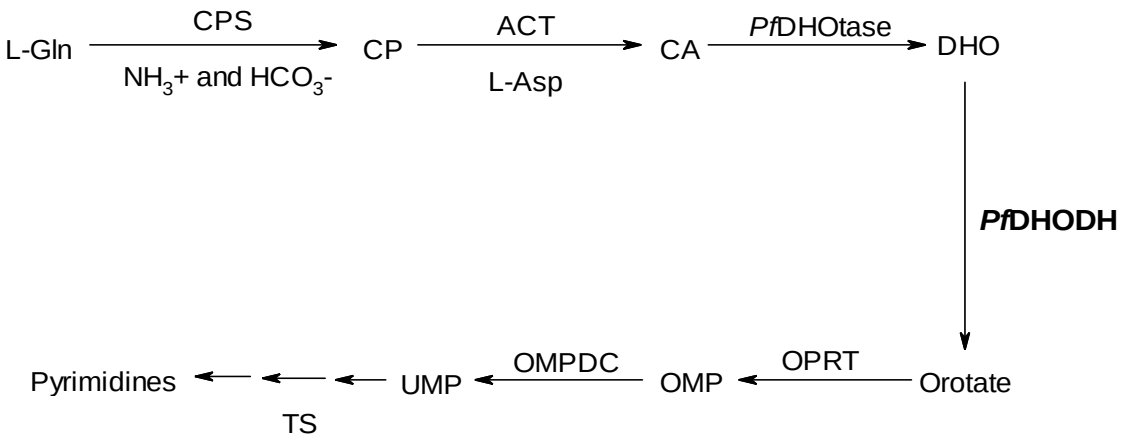


Figure 2.3: Pyrimidine biosynthetic pathway for Plasmodium parasite

Studies have shown *Pf*DHODH as an attractive new target for the development of novel anti-malarial agents (Rodrigues *et al*., 2010). This is based on the fact that the malaria parasite relies entirely on the *de novo* pathway as a source of pyrimidines as opposed to human beings who can salvage pyrimidines (Kumar Ojha *et al.,* 2012). Inhibition of *Pf*DHODH enzyme results in the shutdown of the mitochondrial electron transport chain thereby, arresting crucial metabolic pathways within the microorganism leading to the inhibition of pyrimidine biosynthesis; eventually the parasite dies (Rodrigues *et al*., 2010).

The first *de novo* design of *Pf*DHODH inhibitors showed high selective inhibition against human dihydroorotate dehydrogenase (hDHODH) over *Pf*DHODH and vise versa (Heikkilä *et al*., 2006). For instance, 2-[methyl-(4-phenylbenzoyl)amino]benzoic (**10**) acid showed 42.6±4.6 and >200(µM) against *Pf*DHODH and *h*DHODH respectively

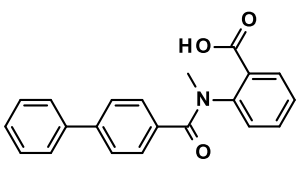


**10**

Research on *Plasmodium falciparum* dihydroorotate dehydrogenase inhibitors has provided a number of lead compounds with inhibitory concentrations whose studies are still in progress (Wadood and Ulhaq, 2013). The triazolopyrimidine scaffold has become of interest in the discovery of *Pf*DHODH lead compounds with good binding affinities and inhibitory concentrations (Deng *et al*., 2009). For example 5-methyl-7-(naphthalen-2-ylamine)-2-(trifluoromethyl)[1,2,4]triazolo[1,5-a]pyrimidine (**11)** showed strong inhibitory concentration of 0.023±0.002 µM against the chloroquine resistant $W_2$ strain of *Plasmodium falciparum* with a selectivity index of 18,478 *(Gujjar et al*., 2009;Boechat *et al*., 2012).

Structure-guided optimization of compound **11** via bioisosteric substitution led to the development of various triazolopyrimidine derivatives that are more potent against *Pf*DHODH (Coteron *et al*., 2011). Among the many triazolopyrimidine analogs discovered is DSM265 (**12**) that has shown excellent *in vivo* activity ($IC_{50}$ of 13nM) against the chloroquine resistant Dd2 strain of *Plasmodium falciparum* (Flannery *et al*., 201; Coteron *et al*., 2011). Similarity of *in vivo* activity of DSM265 (**12**) to that of chloroquine, excellent bioavailability and long half-life has made it a compound of interest and is currently at the phase one clinical studies due to its pharmacokinetic qualification (Gamo, 2014).

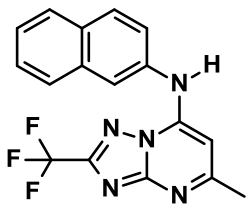

**11**

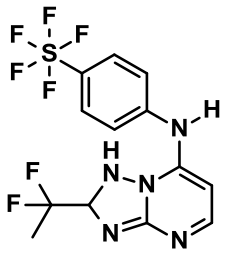

**12**

Considering the attractive selectivity observed for amides of anthranilic acid (Heikkilä *et al*., 2006) and promising potency of triazolopyrimidines (Boechat *et al*., 2012), this study intends to establish the inhibitory potential of the chromone scaffold and its derivatives against *Pf*DHODH.

## 2.5 Chromone Scaffold

The chromone scaffold (**13**) is a benzopyran derivative substituted with a keto group on a γ-pyrone ring and occurs in flavonoids (flavones, isoflavones, flavanones etc) which are ubiquitous in nature (Keri**,** *et al*., 2014).

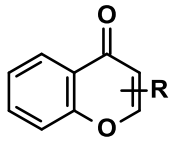


**13**

Due to their abundance in plants and their low mammalian toxicity, chromone derivatives are consumed in large amounts by humans (Patel *et al*., 2011). Numerous biologically active compounds obtained from nature (Yenesew *et al*., 2004a; Zelefack *et al*., 2012) or synthetic pathways (Auffret *et al*., 2007; Keri *et al*., 2014) contain the chromone scaffold.

The first clinically used chromone was khellin (**14**) which was extracted and isolated from the seeds of *Ammi visnaga* (Keri *et al*., 2014). It was used as a relaxing agent for visceral smooth muscle and was later found to treat bronchial asthma. Synthetic furoflavones, derivatives of khellin also showed promising gastro-protective activity (Ragab *et al*., 2007).

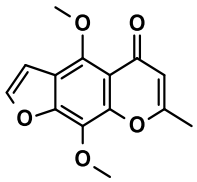

**14**

The foregoing examples illustrate the potential of the chromone scaffold and its derivatives in drug discovery and are the inspiration for establishing its antiplasmodial potential in this study.

### 2.5.1 Antiplasmodial Compounds Containing Chromone, Chromanone and Chalcone Scaffolds

#### 2.5.1.1 Natural Products

A number of natural flavonoids with chromone scaffold (e.g. flavones and isoflavones) have been found to exhibit antiplasmodial activities, 5-prenylpratensein (**15)** (Andayi et al., 2006), artocarpesin (**16**) and artochamin C (**17**) (Zelefack *et al*., 2012), Table 2.1.

Table 2.1: *In vitro* antiplasmodial activity of some chromone natural products

| **COMPOUND** | **$IC_{50}$(µM)** | |
|---|---|---|
| | **D6** | **W2** |
| 5'-Prenylpratensein (**15)** | 6.3±0.3 | 8.7±1.5 |
| Artocarpesin (**16**) | 7.4±1.2* | |
| Artochamin C (**17**) | 24.3±0.3* | |

* Antiplasmodial activity for compounds **16-17** was determined against chloroquine-resistant FcB1 CQR strain of *P. falciparum*

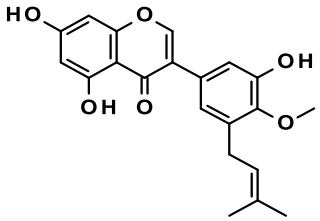

15

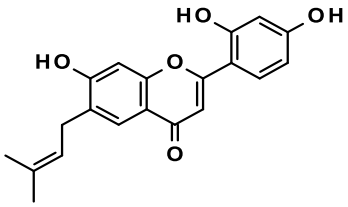

16

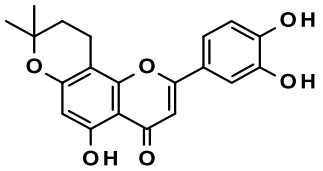

17

Flavanoids with a chromanone (e.g. flavanones) scaffold have also shown promising activity against W2 and D6 strains of *Plasmodium falciparum* (Yenesew *et al*., 2004; Zakaria, *et al.*, 2012), Table 2.2.

Table 2.2: *In vitro* antiplasmodial activity of some chromanones (flavanones) isolated from nature

| **COMPOUND** | **Source** | **$IC_{50}$(µM)** | | **Reference** |
|---|---|---|---|---|
| | | **D6** | **W2** | |
| Abyssinone IV (**18**) | *Erythrina abyssinica* | 5.4±1.5 | 5.9±1.8 | Yenesew *et al*., 2004 |
| Abyssinone V (**19**) | | 2.4±0.2 | 3.6±0.2 | |
| Sigmoidin A (**20**) | | 5.8±0.6 | 5.9±1.1 | |
| Abyssinone V-4'-methyl ether (**21**) | | 11.3±2.1 | 11.1±2.4 | |
| 6-Farnesyl-3′,4′,5,7-tetrahydroxyflavanone (**22**) | *Macaranga triloba* | 0.06* | | Zakaria, *et al.*, 2012 |
| Nymphaeol B (**23**) | | 4.02±0.9* | | |
| Nymphaeol C (**24**) | | 2.04±0.6* | | |

* Antiplasmodial activity for compounds **22-24** was determined against 3D7 CQS strain of *P. falciparum*

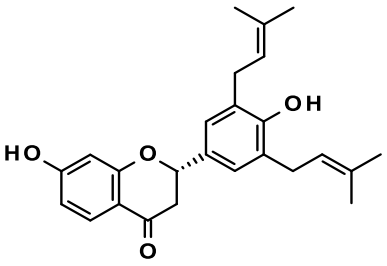

18

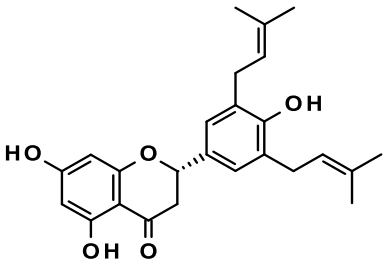

19

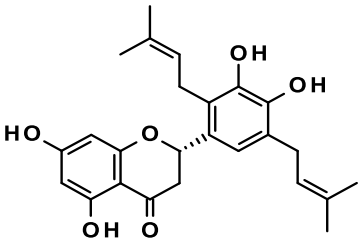

20

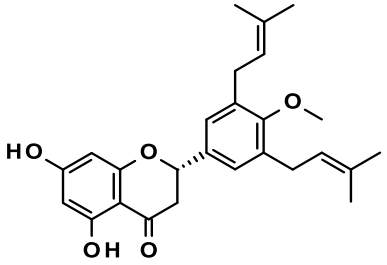

21

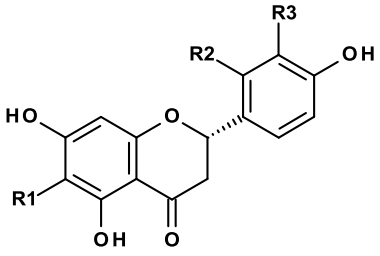

| | $R_1$ | $R_2$ | $R_3$ |
|---|---|---|---|
| **22** | 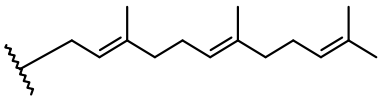 | H | OH |
| **23** | H | 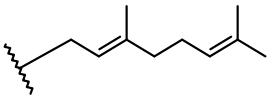 | OH |
| **24** | 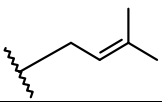 | 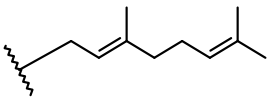 | OH |

Chalcones, which are biosynthetic precursors of flavones, isoflavones and flavanones, have been reported to possess antiplasmodial activity (Ziegler et al., 2004; Yenesew *et al*., 2004), Table 2.3.

Table 2.3: *In vitro* antiplasmodial activity of some chalcones isolated from nature

| **COMPOUND** | **Source** | **$IC_{50}$(µM)** | | **Reference** |
|---|---|---|---|---|
| | | **D6** | **W2** | |
| Licochalcone A (**25**) | *Glycyrrhiza glabra* | 5.97±0.57* | | Ziegler *et al*., 2004 |
| 5-Prenylbutein (**26**) | *Erythrina abyssinica* | 10.3 ±1.3 | 11.2±1.9 | Yenesew *et al*., 2004 |
| Licoagrochalcone A (**27**) | | 12.7±3.2 | 12.0±2.6 | |
| Homobutein (**28**) | | 15.0±2.8 | 16.1±2.1 | |

* Antiplasmodial activity for compounds **35** was determined against 3D7 CQS strain of *P. falciparum*

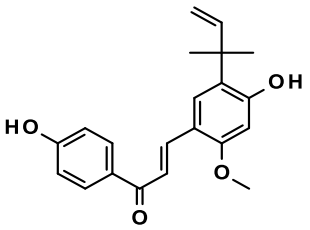


**25**

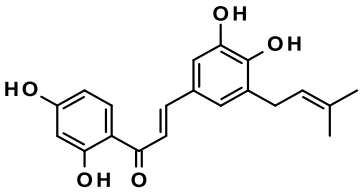


**26**

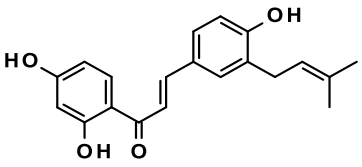


**27**

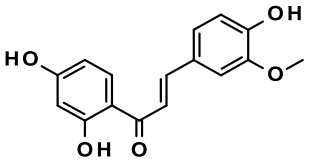


**28**

### 2.5.1.2 Synthetic Chromone-Based Compounds

Promising antiplasmodial activity of synthetic chromones has been observed in both *In vitro* and *in vivo* bioassays (Keri *et al.*, 2014). *In vitro* antiplasmodial activity of

chromone-based compounds against the D6 *strain of Plasmodium falciparum* is summarized in Table 2.4. Compound **29** showed an *in-vivo* percentage inhibition of 27.1 ± 9.0 hence a potential antiplasmodial compound (Auffret *et al*., 2007).

Table 2.4: *In vitro* antiplasmodial activity of synthetic chromone-based compounds

| **Entry** | **Name** | **$IC_{50}$ (µM)** |
|---|---|---|
| **29** | Ethyl 2-[5-[5-hydroxy-4-oxo-7-[2-oxo-2-[4-[(2,3,4-trimethoxyphenyl)methyl]piperazin-1-yl]ethoxy]chromen-2-yl]-2-methoxy-phenoxy]acetate | 0.5 |
| **30** | Ethyl 2-[5-[7-[2-[4-[(2,3-dimethoxyphenyl)methyl]piperazin-1-yl]-2-oxo-ethoxy]-5-hydroxy-4-oxo-chromen-2-yl]-2-methoxy-phenoxy]acetate | 2.4 |
| **31** | Ethyl 2-[5-[5-hydroxy-4-oxo-7-[2-oxo-2-[4-[(3,4,5-trimethoxyphenyl)methyl]piperazin-1-yl]ethoxy]chromen-2-yl]-2-methoxy-phenoxy]acetate | 4.0 |
| **32** | Ethyl 2-[5-[7-[2-[4-[(3,4-dimethoxyphenyl)methyl]piperazin-1-yl]-2-oxo-ethoxy]-5-hydroxy-4-oxo-chromen-2-yl]-2-methoxy-phenoxy]acetate | 4.7 |
| **33** | Ethyl 2-[5-[7-[2-[4-[(4-chlorophenyl)methyl]piperazin-1-yl]-2-oxo-ethoxy]-5-hydroxy-4-oxo-chromen-2-yl]-2-methoxy-phenoxy]acetate | 6.0 |
| **34** | Ethyl 2-[5-[7-[2-(4-benzylpiperazin-1-yl)-2-oxo-ethoxy]-5-hydroxy-4-oxo-chromen-2-yl]-2-methoxy-phenoxy]acetate | 9.5 |

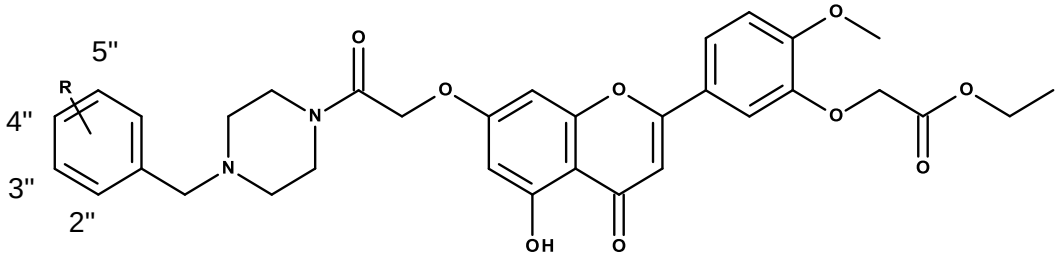


Synthetic chalcones which are intermediates in chromones and chromanones synthesis have shown potential activity against *Plasmodium falciparum* , Table 2.5 (Frölich, *et al*., 2005).

Table 2.5: Antiplasmodial activity of synthetic chalcones

| Compound | $IC_{50}$(µM) | |
|---|---|---|
| | poW | Dd2(µM) |
| **35** | 8.2±0.3 | 24.0±0.8 |
| **36** | 12.9±0.6 | 17±0.6 |
| **37** | 16±0.9 | 10.7±0.3 |

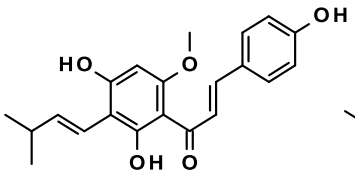


**35**

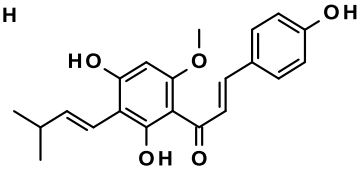


**36**

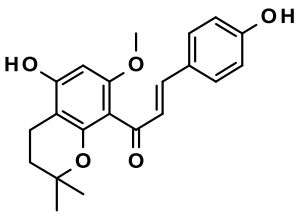


**37**

## 2.6 Synthetic Strategies for Chromones and Chromanones

The various synthetic strategies for chromones use phenols as a common starting material. Subjecting these phenols such as resorcinol to Friedel craft acylation using acetic acid results in the formation of hydroxyacetophenone (Shaibaldain, 2012), Scheme 2.1. The Lewis acids used as catalyst include $ZnCl_2$, $Al_2Cl_3$, $BF_3.Et_2O$, etc. The formation of the hydroxyacetophenone proceeds via *O*-acylation to form an ester, followed by Fries rearrangement under high temperature in presence of a Lewis acid (Shaibaldain, 2012).

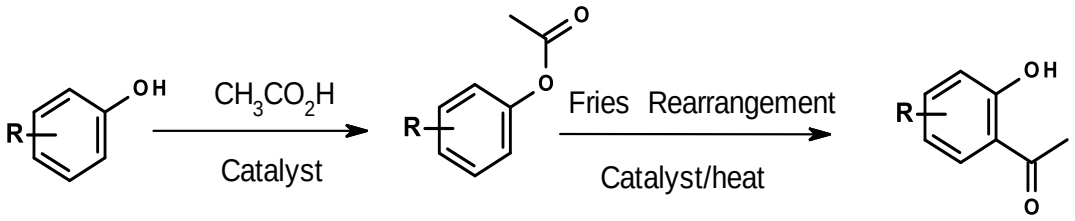


Scheme 2.1: Friedel Craft acylation of phenols

### 2.6.1 Kostanecki-Robinson Strategy

This strategy involves the *O*-acylation of 2-hydroxyacetophenone using aromatic acid anhydride in presence of the corresponding sodium salt (Bird and Cheeseman, 1973). Aromatic acid anhydride are used to avoid the formation of a mixture of chromones and coumarins (Bird and Cheeseman, 1973). The *O*-acylation is followed by base catalyzed Baker-Venkataraman rearrangement and cyclodehydration in presence of an acid, Scheme 2.2.

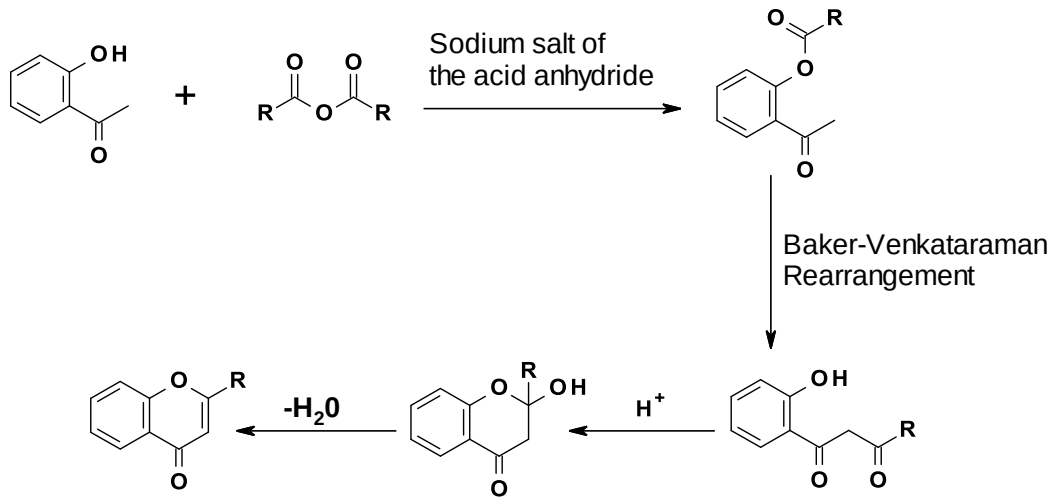


Scheme 2.2: Kostanecki-Robinson strategy

### 2.6.2 Synthesis of Chromones and Chromanones via Chalcone Intermediates

The synthesis of chromones via chalcones involves Aldol condensation of a substituted or non-substituted acetophenone and aldehydes. The Aldol condensation

can be a base or acid catalysed. The most common method is the base catalysed Claisen-Schmidt condensation which uses NaOH or KOH in ethanol or methanol (Masesane and Mazimba, 2014; Cabrera *et al.*, 2007). Other base catalysts include $Ca(OH)_2$ in ethanol (Kulkarni, *et al*., 2013). Solvent free base catalyzed Claisen-Schmidt condensation have been reported to be more effective (Rahman et al., 2012)

Acid catalyzed Aldol condensation whereby silica-supported sulphuric acid is used is also documented (Sultan *et al*., 2013). Other catalysts that have been used include boron triflouride etherate ($BF_3.Et_2O$) (Balsera *et al.*, 2014) and $ZnCl_2$ under microwave irradiation (Reddy, *et al.*, 2001).

The chalcone formed is cyclized to form either a chromone or a chromanone under various conditions. Whereas oxidative cyclization of chalcones using iodine in dimethyl sulphoxide provides chromones (Ghodile *et al*., 2012), cyclization using Algar-Flynn-Oyamada method with alkaline hydrogen peroxide as a catalyst provides 3-hydroxychromones, Scheme 2.3 (Venkatachalam, *et al.*, 2012). However, cyclization in presence of an acid such as oxalic acid yields chromanones (Zambare *et al.*, 2009). In this study, the strategy to synthesize chromones and chromanones was based on the approach via chalcone intermediates.

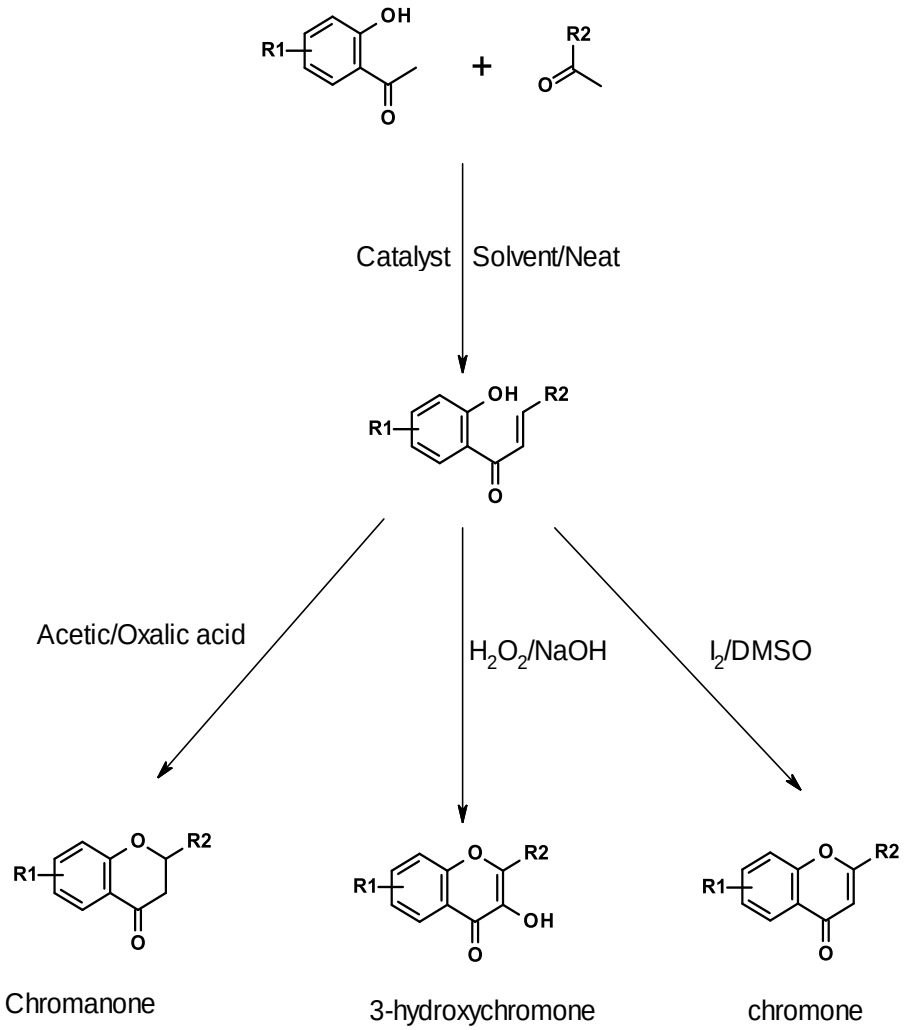


Scheme 2.3: Synthesis of chromones and chromanone via chalcone intermediate

# CHAPTER THREE

# MATERIALS AND METHODS

## 3.1 Database Construction

In this study, a web based *in silico* database of natural products of Kenya was constructed. To generate this web based database, information on natural products were collected from different sources and processed.

### 3.1.1 Data Collection

Information about compounds that have been isolated from natural products of Kenya was collected from various journal articles, review papers, theses, books of abstracts and conference proceedings. The information that was captured was the structure of the compounds, common names, classes of the compounds and biological activities (if available). It also included the plant species, family, parts of the plant where the compounds were extracted, places of collection of the plant and the reference of the source material.

### 3.1.2 Data Processing

The data collected from the various sources was then captured in a Microsoft Excel spreadsheet. Accelrys Draw 4.1 SP1 software- academic version was used to draw the 2D chemical structures of the natural products collected from literature.

The *mol2nam*, a command line utility of *Lexichem* program (OpenEye Scientific Software), was used to generate the IUPAC names of the compounds and to convert the 2D structures into SMILES files (1D format). *Omegsa2,* a command line utility of *Omega* program (OpenEye Scientific Software), was used to convert the 2D to 3D structures and generate the physicochemical properties of the compounds: polar

surface area (PSA), molecular weight (MW), Merck molecular force field energy (MMFF), partition coefficient (log P), rotatable bonds, heavy atoms, hydrogen acceptors and hydrogen donors of the compounds. The data was visualized with VIDA program (OpenEye Scientific Software) and exported into initial MS excel spreadsheet. The data in the MS excel spreadsheet was then transferred into the Discovery Studio 4.1visualizer, a product of Accelrys, where it was organized and a sdf file was generated.

### 3.1.3 Generation of the Web-Based Database of Natural Products of Kenya

Linux computer operating system was used in the generation of the web-based database of natural products from Kenya. The sdf file was exported into the local host database that was then transferred into the web based MySQL relational database using command line. The Information was stored in the MySQL database in normalized tables where each compound was given a unique identification code. The creation of the database search engine was adapted from Nobert Heider's MolDBR6 (Haider, 2010) software package based on the framework summarized in Figure 3.1. The software utilizes the *checkmol* and *matchmo*l search engines (Haider, 2010). Javascript editor JSME and Java molecule editor (JME) by Peter Etrl of Novartis (Bienfait and Ertl, 2013) were used to enable users to search for compounds using structures. The search engine utilizes hypertext preprocessor (PHP) scripts and structured query language (SQL) to achieve its basic utility. The web-based database generated is hosted at the http://m*itishamba*.uonbi.ac.ke

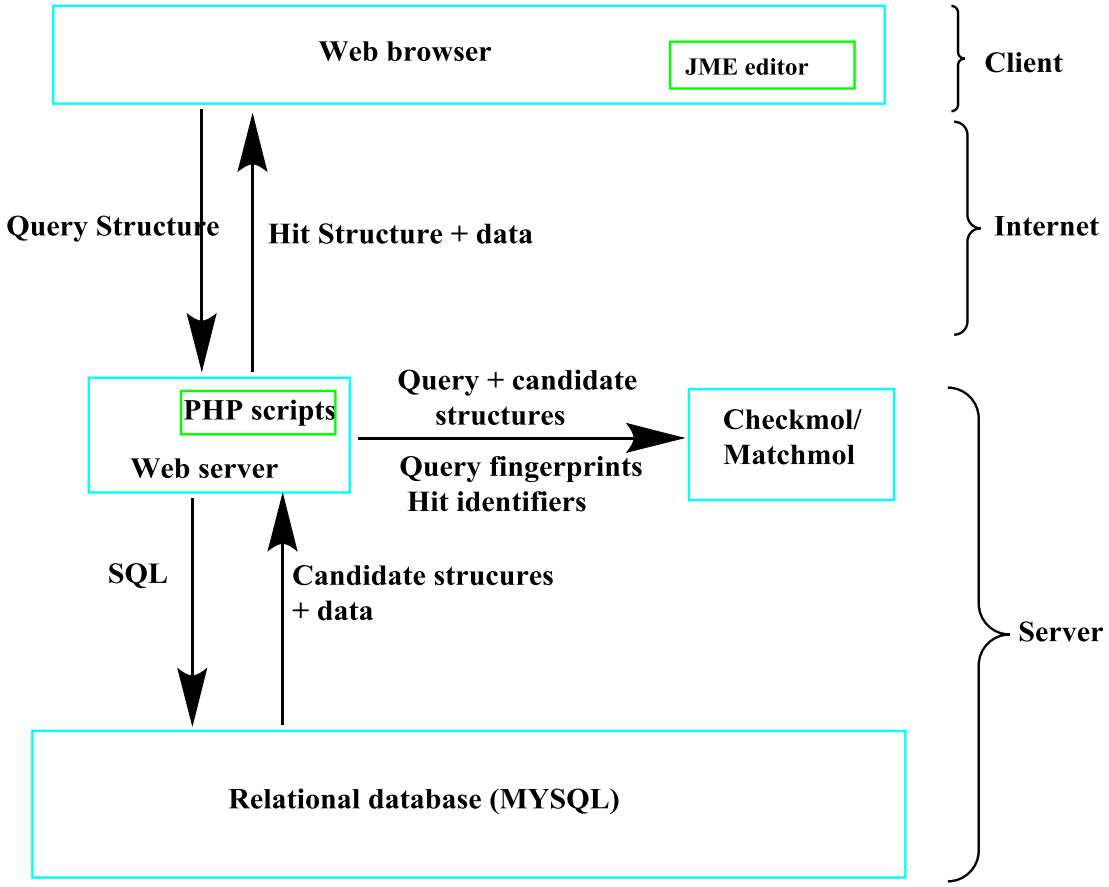


Figure 3.1: Architecture of *mitishamba* database search engine adapted from MOLDBR6

## 3.2 Preparation of the Ligands and the Receptor

The ligands and the receptor were prepared for use in virtual screening process.

### 3.2.1 Preparation of the Ligands

The *mitishamba* database was queried separately for the chromanone, chromone and chalcone ligands and the sdf file of the three hits were downloaded from http://m*itishamba*.uonbi.ac.ke. The three sdf files were combined and filtered using *filter* program (OpenEye Scientific Software). The filter parameters used were based on the Lipinski rule of five (molecular weight<500, hydrogen bond donors<5, hydrogen bond acceptors<10 and Log P<5) (Lipinski *et al.*, 2012). The output was then saved as a zipped file (.oeb.gz).

*Omega2* (OpenEye Scientific Software) was then used to generate 3D conformers of the filtered compounds using default parameters except for number of conformers (maxconfs=10) and stereochemistry (strict stereo=false). The output was saved as a zipped file (.oeb.gz) and visualized using *Vida* (OpenEye Scientific Software).

### 3.2.2 Receptor Preparation

The 1TV5 PDB structure of the *Plasmodium falciparum* dihydroorotate dehydrogenase (*Pf*DHODH) co-crystallised with **A77 1726 (38)** ligand, Figure 3.2, was obtained from the RCSB protein data bank at http://www.rcsb.org/pdb/explore.do?structureId=1tv5. The *Make Receptor* program (OpenEye Scientific Software) was used to define the active binding pocket of the target by selecting the ligand of interest **A77 1726** (**38)** bound to the 1TV5 PDB structure. This was followed by creation of a box that encloses the active site. Then the active site shape potential was created to define the outer and inner contours.

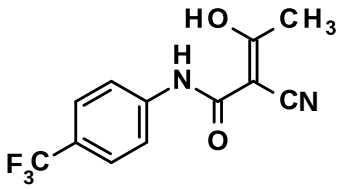


**38**

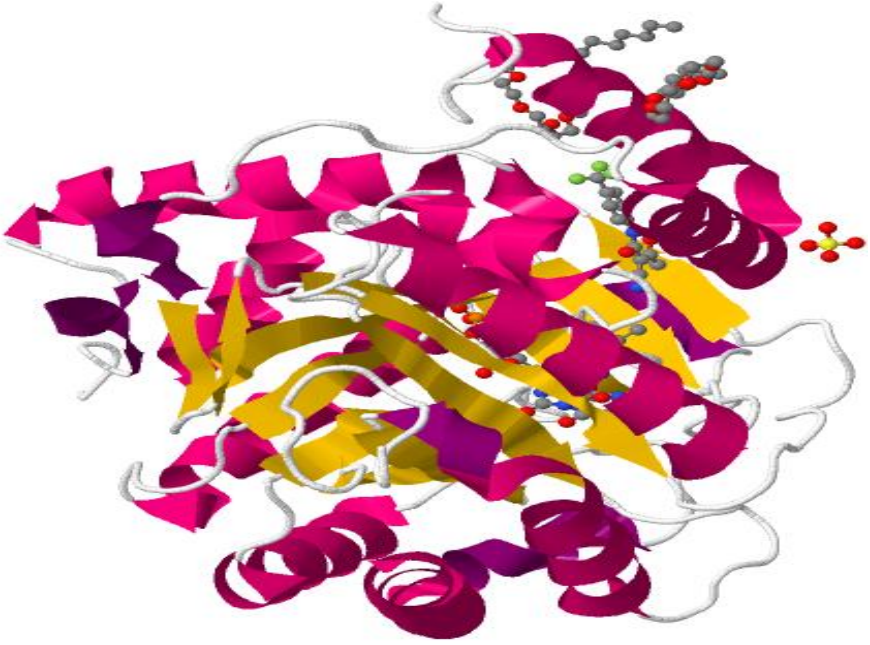

Figure 3.2: 3D Structure of *Pf*DHODH with Bound Ligands

### 3.3 Virtual Screening

The prepared ligands were then subjected to structure based virtual screening against the prepared receptor and ligand based virtual screening with the aim of identifying promising antiplasmodial lead compounds.

#### 3.3.1 Structure-Based Virtual Screening

*Fred* (OEDocking | OpenEye Scientific Software) was used to carry out docking studies against the prepared *Pf*DHODH receptor where the specified binding site contained the inhibitor (**38**). A docking study was done using the command line utility where the inputs were the zipped files of the ligands and the prepared *Pf*DHODH receptor while the output was a zipped file of the docked poses, which were viewed using *Vida* (OpenEye Scientific Software) visualizing program. The zipped file of the docked poses and the receptor were then used to generate a pdf document summarizing ligand receptor interactions.

### 3.3.2 Ligand-Based Virtual Screening

For ligand based virtual screening, shape and electrostatics similarity search was carried out using the validated query.

#### 3.3.2.1 Query Validation

The inhibitor (**38**) bound to 1TV5 *Pf*DHODH receptor was chosen as the query molecule for use in shape and electrostatics similarity. In order to determine whether the chosen query was suitable for similarity search, query validation run was done using *vROCS* program (OpenEye Scientific Software). The decoys and actives were obtained from the Database of Useful Decoys-Enhanced (DUD-E) http://dude.docking.org/target/pyrd. The databases of decoys and actives in the validation run helps in establishing whether the query chosen will differentiate between the already known active and inactive (decoys) molecules against the target protein.

Receiver operating characteristic curve (ROC curve) together with its area under the curve (AUC) and the early enrichment values are the statistical metrics generated by the *vROCS* program (OpenEye Scientific Software) that were used to validate the query (**38**).The validated query (**38**) was then used in ligand based virtual screening of the chromones, chromanones and chalcones to carry out shape matching and electrostatic similarity search.

#### 3.3.2.2 Shape Similarity Search

Using the validated query (**38)** shape similarity search was performed using *vROCS* (OpenEye Scientific Software). The 3D conformers of the ligands, as generated by *Omega* program, were overlaid on the query using the *vROCS* program which employs the Gaussian shape overlap to score the ligands. The ligands are scored based

on shape (Shape Tanimoto score) and color (Color Tanimoto score) and ranked based on Tanimoto Combo score (shape and color).

#### 3.3.2.3 Electrostatics Similarity Search

Using the validated query (**38**), electrostatics similarity studies on 3D conformers of the ligands was done using *EON* (OpenEye Scientific Software). *EON* aligns molecules on the query and calculates the electrostatics potential making use of the Poisson-Boltzmann and Coulombic electrostatics tools. The molecules are scored in terms of Poisson-Boltzmann electrostatics tanimoto (ET_pb), Coulombic electrostatics tanimoto (ET_pb) and *EON* shape tanimoto (*EON*_shape_tani). The ligands were then ranked using electrostatics tanimoto combo (ET_combo) which is a combination of *EON* shape tanimoto and Poisson-Boltzmann electrostatics tanimoto (ET_pb).

The ranking of ligands based on structure and ligand based virtual screening guided the identification of synthetically accessible chromones and chromanones that were targeted for synthesis.

## 3.4 Synthesis of Chromanones and Chromones

The approach for the synthesis of chromanone and chromone based lead compounds was based on retrosynthetic Scheme 3.1 below.

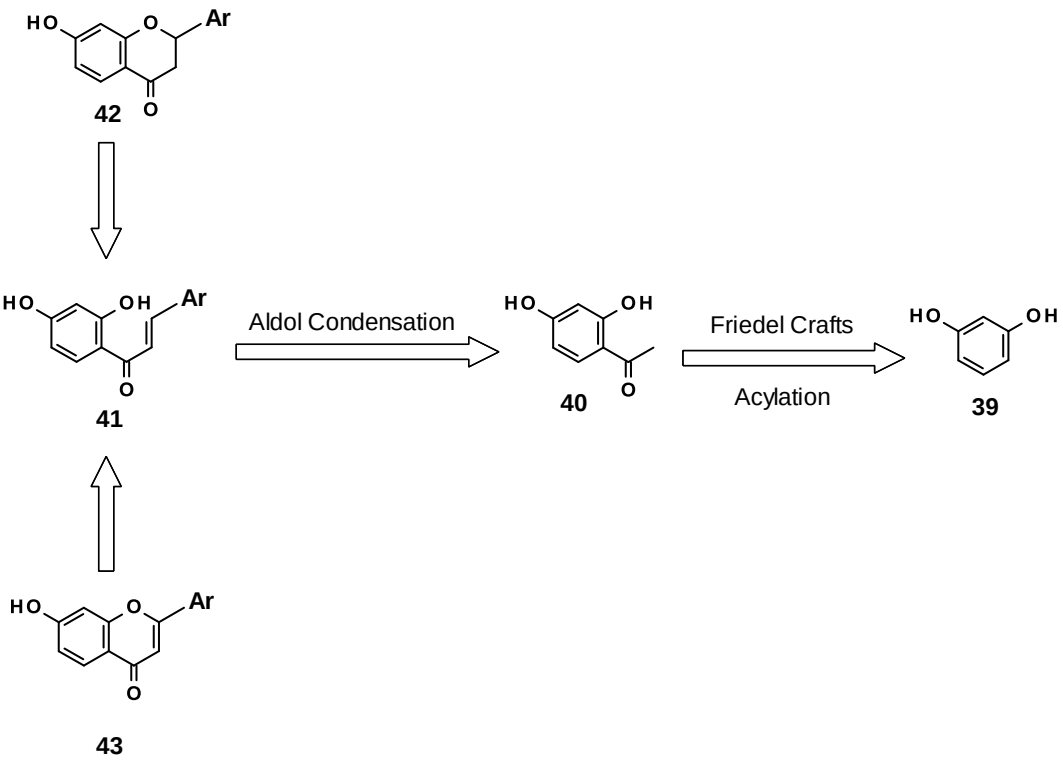


Scheme 3.1: Retrosynthetic pathway to chromanones and chromones

### 3.4.1 General Procedure

Chemicals used in the synthesis were purchased from LOBA Chemie Laboratory reagents and fine chemicals. The purchased chemicals were of synthetic grade and therefore did not need any purification. The solvents used in column and thin layer chromatography were distilled before use. The $^{1}H$ NMR spectra were obtained at 600 and 500 MHz with TMS as an internal standard and deuterated dichloromethane and acetone as the solvents. Reactions were monitored on analytical TLC silica gel plates with fluorescent indicator 254 nm. Purification was done using column chromatography on silica gel 60-120. Purification through recrystallization was done using methanol.

### 3.4.2 Procedure for Synthesis of 2,4–Dihydroxyacetophenone (40)

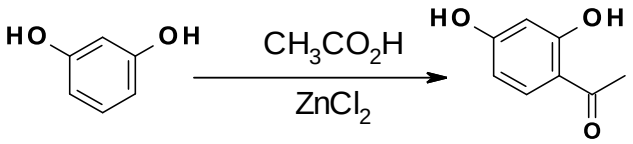


**39** **40**

Anhydrous $ZnCl_2$ (15 g, 110 mmols) was added to acetic acid (30 mL) and refluxed at 150 °C. When all the $ZnCl_2$ was almost dissolved, resorcinol (**39**) (10 g, 90 mmols) was added while stirring and refluxed for 3 hours. Then 50% HCl (50 mL) was added to break the $ZnCl_2$ complex. A bright yellow precipitate formed as the mixture cooled to room temperature. This was further cooled in an ice bath and filtered. The residue was washed with 5% HCl and recrystallised using 20% HCl (Patil *et al*., 2012). Compound **40** was obtained as a yellow crystalline solid (4.6 g, 50%), mp 146 °C: $^{1}$H NMR (600 MHz, Acetone-$d_6$) δ 12.77 (*s*, 1H), 9.48 (*s*, 1H), 7.79 (*d*, *J* = 8.40 Hz, 1H, C-6), 6.45 (*dd*, *J* = 2.40Hz, 8.40Hz, 1H, C-5), 6.34 (*d*, *J* = 2.40 Hz, 1H, C-3), 2.57 (*s*, 3H, $OCH_3$). $^{13}$C NMR (151 MHz, Acetone-$d_6$) δ 202.8(C=O), 164.9(C-4), 164.5(C-2), 133.5(C-1), 113.4(C-6), 107.7(C-5), 102.4(C-3), 25.5 ($CH_3$).

### 3.4.3 Procedure for Synthesis of 2',4'-Dihydroxy-4-methoxychalcone (45 )

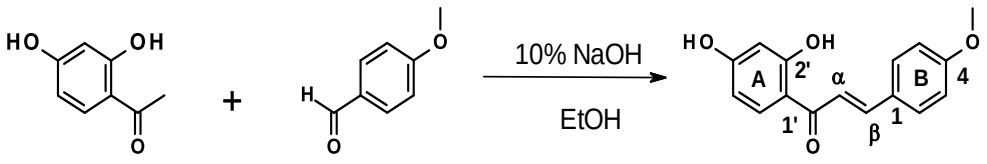


**40** **44** **45**

10% NaOH (20 mL) and 99% ethanol (30 mL) were mixed in a round bottomed flask and cooled in an ice bath for 10 minutes. 4-Methoxybenzaldehyde (6 g, 44 mmols)

was added while stirring then 2, 4-dihydroxyacetophenone (3 g, 20 mmols) was added dropwise. The reaction mixture was left stirring and monitored using TLC until all the 2,4-dihydroxyacetophenone was consumed, this took approximately 48 hours. The reaction mixture was poured over cold water and acidified using 20% HCl. Sodium bicarbonate was added while shaking until there were no bubbles observed to remove the 4-methoxybenzoic acid. It was then transferred into a separatory funnel and extracted three times using ethyl acetate (20 mL). The organic layer was dried using anhydrous $Na_2SO_4$, filtered and concentrated under reduced pressure to provide a yellow precipitate which was purified using column chromatography (5% ethyl acetate in hexane) and recrystallization (methanol). Compound **45** was obtained as a yellow solid (1.6 g, 30 %), mp 186 °C: $^1$H NMR (600 MHz, Acetone-$d_6$) δ 13.64 (*s*, 1H, chelated hydroxyl), 8.16 (*d*, *J* = 8.8 Hz, 1H, C-6'), 7.86 (*m*, 4H, C-2, C-3, β-C and (α-C), 7.05 (*d*, 2H, C-3 and C-5), 6.50 (*dd*, *J* = 8.8, 2.2 Hz, 1H, C-5'), 6.40 (*d*, *J* = 2.2 Hz, 1H, C-3'), 3.89 (*s*, 3H, $OCH_3$), $^{13}$C NMR (150 MHz, Acetone-$d_6$) δ 191.9(C=O), 166.7(C-4'), 164.7 (C-2'), 162.0(C-4), 143.9(β-C), 132.5(C-1'), 130.7(C-2), 130.7(C-6), 128.0(C-1), 118.2(α-C), 114.4(C-3), 114.4(C-5), 113.6(C-6'), 107.8(C-5'), 102.8(C-3'), 54.9($CH_3$).

### 3.4.4 Procedure for Synthesis of 2', 4'-Dihydroxy-4-chlorochalcone (47)

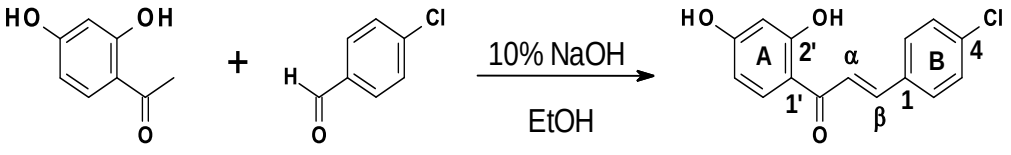


**40** **46** **47**

10% NaOH (10 mL) and 95% EtOH (10 mL) were mixed in a flask and cooled in an ice bath for 10 minutes. 4-Chlorobenzaldehyde (6 g, 43 mmols) was added into the

flask while stirring, and then 2'4-dihydroxyacetophenone (20 mmols) was added dropwise and stirred for 30 minutes. The reaction mixture was heated under reflux at 70 $^{0}$C and monitored using TLC until all the 2'4'-dihydroxyacetophenone was consumed, this took 48 hours. The reaction mixture was poured over cold water and acidified using 20% HCl. Sodium bicarbonate was added while shaking until there were no bubbles observed to remove 4-chlorobenzoic acid. It was then transferred into a separatory funnel and extracted three times using ethyl acetate (20mL). The organic layer was dried using anhydrous $Na_2SO_4$, filtered and concentrated under reduced pressure to provide a yellow precipitate which was purified using column chromatography (5% ethyl acetate in hexane) and recrystallization (methanol). Light yellow crystals (0.84 g, 16%) were obtained: $^{1}$H NMR (500 MHz, Acetone-$d_6$) δ 13.44 (*s*, 1H, chelated hydroxyl), 8.18 (*d*, *J* = 8.9 Hz, 1H, C-6'), 8.00 (*d*, *J* = 15.5 Hz, 1H, $H_\beta$), 7.91 (*d*, *J* = 8.4 Hz, 2H, C-2 and C-6), 7.86 (*d*, *J* = 15.5 Hz, 1H, $H_\alpha$), 7.52 (*d*, *J* = 8.5 Hz, 2H, C-3 and C-5), 6.50 (*dd*, *J* = 8.9, 2.4 Hz, 1H, C-5'), 6.40 (*d*, *J* = 2.4 Hz, 1H, C-3'). $^{13}$C NMR (126 MHz, Acetone-$d_6$) δ 191.7(C=O), 166.8(C-4'), 165.1(C-2'), 142.3(C-β), 135.8(C-4), 133.9(C-1), 132.8(C-6'), 130.3(C-2), 130.3(C-6), 129.0(C-3), 129.0(C-5), 121.6(C-α), 113.6(C-1'), 108.1(C-5'), 102.9(C-3').

### 3.4.5 Procedure for Synthesis of 7-Hydroxy-2-(4-methoxyphenyl)chroman-4-one (48)

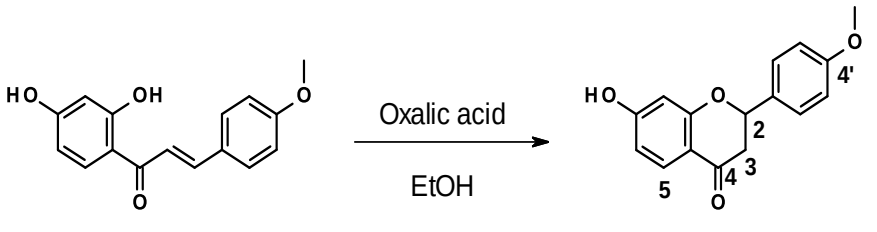


**45** **48**

Oxalic acid (1 g, 7.9 mmols) and 2',4'-dihydroxy-4-methoxychalcone (0.1 g, 0.37 mmols) were dissolved in ethanol (10 mL). The reaction mixture was heated at 80 $^{0}$C for 2 days. It was cooled to room temperature and poured over cold water and extracted three times with ethyl acetate (20 mL). The organic extract was dried using anhydrous $Na_2SO_4$ and concentrated under reduced pressure then purification was done using column chromatography (5% ethyl acetate in hexane) and recrystallization (methanol). A yellow crystalline solid (29 mg, 29%) was obtained: $^{1}$H NMR (600 MHz, $CD_2Cl_2$) δ 7.85 (*d*, *J* = 8.8 Hz, 2H, C-2' and C-6'), 7.44 (*d*, *J* = 8.6 Hz, 1H, C-5), 6.99 (*d*, *J* = 8.8 Hz, 2H, C-3' and C-5'), 6.59 (*dd*, *J* = 8.6, 2.3 Hz, 1H, C-6), 6.49 (*d*, *J* = 2.3 Hz, 1H, C-8), 5.46 (dd, J=2.4, 13.2Hz, 1H, H-2), 3.86 (*s*, 3H, $OCH_3$), 3.09 (*dd*, *J* = 13.2 , 16.8 Hz, 1H, H-$3_{eq}$), 2.81 (*dd*, *J*= 2.4, 16.8 Hz, 1H, H-$_{3ax}$). $^{13}$C NMR (151 MHz, $CD_2Cl_2$) δ 190.5(C=O), 163.6(C-7), 162.7(C-4'), 160.0(C-9), 130.9(C-5), 129.1(C-1'), 127.8(C-2'), 127.8(C-6'), 115.1(C-10), 114.0(C-3'), 114.0(C-5'), 110.3(C-6), 103.2(C-8), 79.7(C-2), 55.3($OCH_3$), 44.0(C-3).

### 3.5 *In vitro* Antiplasmodial Bioassay

*In vitro* antiplasmodial bioassay of compound **45**, **47** and **48** against chloroquine resistant K1 and chloroquine sensitive 3D7 strains of *Plasmodium falciparum* was done using non-radioactive assay technique (Heydenreich et al., 2011). This technique uses the fluorochrome referred to as SYBR Green I, which is a non-radioactive DNA dye that accurately depicts *In vitro* parasite replication. The parasites were cultured to attain 3-8% parasitemia. At the same time two-fold serial dilution of chloroquine (1.953–1000 ng/mL), mefloquine (0.488–250 ng/mL) and test samples (97.7–50,000 ng/mL) were prepared on a 96 well plate. The culture-adapted *P. falciparum* were reconstituted to 1% parasitemia and added onto the plate containing dose range of the

reference drugs and test samples and incubated in gas mixture (5% $CO_2$, 5% $O_2$, and 90% $N_2$) at 37 $^0$C. The assay was stopped after 72 hours by freezing at -80 $^0$C for 24 hours.

Thawing was done followed by direct addition of the lysis buffer containing SYBR Green I (1×final concentration) into the plates and mixing gently using the Beckman Coulter Biomek 2000 automated laboratory workstation. Incubation of the plates was done for 5-15 minutes at room temperature in the dark. Parasite growth inhibition was quantified by measuring the per-well relative fluorescence units (RFU) of SYBR Green 1 dye using the Tecan Genios Plus (Tecan US, Inc., Durham, NC) with excitation and emission wavelengths of 485 nm and 535 nm, respectively, and with the gain set at 60. Differential counts of relative fluorescence units (RFUs) were used in calculating 50% inhibition concentrations ($IC_{50}$'s) for each drug using Prism 4.0 windows software (Graphpad Software, San Diego, CA). A minimum of three separate determinations was carried out for each sample. Replicates had narrow data ranges hence presented as mean ±SD.

# CHAPTER FOUR

# RESULTS AND DISCUSSION

## 4.1 Outline

In this study, a web-based database of natural products of Kenya was developed which was subjected to virtual screening to identify synthetically accessible chromones and chromanones for antiplasmodial assay.

## 4.2 Database Construction

A web-based *in silico* database containing 1112 natural products of Kenya was constructed from data on natural products collected from theses, journal articles, books of abstracts and conference proceedings. The information that was captured was the structure of the compounds (2D sketch files), common names, classes of the compounds and biological activities (if available). It also included the plant species, family, parts of the plant where the compounds were extracted, places of collection of the plant and the reference of the source material.

In addition, the database contains physicochemical properties (polar surface area (PSA), molecular weight (MW), Merck molecular force field energy (MMFF), partition coefficient (log P), rotatable bonds, heavy atoms, hydrogen acceptors and hydrogen donors) of the compounds. The database is named *mitishamba* (a Kiswahili word meaning medicinal herbs) and is hosted at http:/m*itishamba*.uonbi.ac.ke.

### 4.2.1 Features of the *Mitishamba* Web Based Database

The *mitishamba* web based database has features for search (text, structure and advanced search), browsing and downloading the entire database and submitting structures as shown in Figure 4.1.


Figure 4.1: Home page of the *Mitishamba* Database

#### 4.2.1.1 Search Options

The database has three search options: Text, structure and advanced search. In text search, users can search for structures using either trivial names or IUPAC names. For structure search, the database uses Peter Etrl Novartis (Haider, 2010) Javascript molecule editor (JSME) or Java molecule editor (JME) for 2D structure input. The

options are detected automatically on the users' browser and one is used as a fallback incase either Javascript or Java feature is turned off. Optional parameters available for structure search include exact match, substructure similarity search and a ratio similarity on the scale of zero to hundred percent. Once an output is obtained, structures can be downloaded. The advanced search features allow users to search for compounds based on plant family and species.

#### 4.2.1.2 Browse and Download Options

Users can also browse the structures in the entire database. Each structure can either be downloaded individually as a mol file or alternatively, users can download the entire database in sdf, mol, smiles or oeb formats.

#### 4.2.1.3 Submitting Structures

Users can submit their work on natural products of Kenya that has not been captured in the database. In order to submit structure users upload a PDF document that contains the names of the natural products, family and botanical name of the source plant, place of collection of the plant, biological activities of the compounds and appropriately referenced source of the publication.

## 4.3 Virtual Screening Studies

A search in the *mitishamba* database identified a total of 157 chromone, chromanone and chalcone ligands. The ligands were then subjected to structure and ligand-based virtual screening.

### 4.3.1 Ligand and Receptor Preparation

The 157 ligands were filtered using *filter* program based on the Lipinski's rule of five (molecular weight<500, hydrogen bond donors<5, hydrogen bond acceptors<10 and Log P<5) (Lipinski *et al*., 2012) and this yielded 103 ligands. The 3D conformers of

the 103 ligands were then generated using *omega* program for use in both structure and ligand-based virtual screening.

The PDB file of 1TV5 *Pf*DHODH receptor with the bound ligand (**38**) was obtained from RCSB protein data bank at http://www.rcsb.org/pdb/explore.do?structureId=1tv5 and prepared using *Make Receptor* program, Figure 4.2.

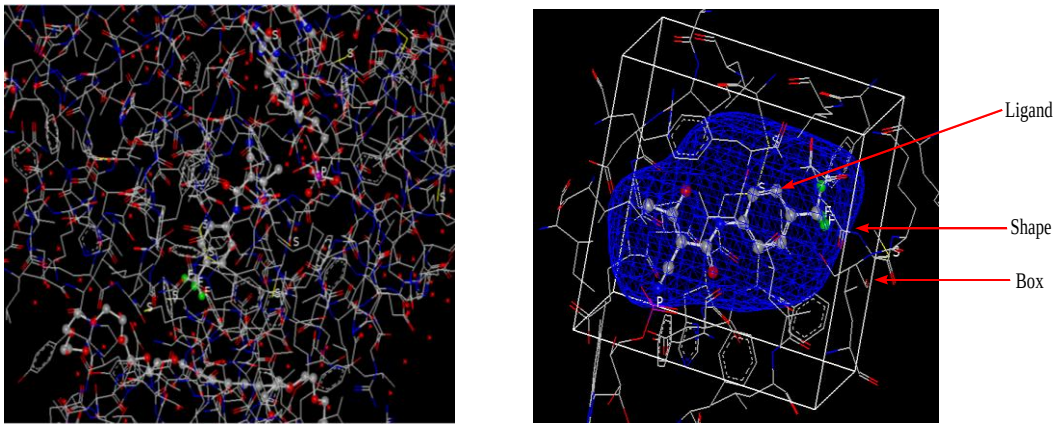


a B

Figure 4.2: (a) 1TV5 PDB file (b) prepared 1TV5 Receptor showing the box enclosing the active site, the defined shape of the active site and the bound ligand.

### 4.3.2 Structure Based Virtual Screening Studies

Docking studies of the filtered ligands against the prepared *Pf*DHODH receptor using *Fred* program ranked the molecules using chemgausse4 docking scores (Kcal/mol). To ease the interpretation of the docking scores (raw data), z-scores were generated (Swann *et al*., 2011). Among the 103 ligands, the ligands with z-score of one and above were 25, Table 4.1. The best scoring ligands were chromones followed by chromanones and chalcones.

Table 4.1: Docking and z-scores of ligands

| Smiles of Compounds | Class of ligand | Docking score (Kcal/mol) | Z-score |
|---|---|---|---|
| COc1c(=O)c2c(cc(cc2oc1c3ccc(c(c3)O)O)O)[O-] | chromone | -14.8608 | 2 |
| COc1cc(c2c(c1)OC(CC2=O)c3ccccc3)[O-] | chromanone | -14.5211 | 2 |
| COc1cc(c2c(c1)OC(CC2=O)c3ccccc3)[O-] | chromone | -14.5211 | 2 |
| c1cc(ccc1c2cc(=O)c3c(cc(cc3o2)O)[O-])O | chromone | -14.5133 | 2 |
| COc1cc(c2c(=O)cc(oc2c1)c3ccc(cc3)O)[O-] | chromone | -14.3959 | 2 |
| COc1c(=O)c2c(cc(cc2oc1c3ccc(cc3)O)O)[O-] | chromone | -14.1036 | 1 |
| c1ccc(cc1)c2cc(=O)c3c(cc(cc3o2)O)[O-] | chromanone | -13.9018 | 1 |
| COc1cc(c2c(c1)OC(CC2=O)c3ccc(cc3)O)[O-] | chromone | -13.8635 | 1 |
| COc1cc(c2c(c1)OC(CC2=O)c3ccc(cc3)O)[O-] | chromone | -13.8635 | 1 |
| c1cc(c(cc1c2c(c(=O)c3c(cc(cc3o2)O)[O-])[O-])O)O | chromone | -13.8531 | 1 |
| c1cc(c(cc1c2c(c(=O)c3c(cc(cc3o2)O)[O-])[O-])O)O | chromone | -13.8531 | 1 |
| c1cc(c(cc1c2cc(=O)c3c(cc(cc3o2)O)[O-])O)O | chromone | -13.8232 | 1 |
| c1cc(ccc1c2c(c(=O)c3c(cc(cc3o2)O)[O-])[O-])O | chromone | -13.7642 | 1 |
| c1c(cc(c(c1O)O)O)c2c(c(=O)c3c(cc(cc3o2)O)[O-])[O-] | chromone | -13.7514 | 1 |
| COc1ccc(c(c1)O)C(=O)C=Cc2ccccc2 | chalcone | -13.6169 | 1 |
| c1ccc(cc1)C2CC(=O)c3c(cc(cc3O2)O)[O-] | chromanone | -13.5869 | 1 |
| COc1cc(cc(c1C(=O)C=Cc2ccccc2)O)O | chalcone | -13.55 | 1 |
| COc1cc(c2c(c1)oc(c(c2=O)OC)c3ccc(cc3)O)[O-] | chromone | -13.5402 | 1 |
| COc1cc(c(c2c1c(=O)cc(o2)c3ccccc3)OC)O | chromone | -13.4887 | 1 |
| COc1cc2c(c(c1OC)[O-])C(=O)CC(O2)c3ccc(cc3)O | chromanone | -13.4786 | 1 |
| COc1cc(c(c(c1)O)C(=O)C=Cc2ccccc2)O | chalcone | -13.4599 | 1 |
| COc1ccc(cc1)c2c(c(=O)c3c(cc(cc3o2)O)[O-])OC | chromone | -13.4357 | 1 |
| COc1c(cc2c(c1[O-])c(=O)c(c(o2)c3ccc(cc3)O)[O-])O | chromone | -13.3051 | 1 |
| c1ccc(cc1)c2cc(=O)c3ccc4c(c3o2)cco4 | chromone | -13.2924 | 1 |
| COc1ccc(cc1)c2cc(=O)c3c(cc(cc3o2)O)[O-] | chromone | -13.2169 | 1 |

The interaction of the ligands with *Pf*DHODH receptor was studied and compared to the binding interaction of the inhibitor (**38**). The inhibitor (**38**) bound to the 1TV5 *Pf*DHODH receptor shows hydrogen bonding interactions with three amino acid residues, ARG 265A, HIS 185A and TRY 528A , Figure 4.3 (Hurt *et al*., 2006).

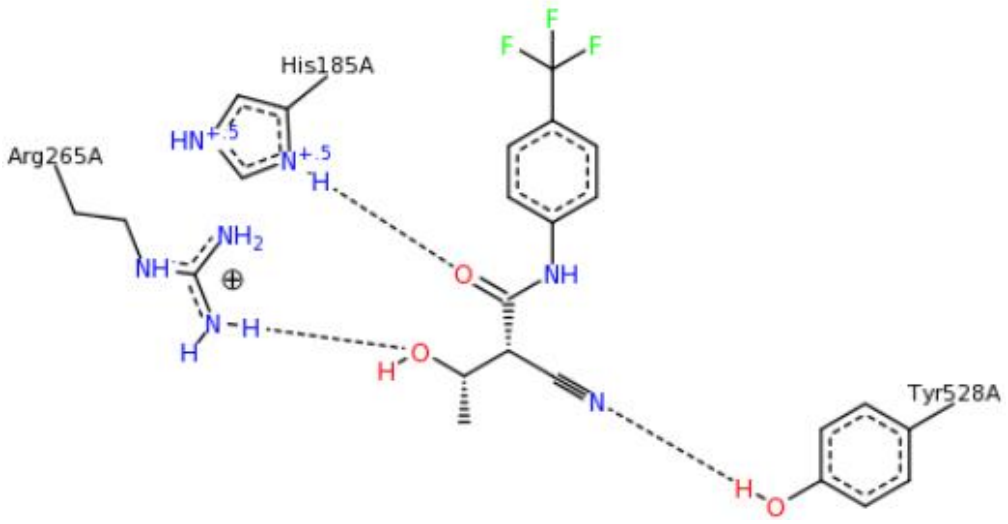


Figure 4.3: Hydrogen bonding interactions of the bound inhibitor (**38**) with amino acid residues of *Pf*DHODH

Comparing the interaction of inhibitor (**38**) with those of the ligands, as expected most of the ligands had at least one interaction with the three amino acid residues, Figure 4.4. Some ligands had additional interactions, for example Figure 4.5 shows interactions with TRY 168A and MET 536A while Figure 4.6 shows interactions with GLY 181A. Other ligands showed further interactions with LEU 531, VAL 532A, LEU 172A and CYS 184.

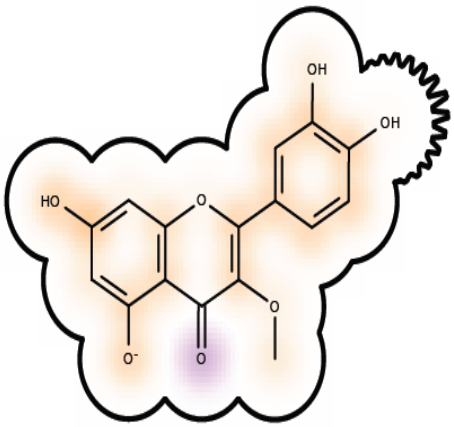

Residue Fingerprint

| | | |
|---|---|---|
| ARG265A | ASN534A | ASP180A |
| ASP186A | CYS175A | CYS184A |
| FMN1002A | GLU182A | GLY181A |
| GLY535A | HIS185A | ILE179A |
| ILE183A | ILE263A | ILE272A |
| LEU172A | LEU176A | LEU187A |
| LEU189A | LEU191A | LEU240A |
| LEU531A | LYS173A | LYS537A |
| MET536A | PHE171A | PHE174A |
| PHE188A | PHE227A | PHE264A |
| PHE533A | TYR168A | TYR528A |
| VAL532A | | |

A B

Figure 4.4: (a) ligand (b) amino acid residues that interracted (blue are donors)

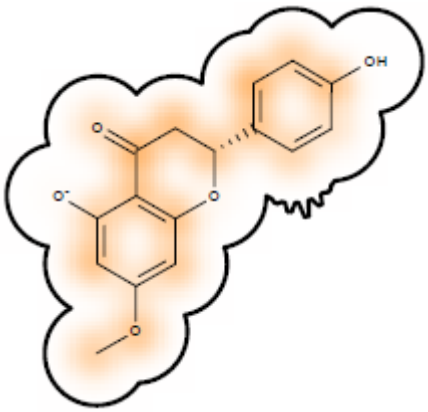


Residue Fingerprint

| | | |
|---|---|---|
| ARG265A | ASN534A | ASP180A |
| ASP186A | CYS175A | CYS184A |
| FMN1002A | GLU182A | GLY181A |
| GLY535A | HIS185A | ILE179A |
| ILE183A | ILE263A | ILE272A |
| LEU172A | LEU176A | LEU187A |
| LEU189A | LEU191A | LEU240A |
| LEU531A | LYS173A | LYS537A |
| MET536A | PHE171A | PHE174A |
| PHE188A | PHE227A | PHE264A |
| PHE533A | TYR168A | TYR528A |
| VAL532A | | |

A B

Figure 4.5: (a) ligand (b) amino acid residues that interacted (blue are donors, red are acceptors)

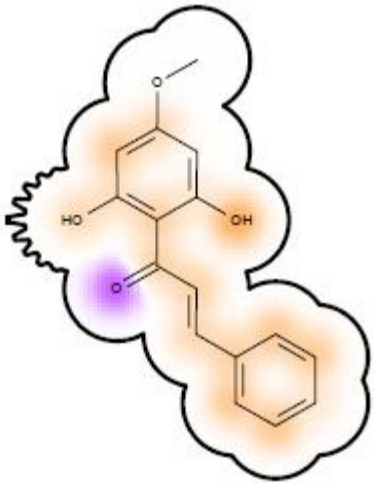


Residue Fingerprint

| | | |
|---|---|---|
| ARG265A | ASN534A | ASP180A |
| ASP186A | CYS175A | CYS184A |
| FMN1002A | GLU182A | GLY181A |
| GLY535A | HIS185A | ILE179A |
| ILE183A | ILE263A | ILE272A |
| LEU172A | LEU176A | LEU187A |
| LEU189A | LEU191A | LEU240A |
| LEU531A | LYS173A | LYS537A |
| MET536A | PHE171A | PHE174A |
| PHE188A | PHE227A | PHE264A |
| PHE533A | TYR168A | TYR528A |
| VAL532A | | |

A B

Figure 4.6: (a) ligand (b) amino acid residues that interacted (blue are donors, red are acceptors and black is by contact)

### 4.3.3 Ligand Based Virtual Screening Studies

The shape and electrostatics of the 103 ligands was compared against a validated query of the inhibitor (**38**).

#### 4.3.3.1 Query Validation

The 3D structure of the 1TV5 *Pf*DHODH inhibitor (**38**), Figure 4.7, was used as the query molecule for shape and electrostatic similarity. In order to determine whether query **38** is valid for shape and electrostatic similarity studies, *vROCs* tanimoto combo scores (combination of shape and color scores) for the actives and decoys were

used to plot ROC curve (Figure 4.8). In the ROCs curve Y-axis is the fraction of actives found and X-axis is the fraction of decoys found.

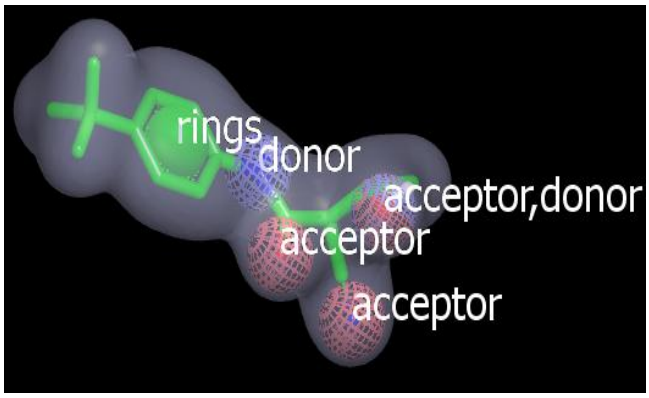


Figure 4.7: 3D structure of the query molecule (**38**) showing shape contour and color and shape atoms.

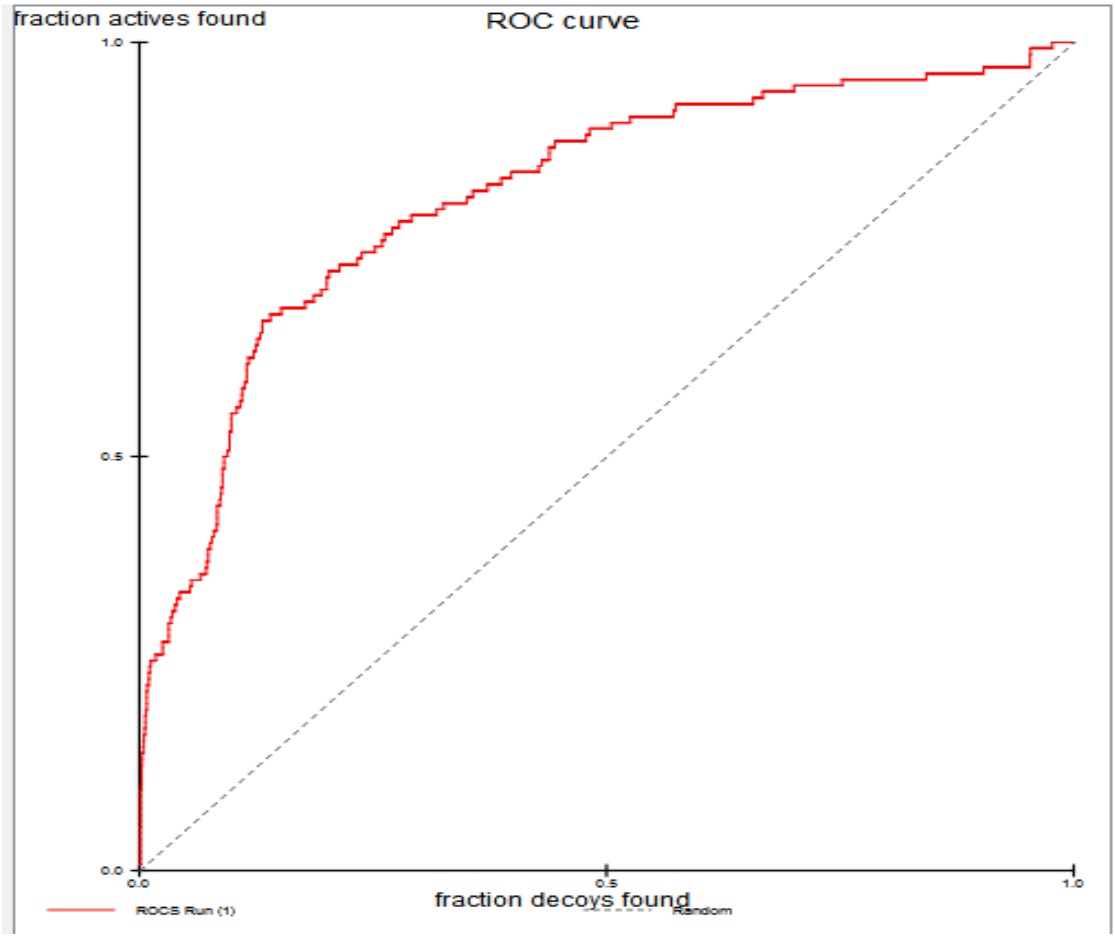


Figure 4.8: ROC curve for the query

The statistical metrics derived from the ROC curve for query validation run is summarized in Table 4.2

Table 4.2: Query validation run statistical metrics

| Statistical Metrics | Values |
|---|---|
| AUC | 0.813 |
| 0.5% enrichment | 31.399 |
| 1.0% enrichment | 22.320 |
| 2.0% enrichment | 12.589 |

The area under the curve (AUC) is the probability that a randomly chosen active has a higher score than a randomly chosen inactive. A highly selective query has 0.8<AUC<1.0 (Jain and Nicholls, 2008). Since the AUC for query **38** is 0.813, the query is highly selective. Table 4.2 indicates that the early enrichment values decrease with increase in the percentage of the decoys. Early enrichment values refer to the fractions of the actives at the particular percentage of the decoys (Senger *et al*., 2003). Therefore, the AUC and early enrichment values indicate that query **38** is selective hence suitable and valid for use in both shape and electrostatics similarity studies.

#### 4.3.3.2 Shape and Electrostatics Similarity Studies

Shape similarity search was done on the 3D conformers of the 103 ligands so as to compare the shape of these ligands to the shape of the validated query. The ligands were ranked based on Tanimoto combo scores and the results are summarized in Table 4.3. Similarly electrostatic similarity comparison between the validated query and the 3D conformers of the 103 ligands were done and ranked using electrostatic tanimoto score (ET score), Table 4.3.

The *ROCS* Tanimoto combo scores and the *EON* electrostatic tanimoto scores were combined into total tanimoto score. The total tanimoto score were then used to calculate z scores which were used to identify the top 29 ligands, Table 4.3. Just as in structure based virtual screening studies (Table 4.1), ligands-based virtual screening identified chromones to be the most virtually active, followed by chromanones and chalcones.

Table 4.3: Ligand-based virtual screening results

| Smiles of Compounds | Tanimoto combo | ET combo | Total | Z-score |
|---|---|---|---|---|
| c1cc(c(cc1c2c(c(=O)c3ccc(cc3o2)O)[O-])O)O | 0.955 | 0.754 | 1.709 | 2 |
| c1cc(c(cc1c2c(c(=O)c3c(cc(cc3o2)O)[O-])[O-])O)O | 0.941 | 0.754 | 1.695 | 2 |
| c1cc(c(cc1c2cc(=O)c3c(cc(cc3o2)O)[O-])O)O | 0.942 | 0.741 | 1.683 | 2 |
| COc1ccc(cc1O)[C@H]2[C@@H](C(=O)c3c(cc(cc3O2)OC)[O-])O | 0.946 | 0.706 | 1.652 | 2 |
| COc1ccc(cc1)c2cc(=O)c3c(cc(cc3o2)O)[O-] | 0.888 | 0.755 | 1.643 | 2 |
| COc1ccc(cc1O)c2c(c(=O)c3c(o2)cc(c(c3[O-])O)O)[O-] | 0.922 | 0.706 | 1.628 | 2 |
| COc1cc(c2c(=O)cc(oc2c1)c3ccc(c(c3)OC)O)[O-] | 0.903 | 0.711 | 1.614 | 1 |
| COc1ccc(cc1)c2cc(=O)c3c(cc(cc3o2)OC)[O-] | 0.875 | 0.732 | 1.607 | 1 |
| COc1c(=O)c2c(cc(cc2oc1c3ccc(c(c3)O)O)O)[O-] | 0.897 | 0.707 | 1.604 | 1 |
| COc1cc(c2c(c1)oc(c(c2=O)[O-])c3ccc(c(c3)OC)O)[O-] | 0.889 | 0.71 | 1.599 | 1 |
| COc1ccc(cc1O)c2c(c(=O)c3c(cc(cc3o2)OC)[O-])OC | 0.92 | 0.674 | 1.594 | 1 |
| c1c(cc(c(c1O)O)O)c2c(c(=O)c3c(cc(cc3o2)O)[O-])[O-] | 0.893 | 0.698 | 1.591 | 1 |
| c1cc(ccc1c2cc(=O)c3c(cc(cc3o2)O)[O-])O | 0.854 | 0.73 | 1.584 | 1 |
| CC1(C=Cc2cc(cc(c2O1)O)[C@@H]3CC(=O)c4c(cc(cc4O3)O)[O-])C | 0.836 | 0.732 | 1.568 | 1 |
| COc1ccc(cc1OC)c2c(c(=O)c3c(cc(cc3o2)OC)[O-])OC | 0.873 | 0.681 | 1.554 | 1 |
| COc1cc(c2c(=O)cc(oc2c1)c3ccc(cc3)O)[O-] | 0.839 | 0.707 | 1.546 | 1 |
| COc1ccc(cc1)[C@H]2CC(=O)c3c(ccc(c3O2)OC)[O-] | 0.844 | 0.698 | 1.542 | 1 |
| COc1cc(ccc1O)c2c(c(=O)c3c(cc(c(c3o2)OC)O)[O-])[O-] | 0.842 | 0.685 | 1.527 | 1 |
| c1ccc(cc1)c2cc(=O)c3c(cc(cc3o2)O)[O-] | 0.83 | 0.686 | 1.516 | 1 |
| COc1ccc(cc1)c2c(c(=O)c3c(cc(cc3o2)O)[O-])OC | 0.819 | 0.696 | 1.515 | 1 |
| COc1cc2c(c(c1OC)[O-])C(=O)C[C@@H](O2)c3ccc(cc3)O | 0.79 | 0.723 | 1.513 | 1 |
| COc1cc(c2c(c1)O[C@H](CC2=O)c3ccc(cc3)O)[ | 0.839 | 0.666 | 1.505 | 1 |

| Smiles of Compounds | Tanimoto combo | ET combo | Total | Z-score |
|---|---|---|---|---|
| c1cc(c(cc1c2c(c(=O)c3ccc(cc3o2)O)[O-])O)O | 0.955 | 0.754 | 1.709 | 2 |
| c1cc(c(cc1c2c(c(=O)c3c(cc(cc3o2)O)[O-])[O-])O)O | 0.941 | 0.754 | 1.695 | 2 |
| c1cc(c(cc1c2cc(=O)c3c(cc(cc3o2)O)[O-])O)O | 0.942 | 0.741 | 1.683 | 2 |
| COc1ccc(cc1O)[C@H]2[C@@H](C(=O)c3c(cc(cc3O2)OC)[O-])O | 0.946 | 0.706 | 1.652 | 2 |
| COc1ccc(cc1)c2cc(=O)c3c(cc(cc3o2)O)[O-] | 0.888 | 0.755 | 1.643 | 2 |
| COc1ccc(cc1O)c2c(c(=O)c3c(o2)cc(c(c3[O-])O)O)[O-] | 0.922 | 0.706 | 1.628 | 2 |
| COc1cc(c2c(=O)cc(oc2c1)c3ccc(c(c3)OC)O)[O-] | 0.903 | 0.711 | 1.614 | 1 |
| COc1ccc(cc1)c2cc(=O)c3c(cc(cc3o2)OC)[O-] | 0.875 | 0.732 | 1.607 | 1 |
| COc1c(=O)c2c(cc(cc2oc1c3ccc(c(c3)O)O)O)[O-] | 0.897 | 0.707 | 1.604 | 1 |
| COc1cc(c2c(c1)oc(c(c2=O)[O-])c3ccc(c(c3)OC)O)[O-] | 0.889 | 0.71 | 1.599 | 1 |
| COc1ccc(cc1O)c2c(c(=O)c3c(cc(cc3o2)OC)[O-])OC | 0.92 | 0.674 | 1.594 | 1 |
| O-] | | | | |
| COc1cc2c(c(c1OC)[O-])c(=O)c(c(o2)c3ccc(c(c3)O)O)OC | 0.849 | 0.656 | 1.505 | 1 |
| CC(=CCc1cc(ccc1O)[C@@H]2CC(=O)c3ccc(cc3O2)O)C | 0.849 | 0.653 | 1.502 | 1 |
| COc1ccc(cc1)c2c(c(=O)c3c(cc(cc3o2)OC)[O-])OC | 0.816 | 0.684 | 1.5 | 1 |
| c1cc(ccc1c2c(c(=O)c3c(cc(cc3o2)O)[O-])[O-])O | 0.812 | 0.68 | 1.492 | 1 |
| COc1cc(c(c(c1O)OC)OC)c2cc(=O)c3c(cc(cc3o2)O)[O-] | 0.819 | 0.663 | 1.482 | 1 |
| CC(=CCc1cc(ccc1O)/C=C/C(=O)c2ccc(cc2O)O)C | 0.857 | 0.619 | 1.476 | 1 |
| COc1ccc(cc1)c2c(c(=O)c3c(cc(cc3o2)OC)[O-])[O-] | 0.81 | 0.658 | 1.468 | 1 |

### 4.4 Selection of Compounds for Synthesis

Generally both structure and ligand based virtual screening studies identified chromones (flavones) as the best inhibitors of *Pf*DHODH followed by chromanones (flavanones) and chalcones. Although the specific ranking order varies, the general trend remains the same. The ranking of ligands based on structure and ligand based virtual screening guided the identification of synthetically accessible chromones and chromanones that were targeted for synthesis.

### 4.4.1 Synthesis of Chromanones and Chromones

The approach for the synthesis of chromanone and chromone based lead compounds was based on retrosynthetic Scheme 4.1. The starting material for the synthesis was resorcinol (**39**), which was acylated then subjected to Aldol condensation and cyclization to access the target chromanones (**42**) and chromones (**43**).

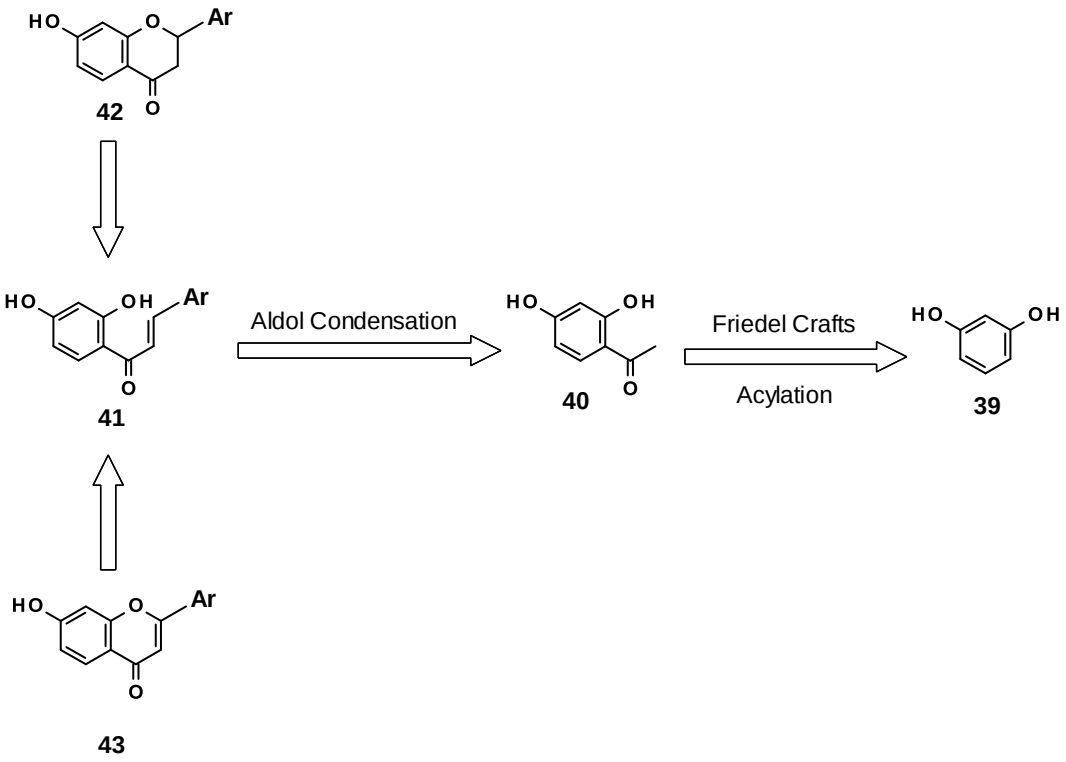


Scheme 4.1: Retrosynthetic pathway for chromanones and chromones

#### 4.4.1.1 Synthesis of 2,4–Dihydroxyacetophenone (40)

2,4-Dihydroxyacetophenone (**40**) was synthesized through Friedel Craft acylation of resorcinol (**39**) using acetic acid in presence of $ZnCl_2$ as the Lewis acid (Scheme 4.2) (Patil *et al*., 2012).

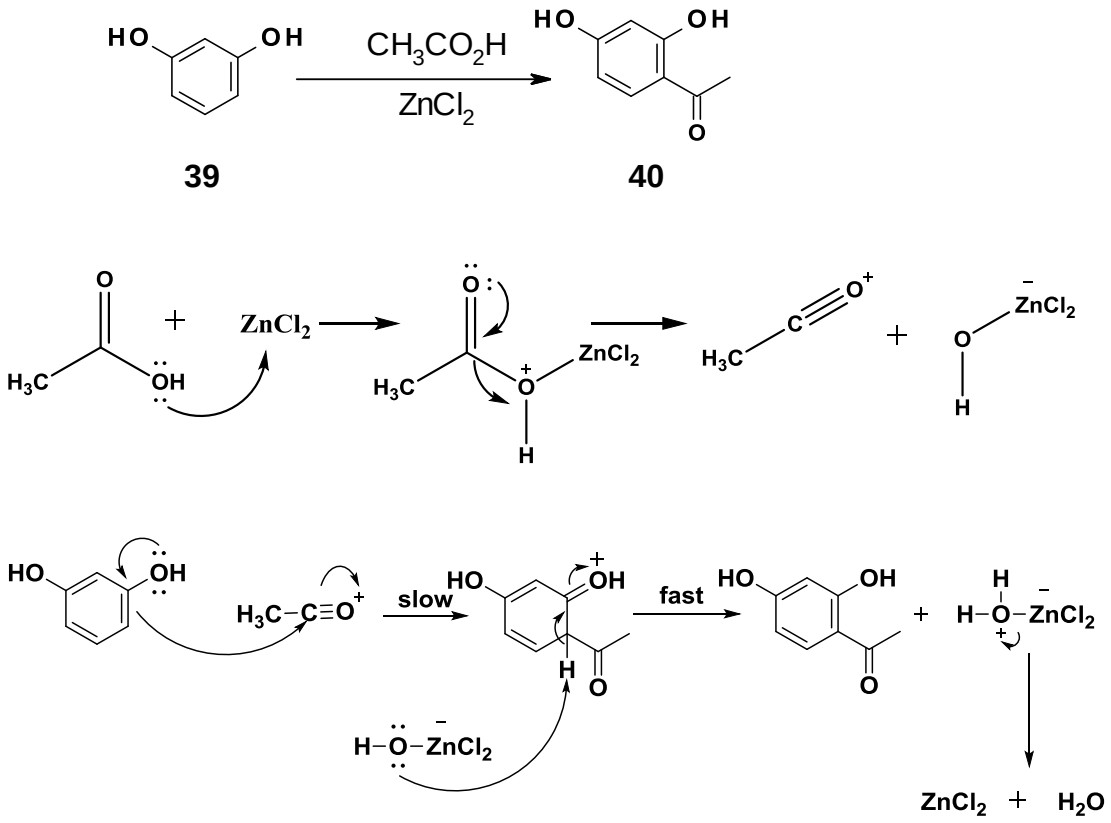


Scheme 4.2: Mechanism of acylation

The product was obtained as a yellow crystalline solid with 50% yield. The structure of the product was determined using $^{1}H$ and $^{13}C$ NMR. The $^{1}H$ NMR signals of an acetoxy methyl at δ 2.57 (*s*, 3H), a chelated hydroxyl (δ 12.77 (*s*, 1H)), a hydroxyl (δ 9.48 (*s*, 1H)) and three mutually coupled aromatic protons at δ 7.79 (*d*, *J* = 8.40 Hz, 1H), 6.45 (*dd*, *J* = 2.40, 8.80Hz, 1H), 6.34 (*d*, *J* = 2.40 Hz, 1H) are consistent with literature (Patil *et al*., 2012). The $^{13}C$ NMR signals at δ 202.8(C=O), 164.9(C-4), 164.5(C-2) 133.5(C-1), 113.4(C-6), 107.7(C-5), 102.4(C-3), 25.5($CH_3$) are also consistent with literature (Patil *et al*., 2012).

#### 4.4.1.2 Synthesis of 2',4'-Dihydroxy-4-methoxychalcone (45)

2',4'-Dihydroxy-4-methoxychalcone (**45**) was synthesized through base-catalyzed Aldol condensation of 2,4-dihydroxyacetophenone (**40**) and 4-methoxybenzaldeyde (**44**)

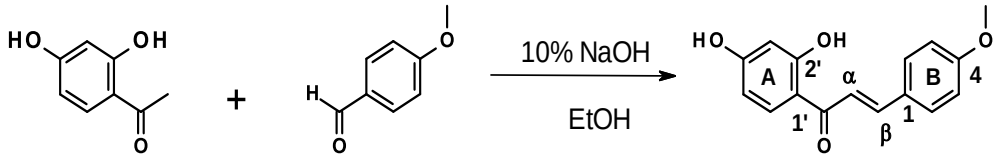


**40** **44** **45**

The product was obtained as yellow crystals in 30% yield. Formation of 2',4'-dihydroxy-4-methoxychalcone (**45)** was found to be slow (48 hrs) which could be attributed to the presence of two hydroxyl groups on the acetophenone (**40**). Under basic conditions, the phenolic protons are picked thus increasing the electron density in the system and reducing the electrophilicity of the carbonyl group, thereby lowering the acidity of the methyl hydrogens (Scheme 4.3).

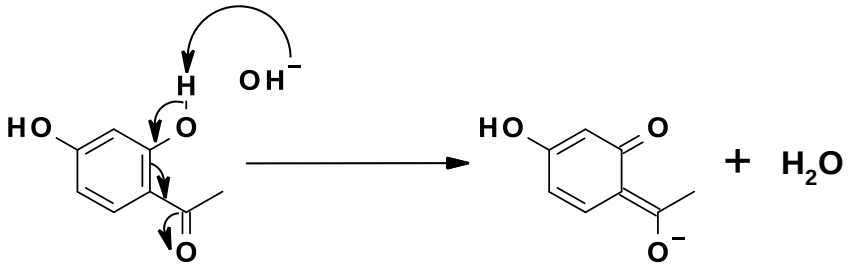


Scheme 4.3: Mechanism of de-protonation of phenolic protons

The $^{1}H$ NMR signals for compound **45** were similar to those of compound **40** except for the incorporation of a methoxy δ 3.89 (*s*, 3H, $OCH_3$). In the $^{13}C$ NMR the signal for the carbonyl is more shielded (δ 191.9) compared to the starting material (δ 202.8)

consistent with an α,β-unsaturated carbonyl system (118.2(α-C) and 143.9(β-C)) as would be expected from an Aldol condensation product.

#### 4.4.1.3 Synthesis of 2',4'-Dihydroxy-4-chlorochalcone (47)

2',4'-Dihydroxy-4-chlorochalcone (**47**) was synthesized through base-catalyzed Aldol condensation of 2,4-dihydroxyacetophenone (**40**) and 4-chlorobenzaldeyde (**46**).

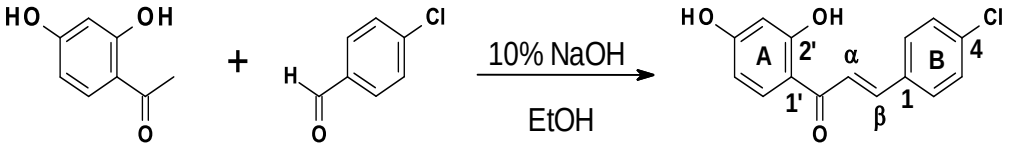


**40** **46** **47**

Compound **47** was obtained as yellow crystals in 16% yield. Unlike the previous Aldol condensation which took place at room temperature, this reaction required refluxing at 70 $^{0}$C for 48 hrs.

The $^{1}$H NMR signals for compound **47** were similar to those of compound **40** except for the incorporation of two *trans* olefinic protons at δ 8.00 (*d*, *J* = 15.5 Hz, 1H, $H_{\beta}$) and 7.86 (*d*, *J* = 15.5 Hz, 1H, $H_{\alpha}$) and an AA'BB' aromatic spin system resonating at δ 7.91 (*d*, *J* = 8.4 Hz, 2H, C-2 and C-6) and 7.52 (*d*, *J* = 8.5 Hz, 2H, C-3 and C-5). In the $^{13}$C NMR the signal for the carbonyl is more shielded (δ 191.7) compared to the starting material (δ 202.8) consistent with an α,β-unsaturated carbonyl system (121.6(α-C) and 142.3(β-C)) as would be expected from an Aldol condensation product.

The low yield of chalcones 2', 4'-dihydroxy-4-methoxychalcone (**45**) and 2', 4' -dihydroxy-4-chlorochalcone (**47)** could be due to side reaction (Cannizaro reaction of

the aldehydes) which led to the formation of a mixture of more than two products, which necessitated purification through column chromatography. Cannizaro reaction involves the conversion of non-enolizable aldehydes into an alcohol and carboxylic acid and takes place in presence of a strong base. The side products formed which included *p*-chlorobenzoic acid was produced in large quantity therefore it prompted the use of excess of the benzaldehyde to ensure that the 2,4-dihydroxyacetophenone was completely consumed in the reaction.

#### 4.4.1.4 Synthesis of 7-Hydroxy-2-(4-methoxyphenyl)chroman-4-one (48)

The synthesis of 7-hydroxy-2-(4-methoxyphenyl)chroman-4-one (7-hydroxy-4'-methoxyflavanone) (**48**) was achieved through the acid catalyzed cyclization of 2',4'-dihydroxy-4-methoxychalcone(**45**).

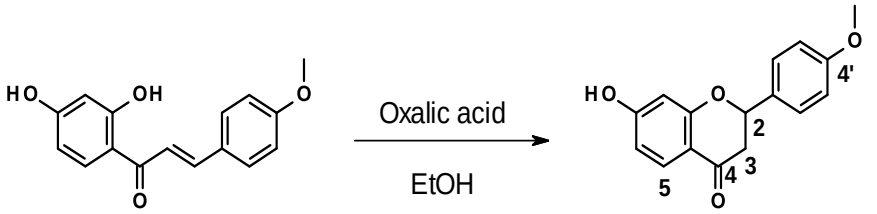


**45** **48**

Compound **48** was isolated as a yellow crystalline solid in 29% yield. The low yield of compound **48** is due to the decomposition of the chalcone hence forming mixtures that needed to be purified by column chromatography. Compound **48** was characterized as a flavanone based on its characteristic $^{1}$H NMR δ at (5.46 (*dd*, 1H, *J*=2.4, 13.2 Hz, H-2), 3.09 (*dd*, *J* = 13.2, 16.8 Hz, 1H, H-$3_{eq}$), 2.81 (*dd*, *J*=16.8, 2.4 Hz, 1H, H-$3_{ax}$)) and $^{13}$C NMR (δ 190.5(C=O), 79.7(C-2), 44.0(C-3)) peaks.

An attempt was made to synthesize chromones (flavones) through oxidative cyclization under two separate reaction conditions (Ghodile *et al*., 2012,Venkatachalam, *et al.*,

2012), Scheme 4.4, was unsuccessful. Under the conditions employed in the attempted cyclization, the chalcones decomposed.

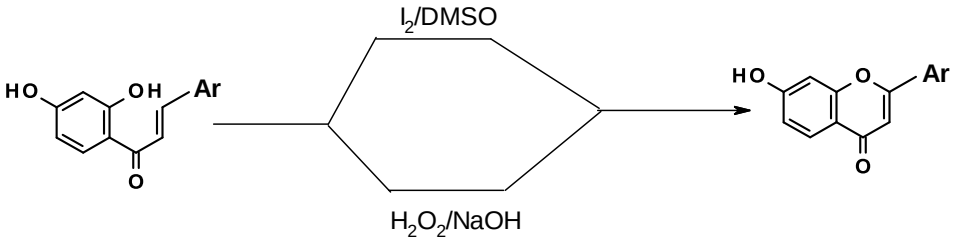


Scheme 4.4: Oxidative cyclization of chalcones to chromones

## 4.5 *In vitro* Antiplasmodial Activity

*In vitro* antiplasmodial bioassay of 2',4'-dihydroxy-4-methoxychalcone (**45)**, 2',4'-dihydroxy-4-chlorochalcone (**47**) and 7-hydroxy-2-(4-methoxyphenyl)chroman-4-one (**48**) against chloroquine resistant K1 and chloroquine sensitive 3D7 strains of *Plasmodium falciparum* was conducted using a non-radioactive assay technique and the results are as shown in Table 4.4.

Table 4.4: *In vitro* $IC_{50}$ values against K1 and 3D7 strains of *P. falciparum*

| **Sample** | **$IC_{50}$ (µg/ml)** | | **Docking score (Kcal/mol)** |
|---|---|---|---|
| | **K1** | **3D7** | |
| 2',4'-Dihydroxy-4-methoxychalcone (**45**) | 4.56 ± 1.66 | 5.14 ± 0.70 | -14.60 |
| 2',4' -Dihydroxy-4-chlorochalcone **(47)** | 20.36 ± 2.77 | | -14.14 |
| 7-Hydroxy-2-(4-methoxyphenyl) chroman-4-one (**48**) | 18.01 ± 2.28 | 4.57 ± 2.17 | -13.34 |
| Chloroquine* | 0.471 ± 0.037 | 0.006 ± 0.0022 | |
| Mefloquine* | 0.004 ± 0.0025 | 0.0008± 0.0004 | |

*standards

Among the compounds tested, 2',4'-dihydroxy-4-methoxychalcone (**45**) showed the highest antiplasmodial activity against both strains. Moderate antiplasmodial activity was observed for compounds **47** and **48** against chloroquine resistant K1 strain of *P.*

*falciparum.* 2',4'-Dihydroxy-4-methoxychalcone (**45**) and 7-hydroxy-2-(4-methoxyphenyl) chroman-4-one (**48**) showed strong antiplasmodial activity against the chloroquine sensitive 3D7 strain of *P. falciparum.* It is worth noting that, from the docking reports, 2',4'-dihydroxy-4-methoxychalcone (**45**) ranks the best among the three synthesized and assayed compounds which is consistent with the assay results, Table 4.4 and Figures 4.9-4.11.

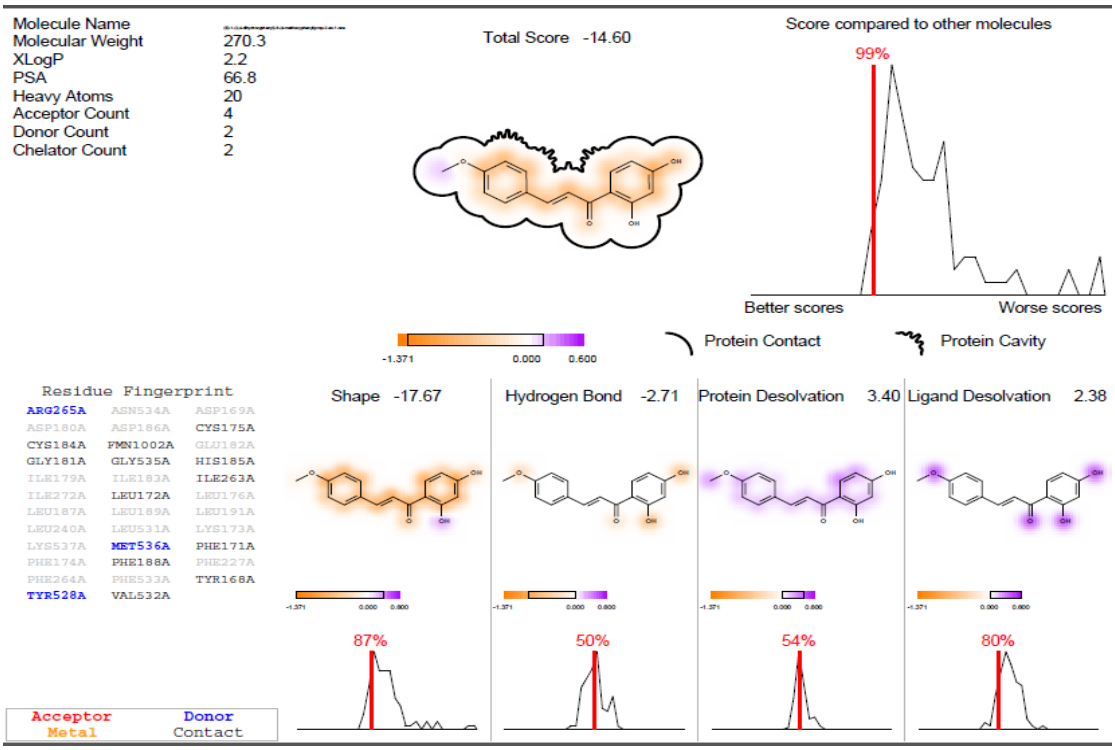

Figure 4.9: Docking report for 2', 4'-dihydroxy-4-methoxychalcone **(45)**

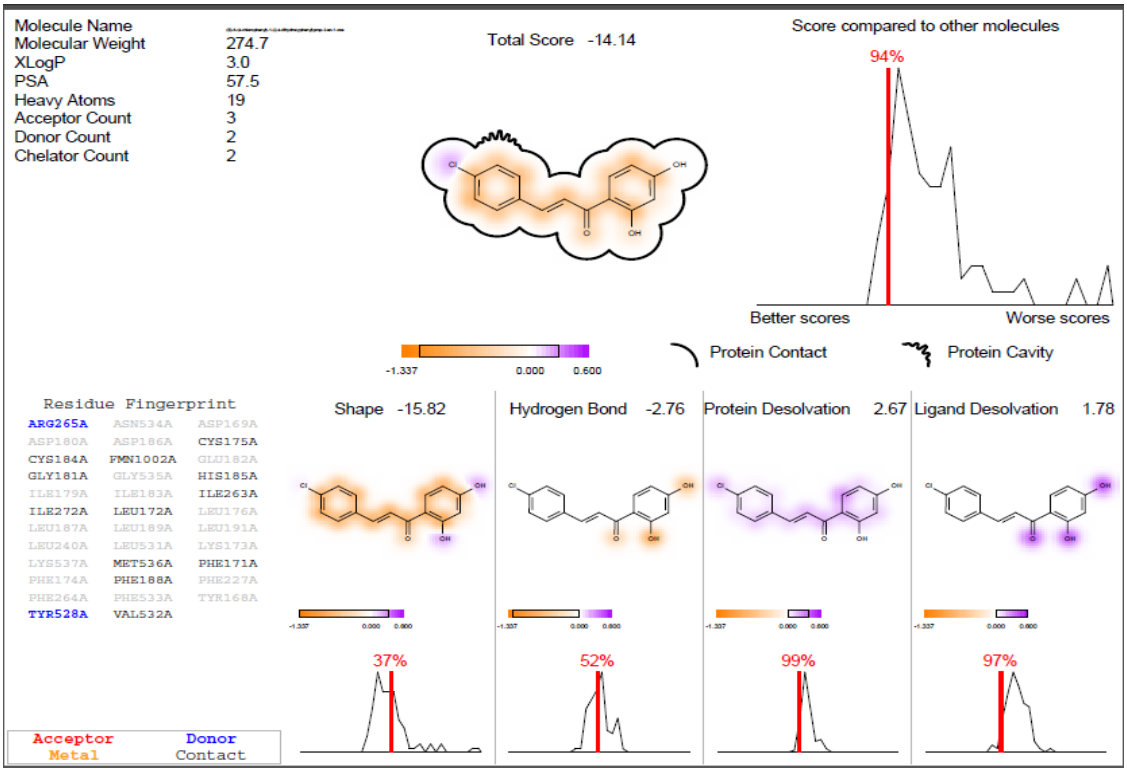


Figure 4.10: Docking report for 2', 4' -dihydroxy-4-chlorochalcone (**47**)

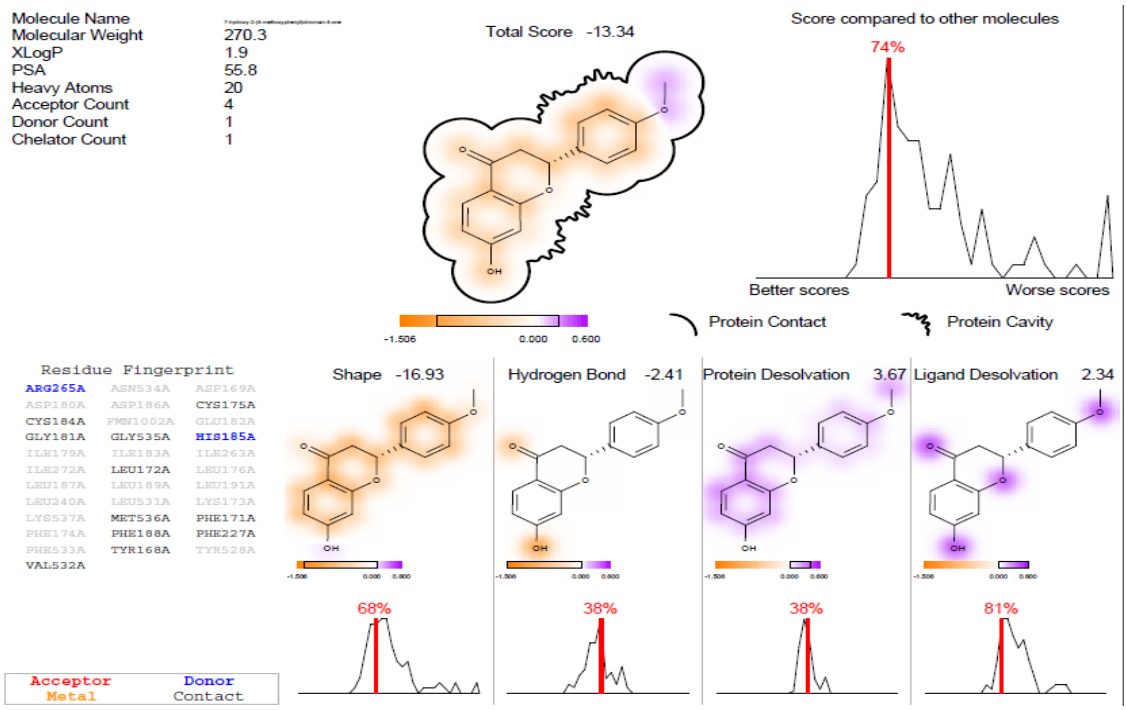


Figure 4.11: Docking report for 7-hydroxy-2-(4-methoxyphenyl) chroman-4-one (**48**)

# CHAPTER FIVE

# CONCLUSIONS AND RECOMMENDATIONS

The contributions of this study in developing a web-based *in silico* database of natural products of Kenya for design and synthesis of antiplasmodial lead compounds are summarized in the conclusions and recommendations below.

## 5.1 Conclusions

In this study:

1. The first web-based *in silico* database of natural products from Kenya was successfully generated and named *mitishamba* Database.
2. The 157 chromone, chromanone and chalcone ligands obtained from the *mitishamba* database were subjected to structure and ligand based virtual screening leading to identification of three synthetically accessible ligands for synthesis and antiplasmodial assay.
3. The three ligands synthesized and assayed were a chromanone (flavanone), 7-hydroxy-2-(4-methoxyphenyl) chroman-4-one (**48**), and two chalcones, 2',4'-dihydroxy-4-methoxychalcone **(45)** and 2',4'-dihydroxy-4-chlorochalcone (**47**). Among the compounds synthesized, 2',4'-dihydroxy-4-methoxychalcone (**45**) showed the highest antiplasmodial activity against chloroquine sensitive 3D7 and chloroquine resistant K1 strains of *P. falciparum* with $IC_{50}$ values of 5.14 ± 0.70 and 4.56±1.66 µg/ml, respectively.

## 5.2 Recommendations

Now that the database of natural products of Kenya is successfully developed, it is recommend that:

1. Further *in silico* design of the chalcones and chromanones be undertaken in order to optimize their antiplasmodial activity.
2. Enzyme inhibition assay of the synthesized compounds be undertaken against the *Pf*DHODH enzyme.
3. Synthetic methods for the cyclization of chalcones to chromones (flavones) be optimized.
4. The database be used in computer-aided drug design to design drugs against other diseases.

# REFERENCES


Achan, J., Talisuna, A. O., Erhart, A., Yeka, A., Tibenderana, J. K., Baliraine, F. N and D'Alessandro, U. (2011). Quinine, an old anti-malarial drug in a modern world: role in the treatment of malaria. *Malar J*, ***10***(144), 1475–2875.

Andayi, A. W., Yenesew, A., Derese, S., Midiwo, J. O., Gitu, P. M., Jondiko, O. J., and Peter, M. G. (2006). Antiplasmodial Flavonoids from *Erythrina sacleuxii*. *Planta Medica*, ***72***(2), 187–189.

Auffret, G., Labaied, M., Frappier, F., Rasoanaivo, P., Grellier, P., and Lewin, G. (2007). Synthesis and antimalarial evaluation of a series of piperazinyl flavones. *Bioorganic* and *Medicinal Chemistry Letters*, **17**(4), 959–963.

Balaramnavar, V. M., Srivastava, R., Rahuja, N., Gupta, S., Rawat, A. K., Varshney, S., and Saxena, A. K. (2014). Identification of novel PTP1B inhibitors by pharmacophore based virtual screening, scaffold hopping and docking. *European Journal of Medicinal Chemistry*, *87*, 578–594.

Balsera, B., Mulet, J., Fernández-Carvajal, A., Torre-Martínez, R. de la, Ferrer-Montiel, A., Hernández-Jiménez, J. G., and Criado, M. (2014). Chalcones as positive allosteric modulators of α7 nicotinic acetylcholine receptors: A new target for a privileged structure. *European Journal of Medicinal Chemistry*, *86*, 724–739.

Biamonte, M. A., Wanner, J., and Le Roch, K. G. (2013). Recent advances in malaria drug discovery. *Bioorganic* and *Medicinal Chemistry Letters*, ***23***(10), 2829–2843.

Bielska, E., Lucas, X., Czerwoniec, A., Kasprzak, J. M., Kaminska, K. H., and Bujnicki, J. M. (2011). Virtual screening strategies in drug design–methods

and applications. *BioTechnologia. Journal of Biotechnology Computational Biology and Bionanotechnology*, **92**(3), 249-264

Bienfait, B., and Ertl, P. (2013). JSME: a free molecule editor in JavaScript. *Journal of Cheminformatics*, **5**(1), 1-6

Bird, C. W., and Cheeseman, G. W. H. (1973). *Aromatic and Heteroatomic Chemistry*. Royal Society of Chemistry. 420-425

Birkholtz, L.-M., Bornman, R., Focke, W., Mutero, C., and De Jager, C., (2012). Sustainable malaria control: transdisciplinary approaches for translational applications. *Malaria Journal*, ***11***(1), 431-442

Boechat, N., Pinheiro, L. C. S., Silva, T. S., Aguiar, A. C. C., Carvalho, A. S., Bastos, M. M., and Krettli, A. U. (2012). New Trifluoromethyl Triazolopyrimidines as Anti-Plasmodium falciparum Agents. *Molecules*, **17**(12), 8285–8302.

Cabrera, M., Simoens, M., Falchi, G., Lavaggi, M. L., Piro, O. E., Castellano, E. E., and González, M. (2007). Synthetic chalcones, flavanones, and flavones as antitumoral agents: Biological evaluation and structure–activity relationships. *Bioorganic* and *Medicinal Chemistry*, **15**(10), 3356–3367.

Castellini, M. A., Buguliskis, J. S., Casta, L. J., Butz, C. E., Clark, A. B., Kunkel, T. A., and Taraschi, T. F. (2011). Malaria drug resistance is associated with defective DNA mismatch repair. *Molecular and Biochemical Parasitology*, **177**(2), 143–147.

Cheeseright, T. (2009). The identification of bioisosteres as drug development candidates. *Innovations in Pharmaceutical Technology*, *28*, 22–26.

Chen, M., Theander, T. G., Christensen, S. B., Hviid, L., Zhai, L., and Kharazmi, A. (1994). Licochalcone A, a new antimalarial agent, inhibits *In vitro* growth of

the human malaria parasite Plasmodium falciparum and protects mice from P. yoelii infection. *Antimicrobial Agents and Chemotherapy*, **38**(7), 1470–1475.

Coteron, J. M., Marco, M., Esquivias, J., Deng, X., White, K. L., White, J., and Phillips, M. A. (2011). Structure-Guided Lead Optimization of Triazolopyrimidine-Ring Substituents Identifies Potent *Plasmodium falciparum* Dihydroorotate Dehydrogenase Inhibitors with Clinical Candidate Potential. *Journal of Medicinal Chemistry*, **54**(15), 5540–5561.

Deng, X., Gujjar, R., El Mazouni, F., Kaminsky, W., Malmquist, N. A., Goldsmith, E. J., and Phillips, M. A. (2009). Structural Plasticity of Malaria Dihydroorotate Dehydrogenase Allows Selective Binding of Diverse Chemical Scaffolds. *Journal of Biological Chemistry*, **284**(39), 26999–27009.

Derese, S., Yenesew, A., Midiwo, J. O., Heydenreich, M., and Peter, M. G. (2003). A new isoflavone from stem bark of Millettia dura. *Bulletin of the Chemical Society of Ethiopia*, **17**(1), 113–115.

Dike, I. P., Obembe, O. O., and Adebiyi, F. E. (2012). Ethnobotanical survey for potential anti-malarial plants in south-western Nigeria. *Journal of Ethnopharmacology*, **144**(3), 618–626.

Endale, M., Alao, J., Akala, H., Rono, N., Eyase, F., Derese, S. and Yenesew, A. (2012). Antiplasmodial Quinones from *Pentas longiflora* and *Pentas lanceolata*. *Planta Medica*, **78**(01), 31–35.

Fidock, D. A., Rosenthal, P. J., Croft, S. L., Brun, R. and Nwaka, S. (2004). Antimalarial drug discovery: efficacy models for compound screening. *Nature Reviews Drug Discovery*, **3**(6), 509–520.

Flannery, E. L., Chatterjee, A. K., and Winzeler, E. A. (2013). Antimalarial drug discovery approaches and progress towards new medicines. *Nature Reviews Microbiology*, **11**(12), 849–862.

Frölich, S., Schubert, C., Bienzle, U., and Jenett-Siems, K. (2005). *In vitro* antiplasmodial activity of prenylated chalcone derivatives of hops (Humulus lupulus) and their interaction with haemin. *Journal of Antimicrobial Chemotherapy*, **55**(6), 883–887.

Gamo, F.-J. (2014). Antimalarial drug resistance: new treatments options for Plasmodium. *Drug Discovery Today: Technologies*, *11*, 81–88.

Gaspar, A., Silva, T., Yáñez, M., Vina, D., Orallo, F., Ortuso, F. and Borges, F. (2011). Chromone, a privileged scaffold for the development of monoamine oxidase inhibitors. *Journal of Medicinal Chemistry*, **54**(14), 5165–5173.

Ghodile, N. G., Rajput, P. R., Banewar, V., W. and Raut, A. R. (2012). Synthesis and antimicrobial activity of some chalcones and flavones having 2-hydroxy acetophenone moiety. *Int. J. Pharm. Bio Sci*, **3**(3), 389–395.

Gujjar, R., Marwaha, A., El Mazouni, F., White, J., White, K. L., Creason, S. and Phillips, M. A. (2009). Identification of a Metabolically Stable Triazolopyrimidine-Based Dihydroorotate Dehydrogenase Inhibitor with Antimalarial Activity in Mice. *Journal of Medicinal Chemistry*, **52**(7), 1864–1872.

Gumula, I., Heydenreich, M., Derese, S., Ndiege, I. O., and Yenesew, A. (2012). Four isoflavanones from the stem bark of Platycelphium voënse. *Phytochemistry Letters*, **5**(1), 150–154.

Haider, N. (2010). Functionality Pattern Matching as an Efficient Complementary Structure/Reaction Search Tool: an Open-Source Approach. *Molecules*, **15**(8), 5079–5092.

Heikkilä, T., Thirumalairajan, S., Davies, M., Parsons, M. R., McConkey, A. G., Fishwick, C. W. G., and Johnson, A. P. (2006). The first de novo designed inhibitors of Plasmodium falciparum dihydroorotate dehydrogenase. *Bioorganic* and *Medicinal Chemistry Letters*, **16**(1), 88–92.

Heydenreich, M., Muiva, L. M., Eyase, F. L., Akala, H. M., Wanyama, P. J. and Yenesew, A. (2011). Terpurinflavone: An antiplasmodial flavone from the stem of Tephrosia Purpurea. *Phytochemistry letters*, ***4***(2011), 176-178.

Huang, S.-Y., Grinter, S. Z., and Zou, X. (2010). Scoring functions and their evaluation methods for protein–ligand docking: recent advances and future directions. *Physical Chemistry Chemical Physics*, **12**(40), 775-787

Hubbard, R. E. (2011). Structure-based drug discovery and protein targets in the CNS. *Neuropharmacology*, **60**(1), 7–23.

Hurt, D. E., Sutton, A. E., and Clardy, J. (2006). Brequinar derivatives and species-specific drug design for dihydroorotate dehydrogenase. *Bioorganic* and *Medicinal Chemistry Letters*, **16**(6), 1610–1615.

Hurt, D. E., Widom, J., and Clardy, J. (2006). Structure of Plasmodium falciparum dihydroorotate dehydrogenase with a bound inhibitor. *Acta Crystallographica. Section D, Biological Crystallography*, **62**(Pt 3), 312–323.

Jaeger, A. (2012). Quinine and chloroquine. *Medicine*, *40*(3), 154–155.

Jain, A. N., and Nicholls, A. (2008). Recommendations for evaluation of computational methods. *Journal of Computer-Aided Molecular Design*, **22**(3-4), 133–139.

Jain, T., and Jayaram, B. (2005). An all atom energy based computational protocol for predicting binding affinities of protein–ligand complexes. *FEBS Letters*, **579**(29), 6659–6666.

Jana, S., and Paliwal, J. (2007). Novel molecular targets for antimalarial chemotherapy. *International Journal of Antimicrobial Agents*, *30*(1), 4–10.

Jiang, Z., and Zhou, Y. (2005). Using gene networks to drug target identification. *Journal of Integrative Bioinformatics*, **2**(1), 14.

Keri, R. S., Budagumpi, S., Pai, R. K., and Balakrishna, R. G. (2014). Chromones as a privileged scaffold in drug discovery: A review. *European Journal of Medicinal Chemistry*, **78**, 340–374.

Keserű, G. M., and Makara, G. M. (2006). Hit discovery and hit-to-lead approaches. *Drug Discovery Today*, **11**(15-16), 741–748.

Kitchen, D. B., Decornez, H., Furr, J. R., and Bajorath, J. (2004). Docking and scoring in virtual screening for drug discovery: methods and applications. *Nature Reviews Drug Discovery*, **3**(11), 935–949.

Klein, E. Y. (2013). Antimalarial drug resistance: a review of the biology and strategies to delay emergence and spread. *International Journal of Antimicrobial Agents*, **41**(4), 311–317.

Kokwaro, J. (2009). *Medicinal Plants of East Africa. Third Edition* (3 edition). Nairobi, Kenya: Univ. of Nairobi Press.

Krungkrai, S. R., and Krungkrai, J. (2011). Malaria parasite carbonic anhydrase: inhibition of aromatic/heterocyclic sulfonamides and its therapeutic potential. *Asian Pacific Journal of Tropical Biomedicine*, **1**(3), 233–242.

Kulkarni, P. S., Swami, P. M., and Zubaidha, P. K. (2013). Calcium Hydroxide Is an Efficient Catalyst for Synthesis of Polyhydroxy Chalcones. *Synthesis and*

*Reactivity in Inorganic, Metal-Organic, and Nano-Metal Chemistry*, **43**(5), 617–620.

Kumar, A., Paliwal, D., Saini, D., Thakur, A., Aggarwal, S., and Kaushik, D. (2014). A comprehensive review on synthetic approach for antimalarial agents. *European Journal of Medicinal Chemistry*, *85*, 147–178.

Kumar Ojha, P., Mitra, I., Kar, S., Narayan Das, R., and Roy, K. (2012). Lead Hopping for *Pf* DHODH Inhibitors as Antimalarials Based on Pharmacophore Mapping, Molecular Docking and Comparative Binding Energy Analysis (COMBINE): A Three-Layered Virtual Screening Approach. *Molecular Informatics*, **31**(10), 711–718.

Kuntz, I. D. (1992). Structure-Based Strategies for Drug Design and Discovery. *Science*, **257**(5073), 1078–1082.

Langdon, S. R., Ertl, P., and Brown, N. (2010). Bioisosteric Replacement and Scaffold Hopping in Lead Generation and Optimization. *Molecular Informatics*, **29**(5), 366–385.

Lee, C.-H., Huang, H.-C., and Juan, H.-F. (2011). Reviewing Ligand-Based Rational Drug Design: The Search for an ATP Synthase Inhibitor. *International Journal of Molecular Sciences*, **12**(12), 5304–5318.

Lee, S. J., Seo, E., and Cho, Y. (2013). Proposal for a new therapy for drug-resistant malaria using Plasmodium synthetic lethality inference. *International Journal for Parasitology: Drugs and Drug Resistance*, *3*, 119–128.

Lipinski, C. A., Lombardo, F., Dominy, B. W., and Feeney, P. J. (2012). Experimental and computational approaches to estimate solubility and permeability in drug discovery and development settings. *Advanced Drug Delivery Reviews*, *64*, 4–17.

Lukens, A. K., Ross, L. S., Heidebrecht, R., Javier Gamo, F., Lafuente-Monasterio, M. J., Booker, M. L., and Wirth, D. F. (2014). Harnessing evolutionary fitness in Plasmodium falciparum for drug discovery and suppressing resistance. *Proceedings of the National Academy of Sciences*, **111**(2), 799–804.

Manguro, L. O. A., Onyango Okwiri, S., and Lemmen, P. (2006). Oleanane-type triterpenes of Embelia schimperi leaves. *Phytochemistry*, *67*(24), 2641–2650.

Masesane, B., and Mazimba, V O. (2014). Reaction of ethyl acetoacetate and 2′-hydroxychalcones: Efficient route to 9-aryl-6H-benzo[c]chromen-6-ones. *Bulletin of the Chemical Society of Ethiopia*, ***28***(2), 289-294

Meanwell, N. A. (2011). Synopsis of some recent tactical application of bioisosteres in drug design. *Journal of Medicinal Chemistry*, **54**(8), 2529–2591.

Muiva, L. M., Yenesew, A., Derese, S., Heydenreich, M., Peter, M. G., Akala, H. M., and Walsh, D. (2009). Antiplasmodial β-hydroxydihydrochalcone from seedpods of Tephrosia elata. *Phytochemistry Letters*, **2**(3), 99–102.

Muthaura, C. N., Keriko, J. M., Derese, S., Yenesew, A., and Rukunga, G. M. (2011). Investigation of some medicinal plants traditionally used for treatment of malaria in Kenya as potential sources of antimalarial drugs. *Experimental Parasitology*, **127**(3), 609–626.

Nagamani, S., Kesavan, C., and Muthusamy, K. (2012). E-Pharmacophore mapping and docking studies on Vitamin D receptor (VDR). *Bioinformation*, **8**(15), 705-710.

Nair, V. and Vellalath, S. (2008). Molecule matters. *Resonance*, **13**(3), 254–260.

Nicholls, A., McGaughey, G. B., Sheridan, R. P., Good, A. C., Warren, G., Mathieu, M. and Kelley, B. (2010). Molecular Shape and Medicinal Chemistry: A Perspective. *Journal of Medicinal Chemistry*, *53*(10), 3862–3886.

Nogueira, C. R., and Lopes, L. M. X. (2011). Antiplasmodial Natural Products. *Molecules*, **16**(12), 2146–2190.

Omosa, L. K., Midiwo, J. O., Derese, S., Yenesew, A., Peter, M. G., and Heydenreich, M. (2010). neo-Clerodane diterpenoids from the leaf exudate of Dodonaea angustifolia. *Phytochemistry Letters*, **3**(4), 217–220.

Ooms, F. (2000). Molecular modeling and computer aided drug design. Examples of their applications in medicinal chemistry. *Current Medicinal Chemistry*, ***7***(2), 141–158.

Opiyo, S. A., Manguro, L. O. A., Okinda-Owuor, P., Ateka, E. M., and Lemmen, P. (2011). 7α-Acetylugandensolide and antimicrobial properties of Warburgia ugandensis extracts and isolates against sweet potato pathogens. *Phytochemistry Letters*, ***4***(2), 161–165.

Patel, M. C., Rajani, D. P., and others. (2011). Synthesis and characterization of some novel chromones and chromanones derivatives and its biological screening. *Der Pharma Chemica*, ***3***(4), 422-432.

Patil, R. B., Sawant, S. D., and Thombare, P. A. (2012). Design, Synthesis and Pharmacological Evaluation of Chromenones and Related Analogues. *International Journal of PharmTech Research*, *4*(1), 375-381.

Phillips, M. A., and Rathod, P. K. (2010). Plasmodium dihydroorotate dehydrogenase: a promising target for novel anti-malarial chemotherapy. *Infectious Disorders Drug Targets*, **10**(3), 226–239.

Ragab, F. A., Hassan, G. S., Yossef, H. A., and Hashem, H. A. (2007). Synthesis of 6- and 9-alkylaminomethyl furoflavones as gastroprotective agents. *European Journal of Medicinal Chemistry*, **42**(8), 1117–1127.

Rahman, A. F. M. M., Ali, R., Jahng, Y., and Kadi, A. A. (2012). A Facile Solvent Free Claisen-Schmidt Reaction: Synthesis of α,α′-bis-(Substituted-benzylidene)cycloalkanones and α,α′-bis-(Substituted-alkylidene)cycloalkanones. *Molecules*, **17**(12), 571–583.

Ramazani, A., and Borna, H. (2011). In silico analysis and development of anti-malarial compounds against dihydroorotate dehydrogenase using chem-bioinformatic tools. *International Journal of Pharma* and *Bio Sciences*, **2**(2).

Reddy, G. V., Maitraie, D., Narsaiah, B., Rambabu, Y., and Rao, P. S. (2001). Microwave assisted knoevenagel condensation: a facile method for the synthesis of chalcones . *Synthetic Communications*, **31**(18), 2881–2884.

Rodrigues, T., Lopes, F., and Moreira, R. (2010). Inhibitors of the mitochondrial electron transport chain and de novo pyrimidine biosynthesis as antimalarials: the present status. *Current Medicinal Chemistry*, **17**(10), 929–956.

Roy, P. P., and Roy, K. (2010). Pharmacophore mapping, molecular docking and QSAR studies of structurally diverse compounds as CYP2B6 inhibitors. *Molecular Simulation*, **36**(11), 887–905.

Rudrapal, M. (2011). A Brief Review on Malaria and Current Antimalarial Drugs. *Curr. Pharm. Res*, *1*, 286–292.

Schlitzer, M. (2007). Malaria Chemotherapeutics Part I: History of Antimalarial Drug Development, Currently Used Therapeutics, and Drugs in Clinical Development. *ChemMedChem*, **2**(7), 944–986.

Schlitzer, M. (2008). Antimalarial Drugs – What is in Use and What is in the Pipeline. *Archiv Der Pharmazie*, **341**(3), 149–163.

Schneider, G., Schneider, P., and Renner, S. (2006). Scaffold-Hopping: How Far Can You Jump? *QSAR* and *Combinatorial Science*, *25*(12), 1162–1171.

Senger, M., Rice, P., and Oinn, T. (2003). Soaplab-a unified Sesame door to analysis tools. In *Proceedings of the UK e-Science All Hands Meeting* **18**,509–513.

Shaibaldain, N. L. (2012). Fries rearrangement of 3, 5-dimethoxyphenyl acetate. *Journal of Basrah Researches ((Sciences)) Volume*, ***38*(**2), 54-58.

Shanthi, V., Ramesh, M., Srimai, V., Srinivas, P., and Parthasarathy, T. (2013). QSAR, Docking and invitro antioxidant activity study of novel chromone derivatives. *Modern Chemistry*, **1**(1), 8–17.

Sharma, R., Lawrenson, A. S., Fisher, N. E., Warman, A. J., Shone, A. E., Hill, A., and Berry, N. G. (2012). Identification of Novel Antimalarial Chemotypes via Chemoinformatic Compound Selection Methods for a High-Throughput Screening Program against the Novel Malarial Target, PfNDH2: Increasing Hit Rate via Virtual Screening Methods. *Journal of Medicinal Chemistry*, **55**(7), 3144–3154.

Sultan, A., Raza, A., Abbas, M., Khan, K., Tahir, M., and Saari, N. (2013). Evaluation of Silica-H2SO4 as an Efficient Heterogeneous Catalyst for the Synthesis of Chalcones. *Molecules*, **18**(8), 10081–10094.

Swann, S. L., Brown, S. P., Muchmore, S. W., Patel, H., Merta, P., Locklear, J., and Hajduk, P. J. (2011). A Unified, Probabilistic Framework for Structure- and Ligand-Based Virtual Screening. *Journal of Medicinal Chemistry*, **54**(5), 1223–1232.

Theil, F.-P., Guentert, T. W., Haddad, S., and Poulin, P. (2003). Utility of physiologically based pharmacokinetic models to drug development and rational drug discovery candidate selection. *Toxicology Letters*, **138**(1), 29–49.

Thera, M. A., and Plowe, C. V. (2012). Vaccines for Malaria: How Close Are We? *Annual Review of Medicine*, *63*(1), 345–357.

Udatha, D. B. R. K. G., Sugaya, N., Olsson, L., and Panagiotou, G. (2012). How well do the substrates KISS the enzyme? Molecular docking program selection for feruloyl esterases. *Scientific Reports*, *2*.

Van Drie, J. H. (2010). History of 3D pharmacophore searching: commercial, academic and open-source tools. *Drug Discovery Today: Technologies*, **7**(4), e255–e262.

Venkatachalam, H., Nayak, Y., and Jayashree, B. S. (2012). Evaluation of the antioxidant activity of novel synthetic chalcones and flavonols. *Int J Chem Eng Appl*, **3**(3), 216–219.

Wadood, A., and ulhaq, Z.-. (2013). In silico identification of novel inhibitors against Plasmodium falciparum dihydroorate dehydrogenase. *Journal of Molecular Graphics and Modelling*, *40*, 40–47.

Wale, N., Karypis, G., and Watson, I. A. (2007). *Methods for Effective Virtual Screening and Scaffold-Hopping in Chemical Compounds*. DTIC Document.

WHO | World Malaria Report 2010.

WHO | World Malaria Report 2014.

World Health Organization, Tuschman, M., World Health Organization., and Global Malaria Programme. (2013). *World malaria report 2013*.

Wunberg, T., Hendrix, M., Hillisch, A., Lobell, M., Meier, H., Schmeck, C., and Hinzen, B. (2006). Improving the hit-to-lead process: data-driven assessment of drug-like and lead-like screening hits. *Drug Discovery Today*, **11**(3), 175–180.

Yenesew, A., Derese, S., Midiwo, J. O., Bii, C. C., Heydenreich, M., and Peter, M. G. (2005). Antimicrobial flavonoids from the stem bark of Erythrina burttii. *Fitoterapia*, **76**(5), 469–472.

Yenesew, A., Derese, S., Midiwo, J. O., Oketch-Rabah, H. A., Lisgarten, J., Palmer, R., and Waters, N. C. (2003). Anti-plasmodial activities and X-ray crystal structures of rotenoids from Millettia usaramensis subspecies usaramensis. *Phytochemistry*, **64**(3), 773–779.

Yenesew, A., Induli, M., Derese, S., Midiwo, J. O., Heydenreich, M., Peter, M. G., and Waters, N. C. (2004). Anti-plasmodial flavonoids from the stem bark of Erythrina abyssinica. *Phytochemistry*, **65**(22), 3029–3032.

Yenesew, A., Midiwo, J. O., Heydenreich, M., Schanzenbach, D., and Peter, M. G. (2000). Two isoflavanones from the stem bark of Erythrina sacleuxii. *Phytochemistry*, **55**(5), 457–459.

Yenesew, A., Twinomuhwezi, H., Kabaru, J. M., Akala, H. M., Kiremire, B. T., Heydenreich, M., and Walsh, D. S. (2009). Antiplasmodial and larvicidal flavonoids from Derris Trifoliata, **23**(3), 409–414.

Zakaria, I., Ahmat, N., Jaafar, F. M., and Widyawaruyanti, A. (2012). Flavonoids with antiplasmodial and cytotoxic activities of Macaranga triloba. *Fitoterapia*, **83**(5), 968–972.

Zambare, A. S., Sangshetti, J. N., Kokare, N. D., and Shinde, D. B. (2009). Development of mild and efficient method for synthesis of substituted flavones using oxalic acid catalyst. *Chinese Chemical Letters*, **20**(2), 171–174.

Zelefack, F., Guilet, D., Valentin, A., Fongang, R. C. Soh, Kom, B., Chevalley, S., and Dijoux-Franca, M.-G. (2012). Antiplasmodial and cytotoxic activities of flavonoids and arylbenzofuran derivatives Morus mesozygia, **2**(2), 20–24.

Zhu, F., Shi, Z., Qin, C., Tao, L., Liu, X., Xu, F., and Chen, Y. (2012). Therapeutic target database update 2012: a resource for facilitating target-oriented drug discovery. *Nucleic Acids Research*, **40**(D1), D1128–D1136.

Ziegler, H. L., Hansen, H. S., Staerk, D., Christensen, S. B., Hagerstrand, H., and Jaroszewski, J. W. (2004). The Antiparasitic Compound Licochalcone A Is a Potent Echinocytogenic Agent That Modifies the Erythrocyte Membrane in the Concentration Range Where Antiplasmodial Activity Is Observed. *Antimicrobial Agents and Chemotherapy*, **48**(10), 4067–4071.

# APPENDICES

## Appendix A: NMR Spectra for 2,4–Dihydroxyacetophenone (40)

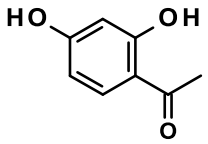


**40**

$^{1}$H NMR Spectrum for **40**

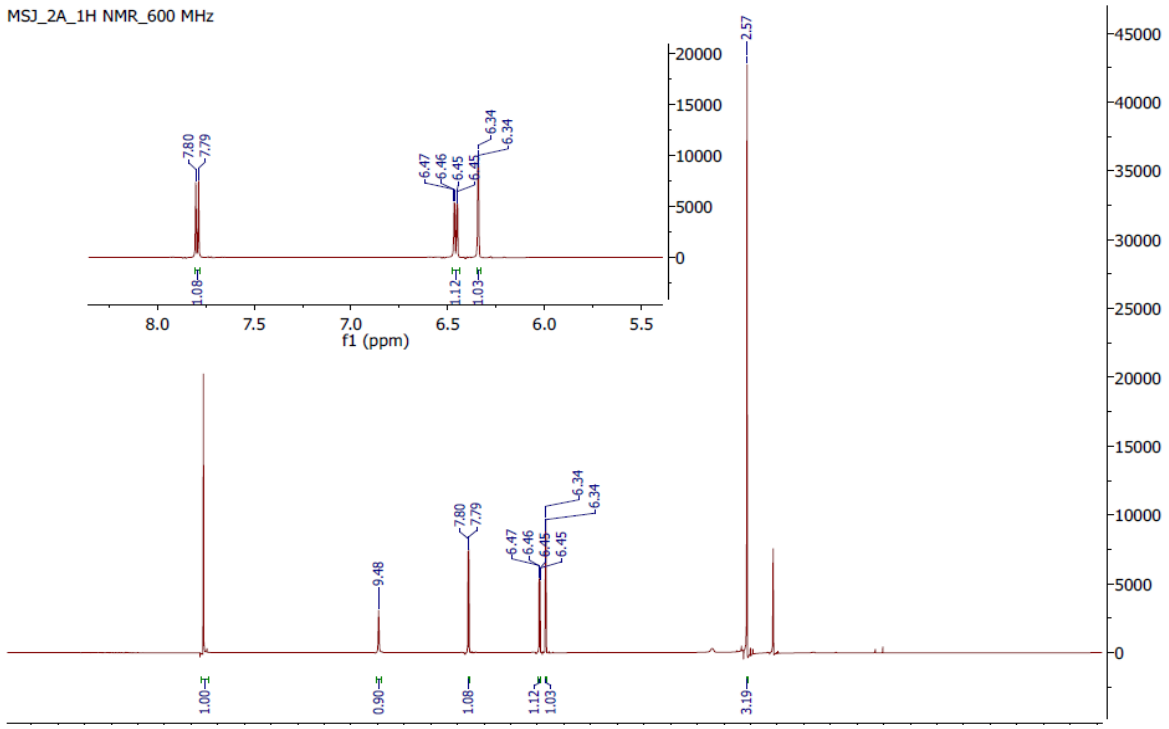


$^{13}$C NMR Spectrum for **40**

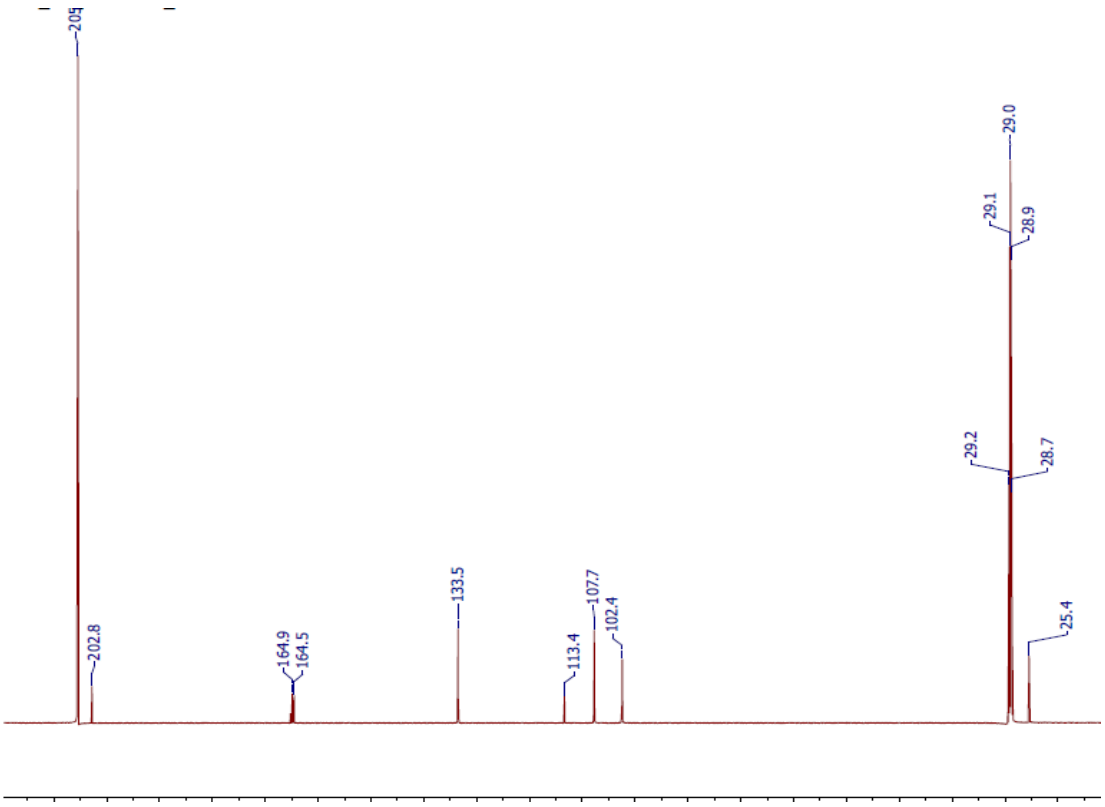

HSQS Spectrum for **40**

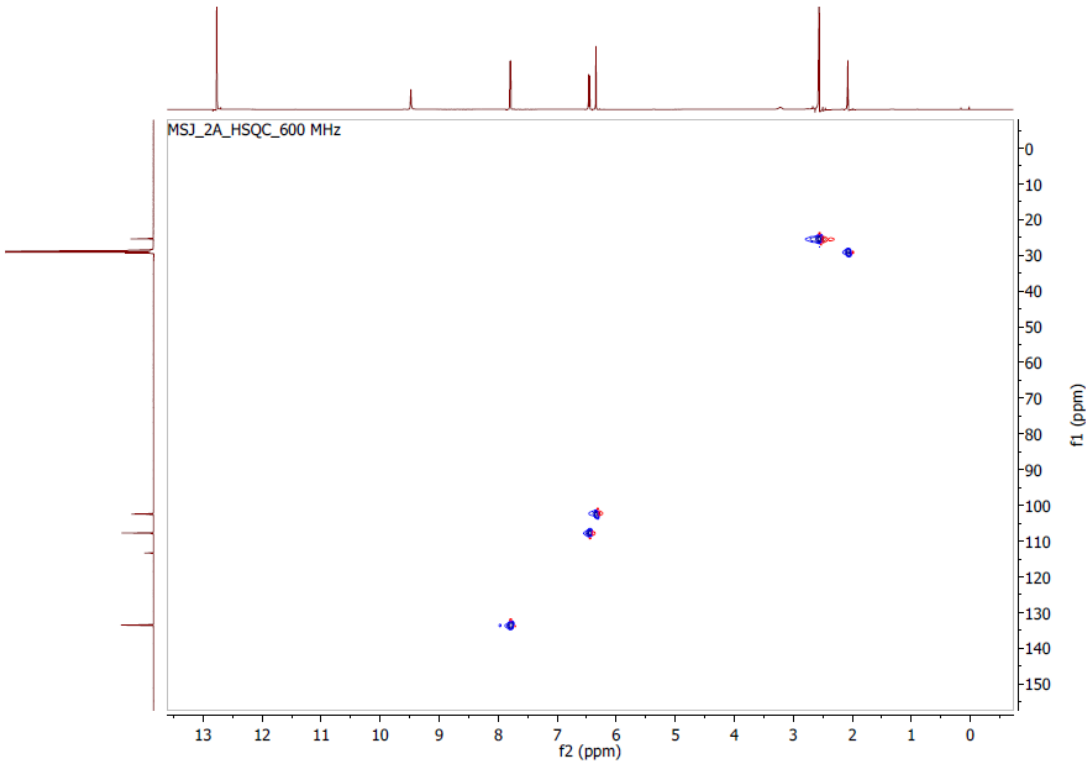


HMBC Spectrum for **40**

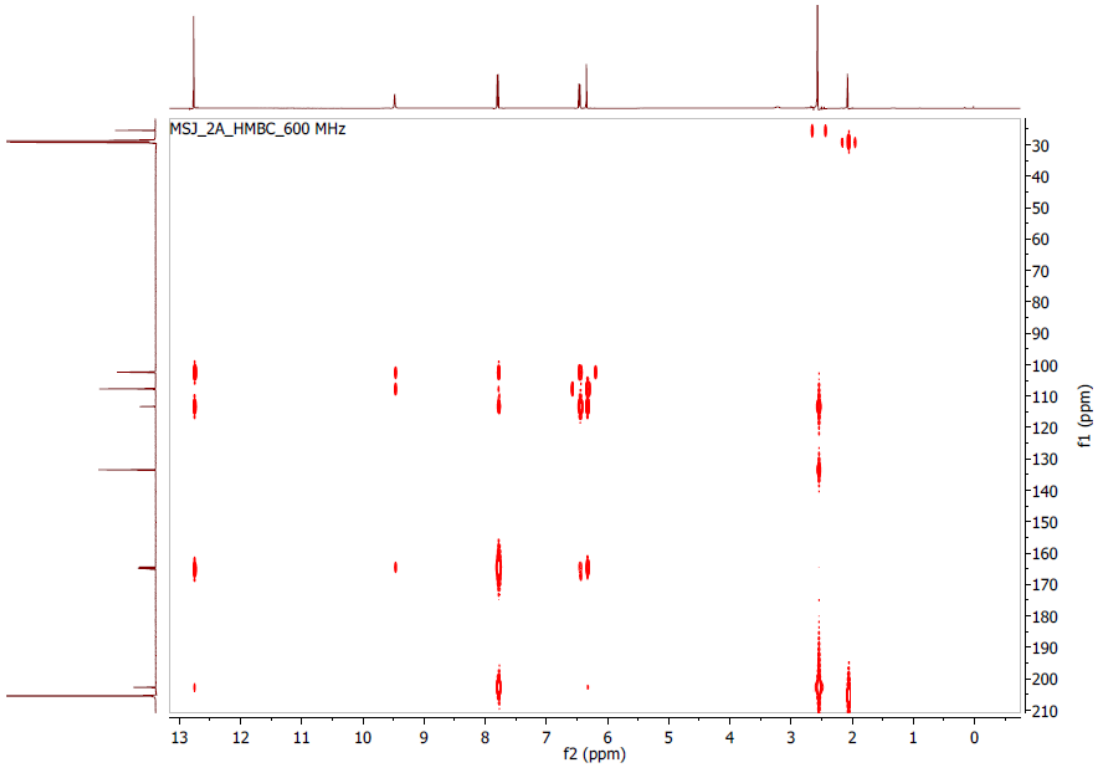

COSY spectrum for **40**

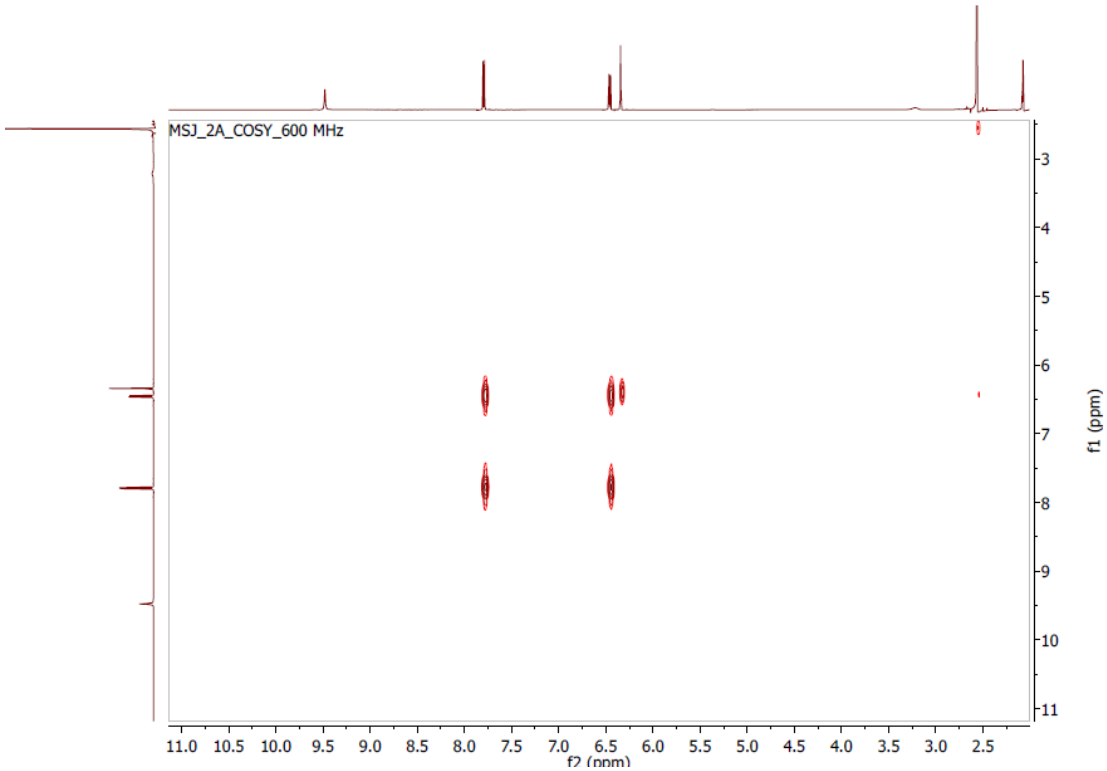

**Appendix B: NMR Spectra for 2',4'-Dihydroxy-4-methoxychalcone (45)**

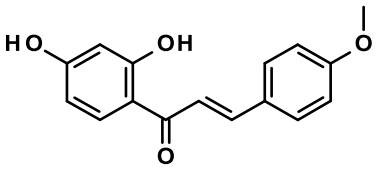


**45**

$^{1}$H NMR Spectrum for **45**

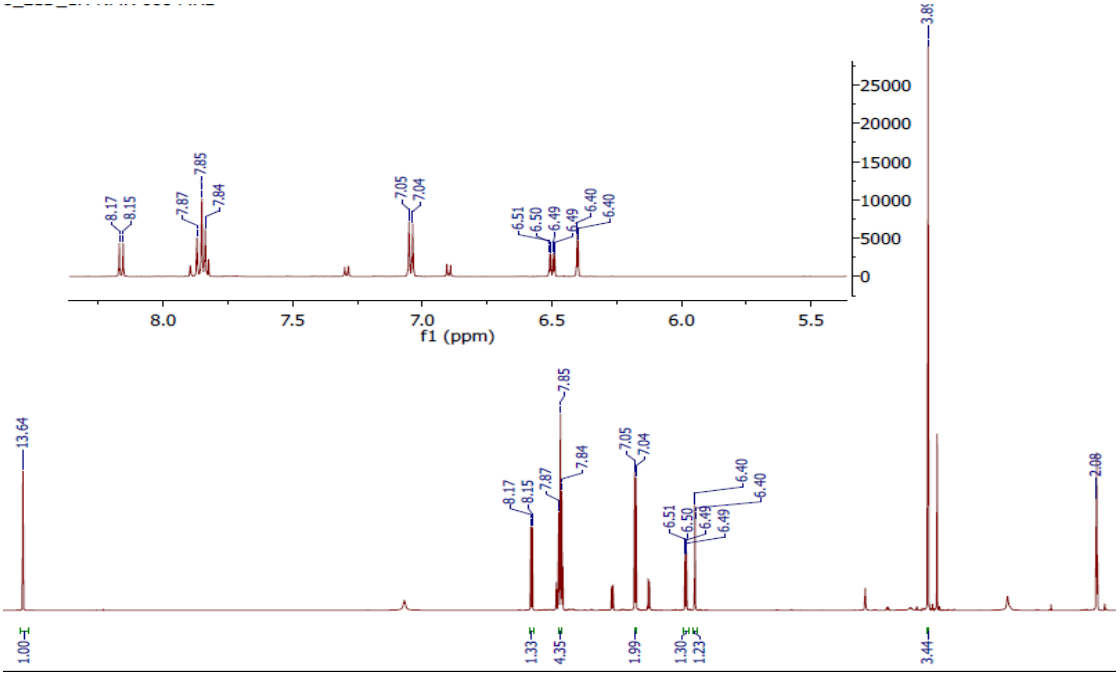


$^{13}$C NMR Spectrum for **45**

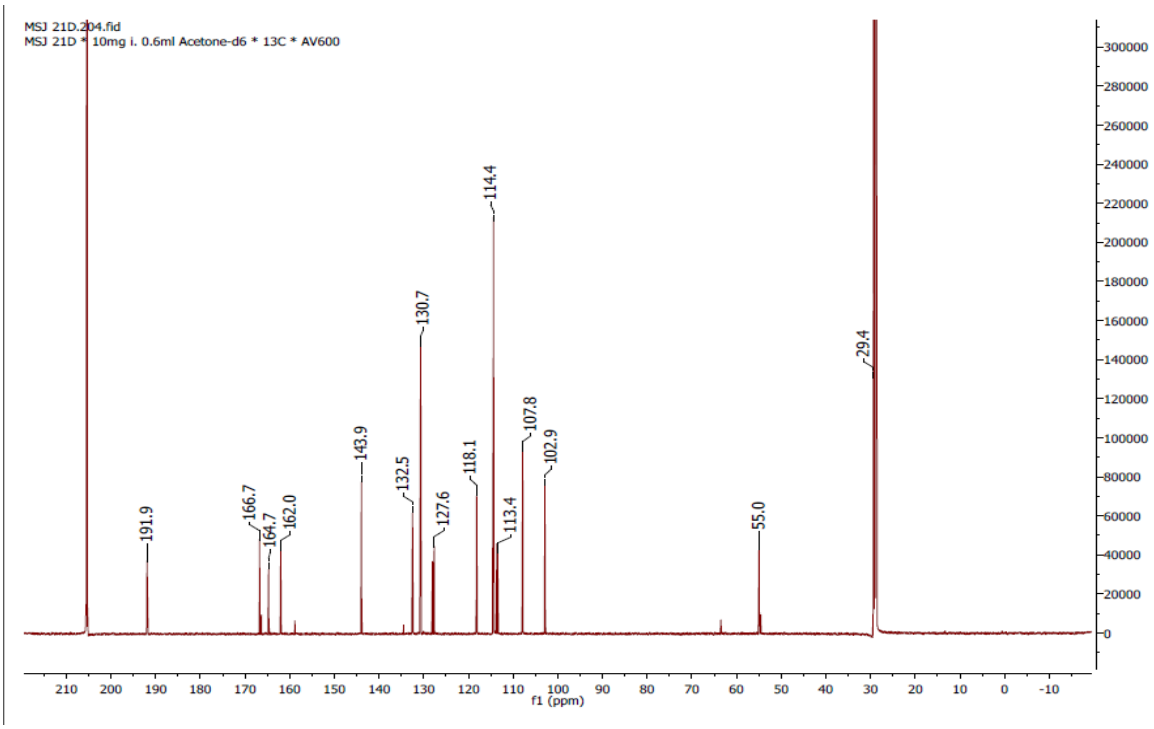

HSQC Spectrum for **45**

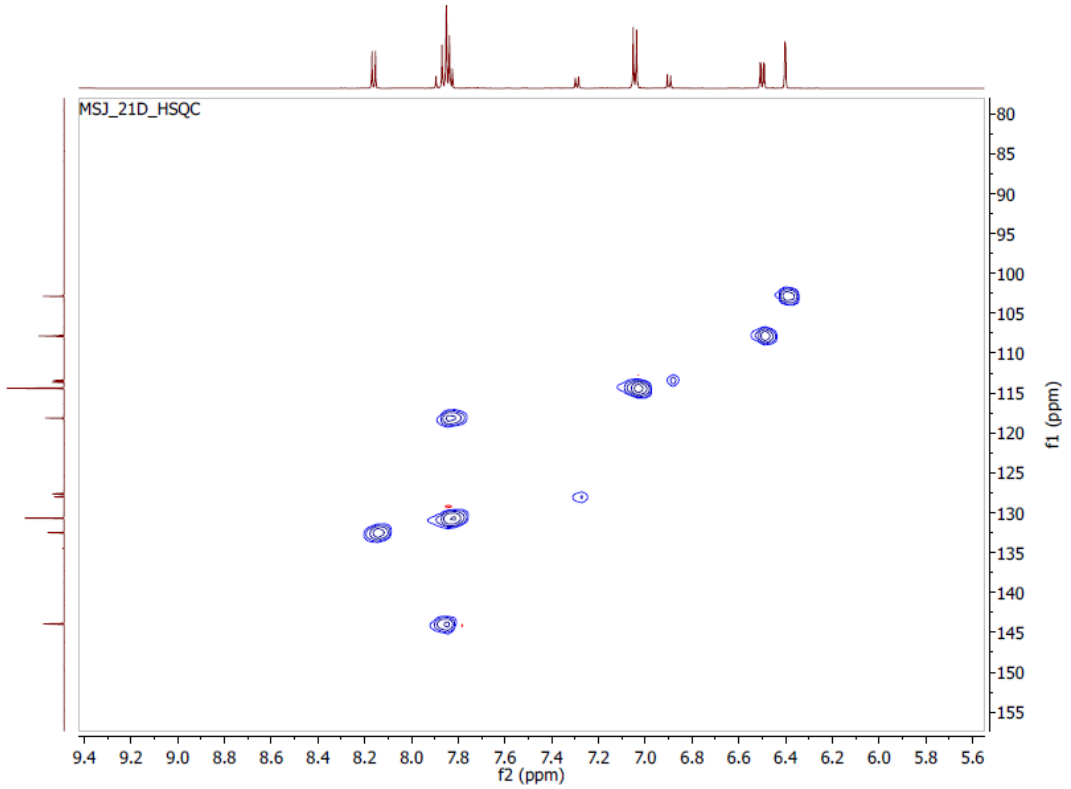


HMBC Spectrum for **45**

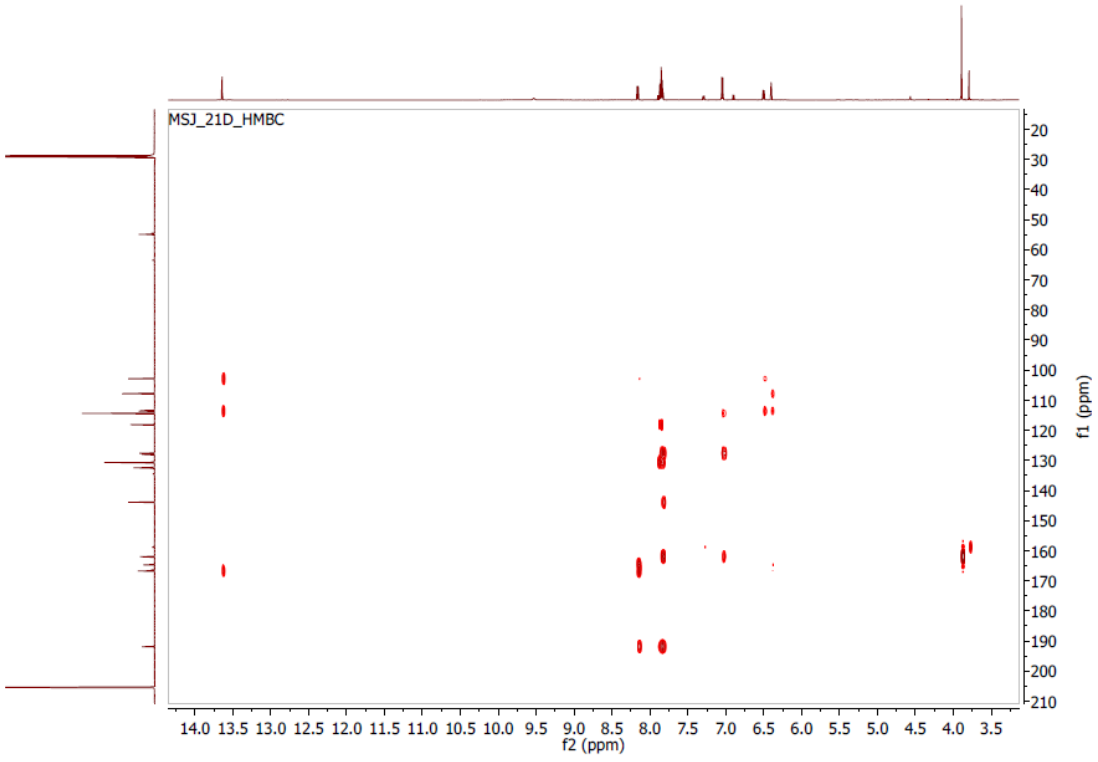

COSY Spectrum for **45**

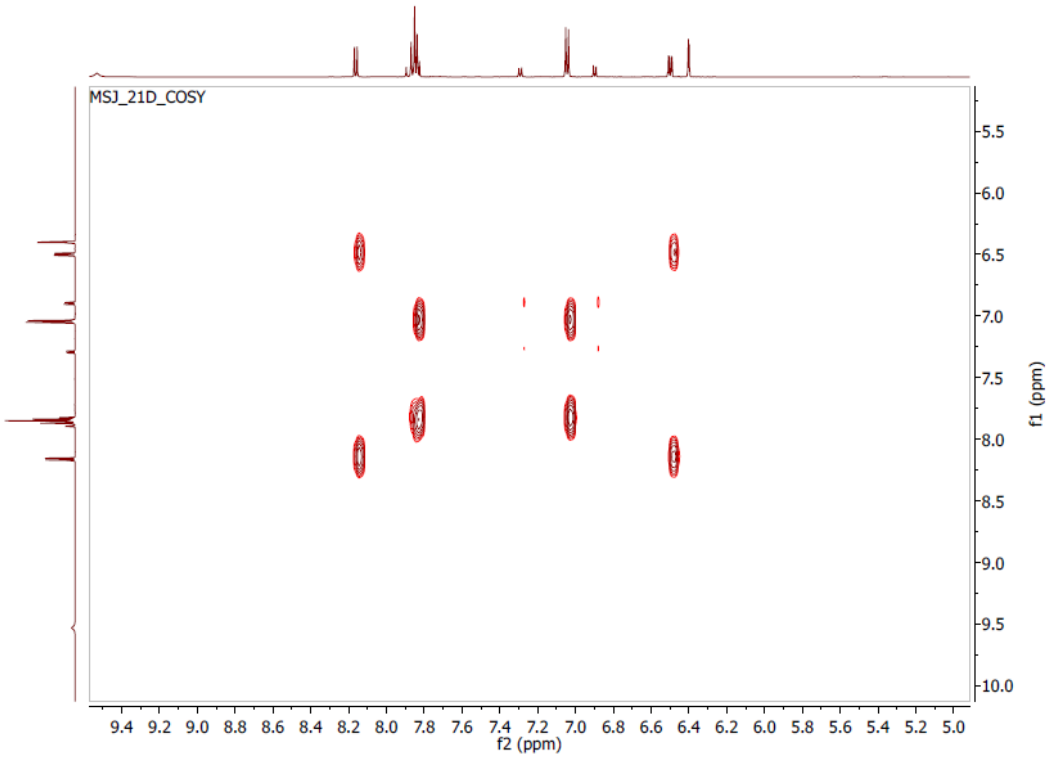

**Appendix C: NMR Spectrum for 2',4'-Dihydroxy-4-chlorochalcone (47)**

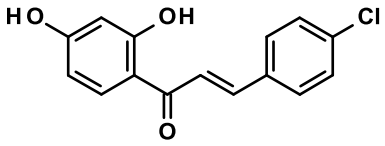


**47**

$^{1}$H NMR Spectrum for **47**

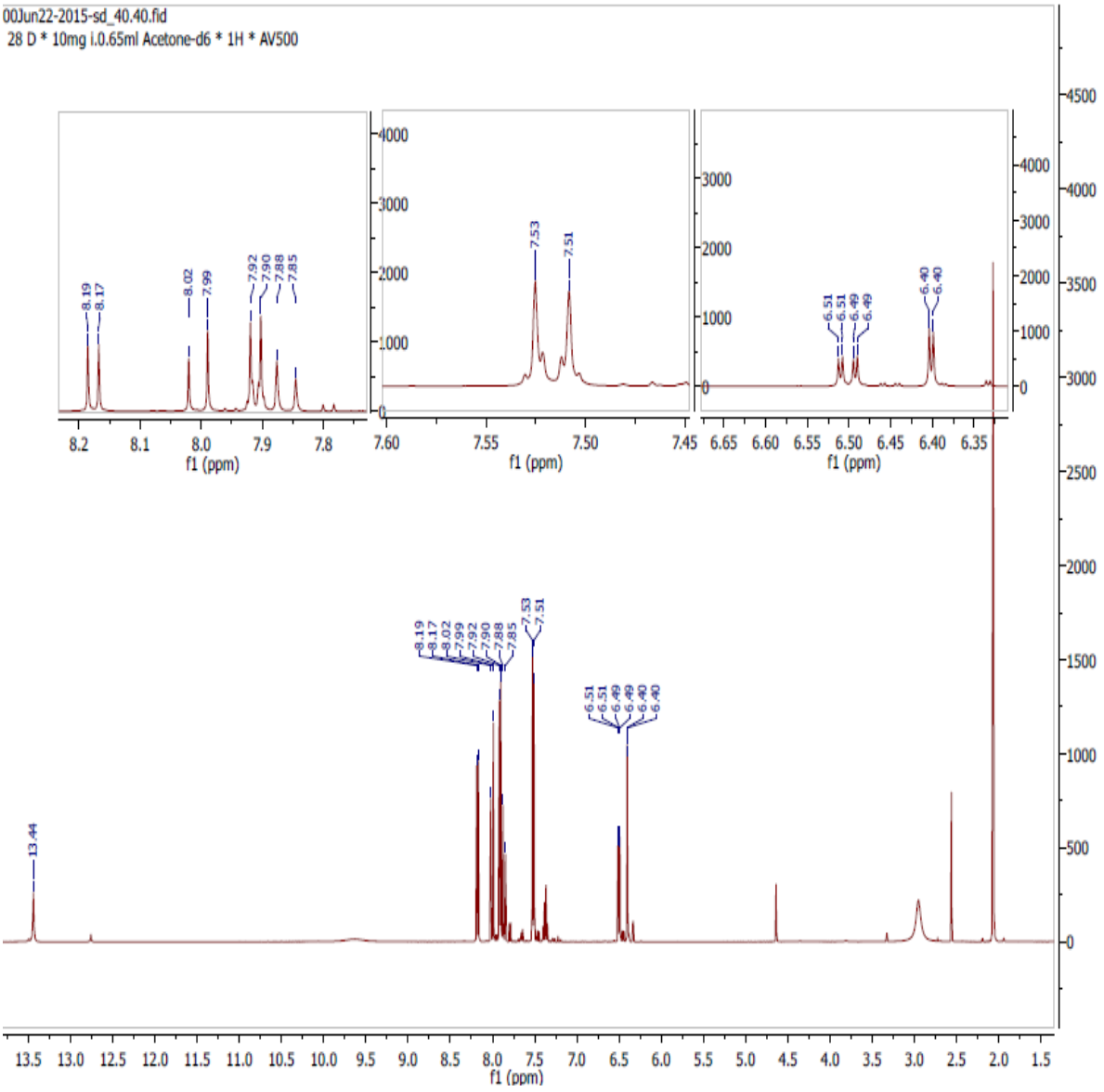

$^{13}$C NMR Spectrum for **47**

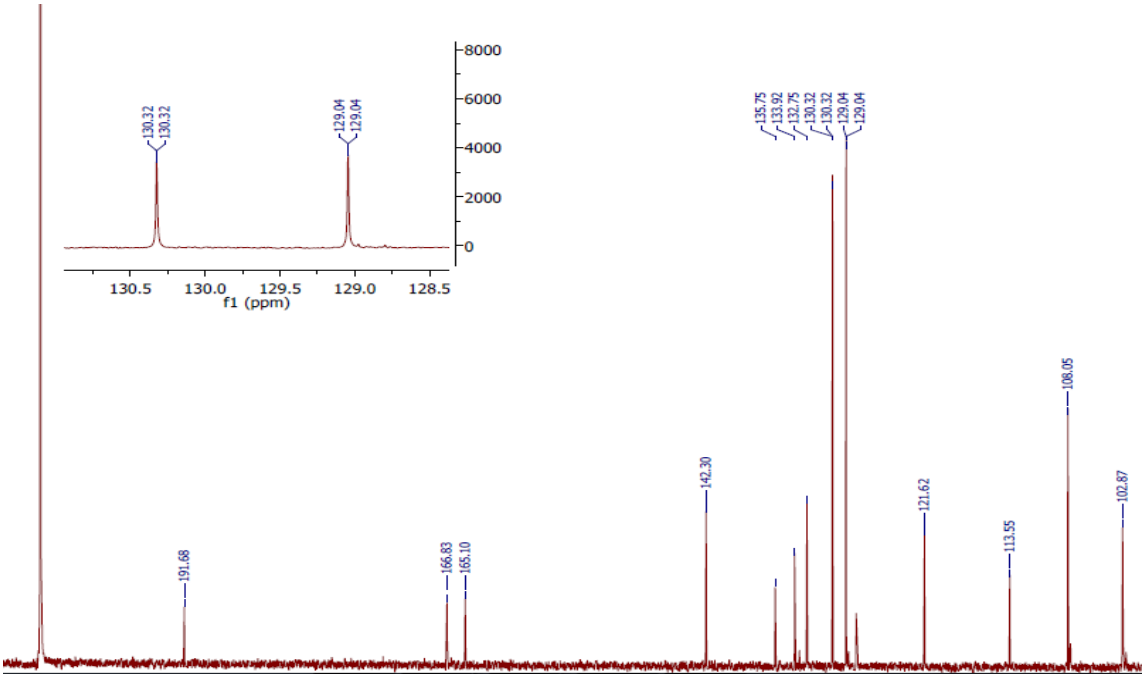


HSQC Spectrum for **47**

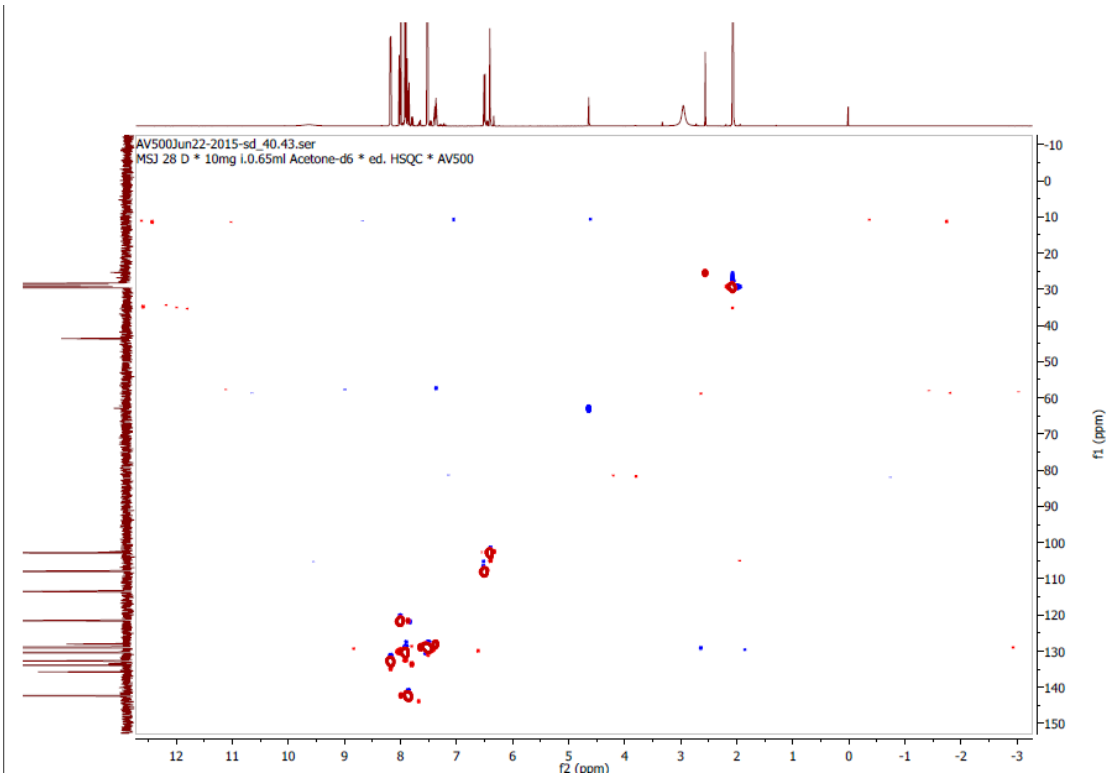

HMBC Spectrum for **47**

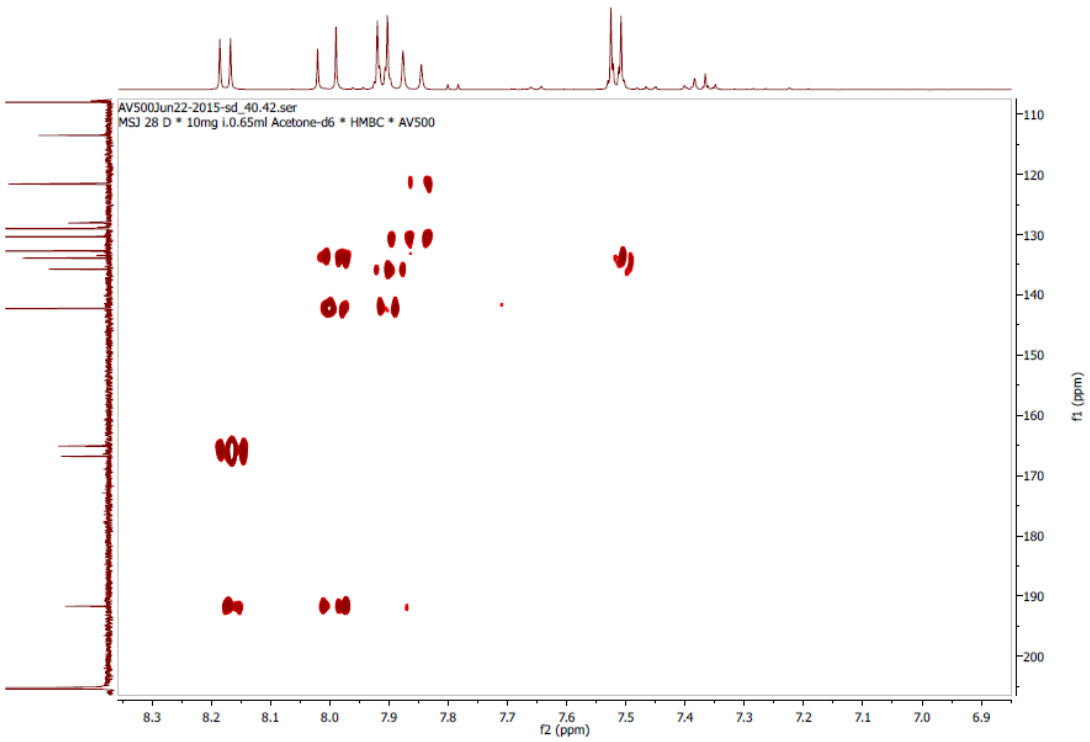


COSY Spectrum for **47**

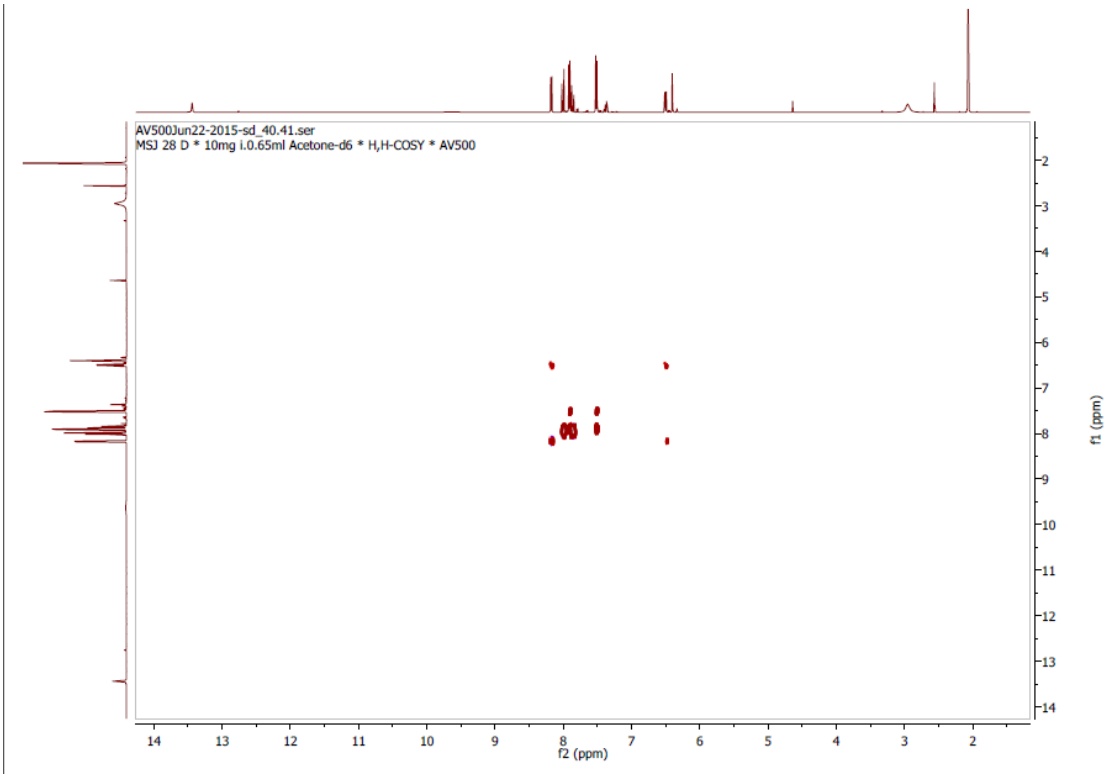

**Appendix D: NMR Spectrum for 7-hydroxy-2-(4-methoxyphenyl)chroman-4-one (48)**

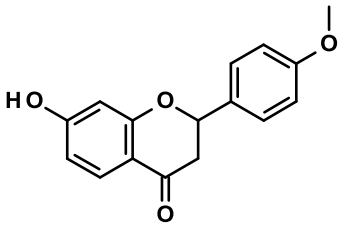


**48**

1H NMR Spectrum for **48**

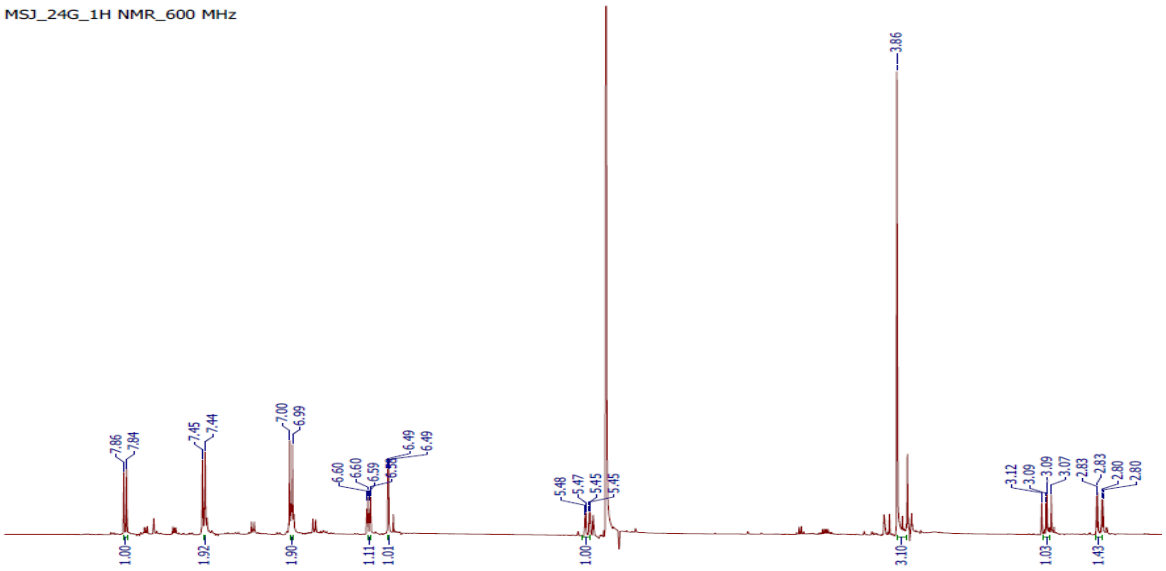


$^{13}$C NMR Spectrum for **48**

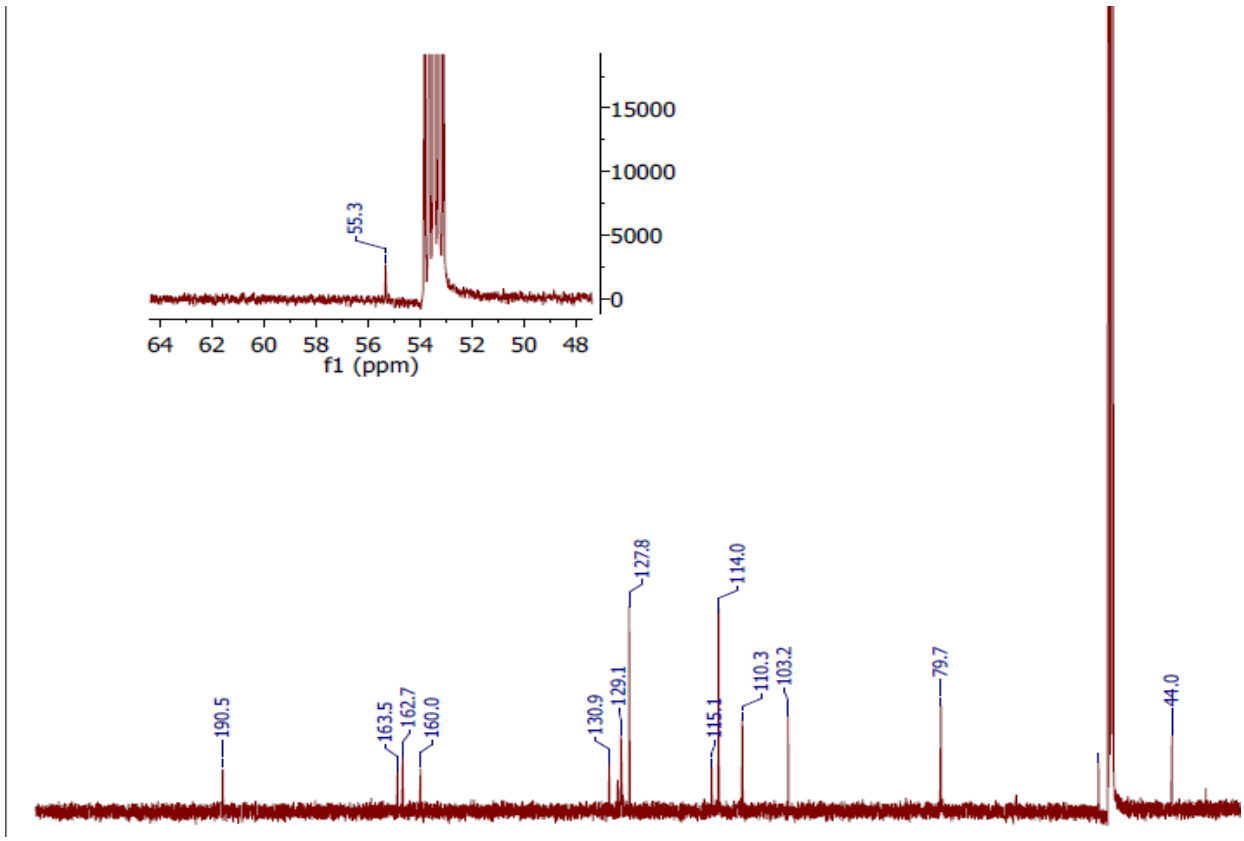

HSQC Spectrum for **48**

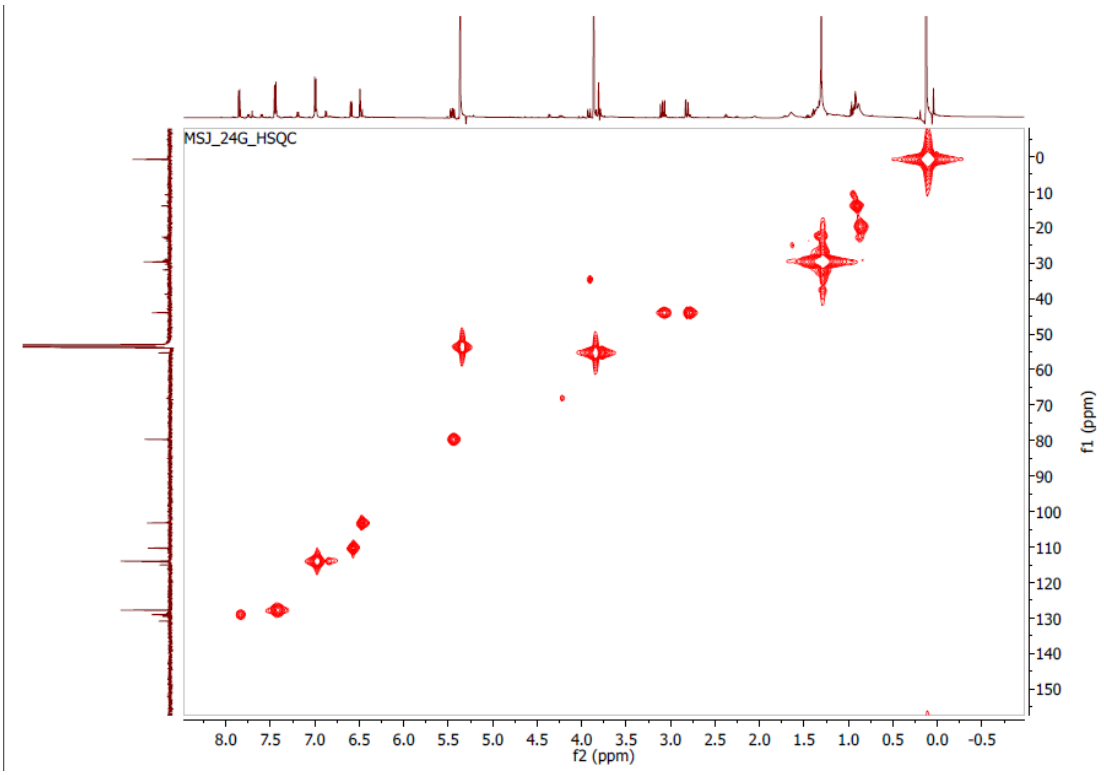


HMBC Spectrum for **48**

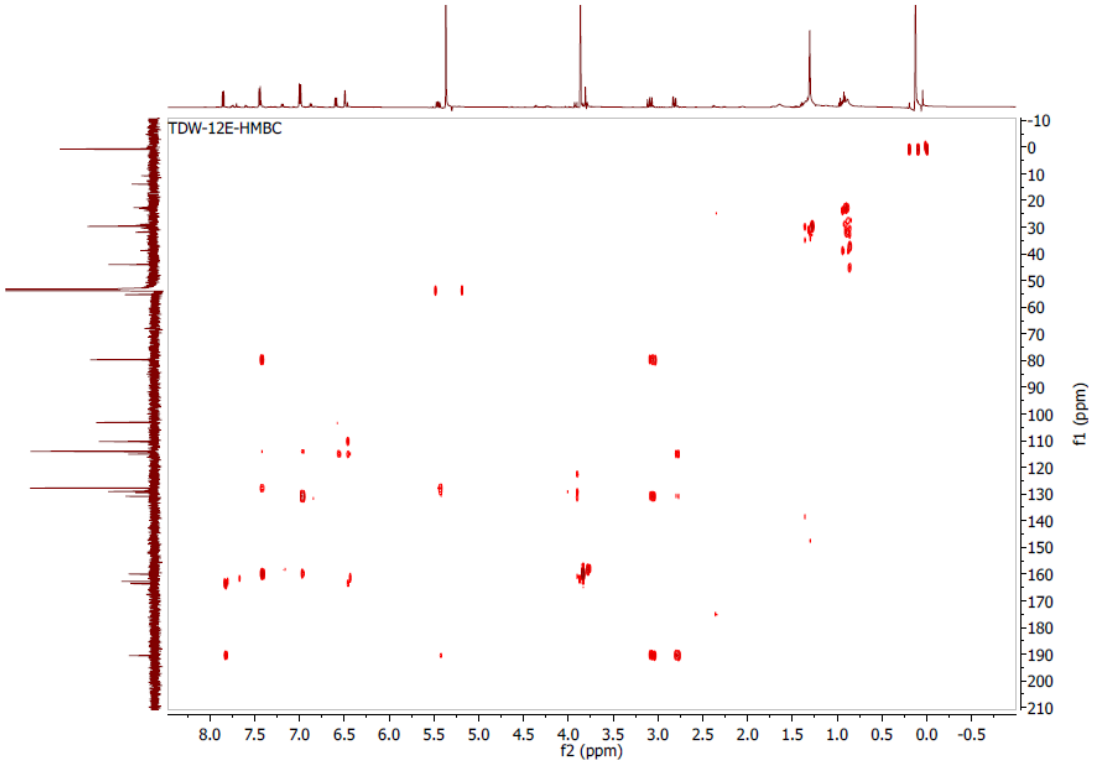

COSY Spectrum for **48**